

Longitudinal Quantification of Neutralizing Antibodies and T cell Responses to
COVID-19 mRNA Vaccines

by

Alexa J. Roeder

A Dissertation Presented in Partial Fulfillment
of the Requirements for the Degree
Doctor of Philosophy

Approved October 2023 by the
Graduate Supervisory Committee:

Douglas Lake, Chair
Grant McFadden
Esther Borges Florsheim
Yung Chang
Masmudur Rahman

ARIZONA STATE UNIVERSITY

December 2023

ABSTRACT

Severe acute respiratory syndrome coronavirus-2 (SARS-CoV-2) is the causative pathogen of Coronavirus Disease 2019 (COVID-19). Successful vaccination aims to elicit neutralizing antibodies (NAbs) which inhibit viral infection. Traditional NAb quantification methods (neutralization assays) are labor-intensive and expensive, with limited practicality for routine use (e.g. monitoring vaccination response). Thus, a rapid (10-minute) lateral flow assay (LFA) for quantification of SARS-CoV-2 NAbs was developed. Using the NAb LFA, an 18-month longitudinal study assessing monthly NAb titers was conducted in a cohort of over 500 COVID-19 mRNA vaccine recipients. Three NAb response groups were identified: vaccine strong responders (VSRs), moderate responders (VMRs), and poor responders (VPRs). VSRs generated high and durable NAb titers. VMRs initially generated high NAb titers but showed more rapid waning with time post-vaccination. Finally, VPRs rarely generated NAb titers $\geq 1:160$, even after 3rd dose.

Although strong humoral responses correlate with vaccine effectiveness, viral-specific CD4⁺ and CD8⁺ T cells are critical for long-term protection. Discordant phenotypes of viral-specific CD8⁺ and CD4⁺CXCR5⁺ T follicular helper (cTfh) cells have recently been associated with differential NAb responses. The second portion of this dissertation was to investigate whether/how SARS-CoV-2 T cell responses differ in individuals with impaired NAb titers following mRNA vaccination. Thus, phenotypic and functional characterization of T cell activation across NAb response groups was conducted. It was hypothesized that VPRs would exhibit discordant SARS-CoV-2 T cell activation and altered cTfh phenotypes. Peripheral blood mononuclear cells were isolated from VPRs, VMRs, VSRs, naturally infected, and normal donors. SARS-CoV-2

responsive T cells were characterized using *in vitro* activation induced marker assays, multicolor flow cytometry, and multiplex cytokine analysis. Further, CXCR5⁺ cTfh were examined for chemokine receptor expression (CCR6 and CXCR3). Results demonstrated that despite differential NAb responses, activation of SARS-CoV-2 responsive CD4⁺ and CD8⁺ T cells was comparable across NAb groups. However, double-positive CD4⁺CD8⁺, CD8^{low}, and activated CD4⁺CXCR5⁺CCR6⁻CXCR3⁺ (Tfh1-like) T cells were expanded in VPRs compared to VMR and VSRs. Interestingly, a unique population of CD8⁺CXCR5⁺ T cells was also expanded in VPRs. These novel findings may aid in identification of individuals with impaired or altered immune responses to COVID-19 mRNA vaccination.

DEDICATION

To all individuals who participated in our studies and believed in the concept,

this is possible only because of you. Thank you.

To Mary, and all others that fail to fit in the boxes built for us.

You are my reason.

To R. Hirshman, A. Roeder, H. Roeder, J. Roeder, and S. Roeder.

I wish you were here.

To S. Graham and D. Glick, your gifts are immortal.

ACKNOWLEDGMENTS

First and foremost, I thank my mentor of the past 8 years, Dr. Douglas Lake, for his intellectual guidance and insight, support in times of personal difficulty, and his unwavering ability to see possibility in pandemonium.

Thank you to my Ph.D. advisory committee, Dr. Grant McFadden, Dr. Esther Borges Florsheim, Dr. Yung Chang, and Dr. Masmudur Rahman, for their time, mentorship, insightful conversation, and expertise shared. I would also like to thank Dr. Karen Kibler, my BSL-3 mentor, for her extensive time taken to train me, help to conduct experiments, and the invaluable expertise she imparted during our time together

I thank our collaborators, Dr. Sergei Svarovsky, Dr. Alim Seit-Nebi, and Dr. Maria Gonzalez-Moa, for their intellectual contribution in development of the NAb LFA.

With profound gratitude and admiration, I thank Yvette Ruiz, for the innumerable lessons she taught me scientifically and otherwise, for her friendship, willingness to help, and invaluable guidance in any situation.

Thank you to Mia Masuda, for your love, friendship, and unconditional support. For your scientific insight, for continuously challenging me to learn and grow myself, and for always laughing and crying alongside me in this journey.

To my lab mates and dear friends, Kirsten Pfeffer, Francisca Grill, and Calvin Koelbel, I extend a sincerest thank you for our time together. For your friendship, support, scientific and intellectual contribution, and meaningful conversation throughout the years. I will remember them fondly and with adoration for years to come.

I wish you all joy, health, and great success.

To my mother and father, how far we've come. Thank you, for everything. I can't believe we're here, together, and I'm so very grateful. To my entire family, whose unconditional love and unwavering belief in my ability to persevere sustains me in moments of discouragement.

Thank you to my lab mates, Austin Blackmon, Megan Koehler, and Patrick Grandinetti, for all of your help, conversation, and friendship. I know the lab is in excellent hands with you all, and I wish for you a successful and exciting graduate journey.

Lastly, I sincerely thank Dr. Jane Maienschein and Arizona State University's Center for Biology and Society, for their gracious funding that allowed me to focus solely on research during the height of the COVID-19 pandemic.

TABLE OF CONTENTS

	Page
LIST OF TABLES	vi
LIST OF FIGURES	vii
CHAPTER	
1 INTRODUCTION	1
<i>Coronaviridae</i> Familial Introduction—Seasonal(s), SARS, and MERS	1
SARS-CoV-2 Pathogenesis and Transmission	4
Rapid Lateral Flow Assay to Detect SARS-CoV-2 Neutralizing Antibodies	8
SARS-CoV-2 Emergence, Expansion, and Evolution	9
COVID-19 Convalescent Plasma (CCP)	12
mRNA Vaccines – Prelude and Present-day Status	16
2 DEVELOPMENT OF A RAPID POINT-OF-CARE TEST THAT MEASURES NEUTRALIZING ANTIBODIES TO SARS-COV-2	22
Abstract	22
Introduction	23
Materials and Methods	24
Results	28
Discussion	38
3 THIRD COVID-19 VACCINE BOOSTS NEUTRALIZING ANTIBODIES IN POOR RESPONDERS	41
Abstract	41
Introduction	42

CHAPTER	Page
Materials and Methods.....	44
Results	50
Discussion.....	56
 4 LONGITUDINAL COMPARISON OF NEUTRALIZING ANTIBODY RESPONSES TO COVID-19 MRNA VACCINES AFTER SECOND AND THIRD DOSES	61
Abstract	61
Introduction	62
Materials and Methods.....	65
Results	68
Discussion	89
 5 DEVELOPMENT OF SARS-COV-2 VARIANT-SPECIFIC NEUTRALIZING ANTIBODY LATERAL FLOW ASSAYS	95
Introduction	95
Materials and Methods.....	96
Results	98
Discussion.....	102
 6 T CELL AND CYTOKINE PROFILING OF SARS-COV-2 MRNA VACCINE- INDUCED NEUTRALIZING ANTIBODY POOR RESPONDERS	104
Introduction	104
Materials and Methods.....	109

CHAPTER	Page
Results	115
Discussion.....	126
7 DISCUSSIONS	130
REFERENCES	142
APPENDIX	
A STATEMENT OF PERMISSIONS	161
B SARS-COV-2 NEUTRALIZING ANTIBODY LATERAL FLOW ASSAY CLINICAL AGREEMENT AND VALIDATION STUDIES.....	163
C PROTOCOL FOR VALIDATION OF FOCUS REDUCTION NEUTRALIZATION TEST AT ARIZONA STATE UNIVERSITY.....	167
D FLOW CYTOMETRIC T CELL ASSAY GATING WORKFLOWS.....	176
E FLOW CYTOMETRIC T CELL MULTICOLOR ANTIBODY PANELS...	178
F CD8 ^{HI} VS CD8 ^{LOW} ACTIVATION INDUCED MARKER EXPRESSION..	180

LIST OF TABLES

Table	Page
1. SARS-CoV-2 NAb LFA Precision Study	36
2. SARS-CoV-2 NAb LFA Density Unit Conversion	51
3. Demographic Information for 3 rd mRNA Vaccine Dose Recipients	53
4. Population Demographics of COVID-19 mRNA Vaccine Study Participants ...	69
5. Breakthrough Infection Population Demographics	88
6. BA.5 NAb LFA Density Unit Conversion	102

LIST OF FIGURES

Figure	Page
1. COVID-19 Convalescent Plasma as a Treatment for SARS-CoV-2 Infection	3
2. Animal Origins of Human Coronaviruses	5
3. SARS-CoV-2 in Domestic and Wild Animals	7
4. Rapid Lateral Flow Assay to Detect SARS-CoV-2 NAb	8
5. NAb LFA Evaluation of COVID-19 Convalescent Plasma	12
6. Focus Reduction Neutralization Test (FRNT) Methodology	15
7. Longitudinal SARS-CoV-2 NAb Quantitation in VPR, VMR, & VSR Groups..	19
8. Principles of SARS-CoV-2 NAb LFA	28
9. RBD-ACE2 Competition LFA Density and IC ₅₀ Value Comparison	30
10. Cross-Reactivity Evaluation of Seasonal Respiratory Virus Convalescent Sera..	31
11. Regression Analyses of Serum NAb titers	32
12. Bland-Altman Analyses of Ortho Virtros and NAb LFA	33
13. Univariate ROC Analyses of Ortho Virtros and NAb LFA	34
14. NAb Levels in Prior Infection and Vaccine-Induced Individuals	37
15. Lateral Flow Assay to Detect SARS-CoV-2 Neutralizing Antibody	45
16. Regression Analysis of LFA Density and Neutralization IC ₅₀ values	49
17. NAb LFA with Density, IC ₅₀ , Titer, and Percent Neutralization Values	52
18. NAb Profile of mRNA Vaccine Recipients Pre- and Post-3 rd Vaccine Dose	55
19. Comparison of NAb After 2 nd dose of mRNA1273 or BNT162b2	56
20. Schematic Diagram of NAb LFA Principle/Mechanism	63
21. NAb LFA Density Units Correspond to Percent Neutralization and NAb titer ..	67

Figure	Page
22. Flowchart of mRNA-Vaccinated Subjects	70
23. Comparison of 2nd and 3rd mRNA Vaccine-Induced NAb Durability	71
24. NAb Durability of 2 nd and 3 rd mRNA Vaccine Doses by Manufacturer	73
25. Comparison of 2 nd and 3 rd Dose NAb Durability by Sex and Age	76
26. 2 nd and 3 rd Vaccine Dose Cluster Analyses of Longitudinal NAb Data	79
27. Percent Neutralization Between 2 nd and 3 rd Vaccine Doses	81
28. Grouping Analyses of Paired Longitudinal NAb Data	83
29. Post Hoc Power Analysis of Paired Longitudinal Data	85
30. NAb Titers of Naturally Infected Subjects Pre and Post Omicron Dominance ..	87
31. Validation of a BA.1-Specific NAb LFA.....	99
32. Validation of a BA.5-Specific NAb LFA.....	101
33. Activation Induced Marker Staining of Spike Peptide Stimulated PBMCs.	116
34. Identification of CD4 ⁺ CD8 ⁺ and CD8 ^{low} T cells in VPR subjects.....	118
35. Characterization of Bulk CD4 ⁺ cTfh in VPR, VMR, and VSR Subjects	120
36. Characterization of Activated CD4 ⁺ cTfh in VPR, VMR, and VSR Subjects. .	122
37. Assessment of Bulk CD8 ⁺ T cell CXCR5, CCR6, and CXCR3 Expression.....	123
38. Cytokine Profiling of Supernatants from Peptide-Stimulated PBMCs	125

CHAPTER I

INTRODUCTION

***Coronaviridae* familial introduction—seasonal(s), SARS, and MERS**

Viral family *Coronaviridae* compose a large group of positive sense, single-stranded, enveloped RNA viruses, and are causative pathogens for many seasonal illnesses that cause disease in human populations annually.¹ Several seasonal coronaviruses include those that cause “common cold” symptoms, such as human coronavirus (HCoV) OC43, HKU1, NL63, and 229E.² Other members of *Coronaviridae* can cause more severe disease phenotypes with increased fatality and hospitalization rates, such as severe acute respiratory syndrome coronavirus (SARS-CoV) and middle eastern respiratory virus syndrome coronavirus (MERS-CoV).

SARS-CoV was first detected late 2002 in the Guangdong Province of China, prior to spreading to Hong Kong,³ and rapidly leading to outbreaks in Singapore, Toronto, and Vietnam.^{4,5} Cumulatively, from emergence in 2002 through 2004, there were more than 8,000 documented cases of SARS-CoV infection and over 900 known deaths (an estimated fatality rate of approximately 10%).⁶ In contrast, MERS, first detected in 2012 in Saudi Arabia,⁷ has a much higher fatality rate of nearly 41%, as more than 900 deaths and at least 2,600 cases have been documented to date.⁸ A subsequent 2015 MERS outbreak in Republic of Korea resulted in an additional 186 cases and 38 fatalities,⁹ though was comparably well contained. Treatment availability at the height of the MERS epidemic lacked in specificity,¹⁰ as main therapeutic interventions involved treatment of symptoms adjunct to oxygen and hydration support. Although, several case

studies were reported to have used corticosteroids, interferons, remdesivir, various experimental treatments, and convalescent plasma transfusion,^{11,12} intervention strategies were subject to availability and case severity at that time.

Convalescent plasma refers an antibody-rich component from the blood of a previously infected and recovered individual. Convalescent plasma transfusion refers to the isolation and intravenous (IV) transfer into a patient with active infection (**Figure 1**), ideally, early in disease.¹³ Although clinical outcomes CP use have historically been low, several decades of literature to support the use in emergency pandemic or epidemic circumstance, and reduction in mortality has been associated with CP use for various infectious diseases.¹⁴ The basis of CP is founded upon an immunologic concept of passive immunity, or the transfer of antibodies from one individual to another.¹⁵ Passive immunity as both a prophylactic and/or therapeutic method of intervention has long been used in an emergency response to infectious disease settings.¹⁶ In 2013-2016, CP was used during the Ebola outbreak in West Africa,¹⁷ in the SARS-CoV and MERS-CoV outbreaks,¹⁸ as well as in 2019 and 2020, in the infancy of the SARS-CoV-2 pandemic.¹⁹

Use of Convalescent Plasma to Treat COVID-19 Patients

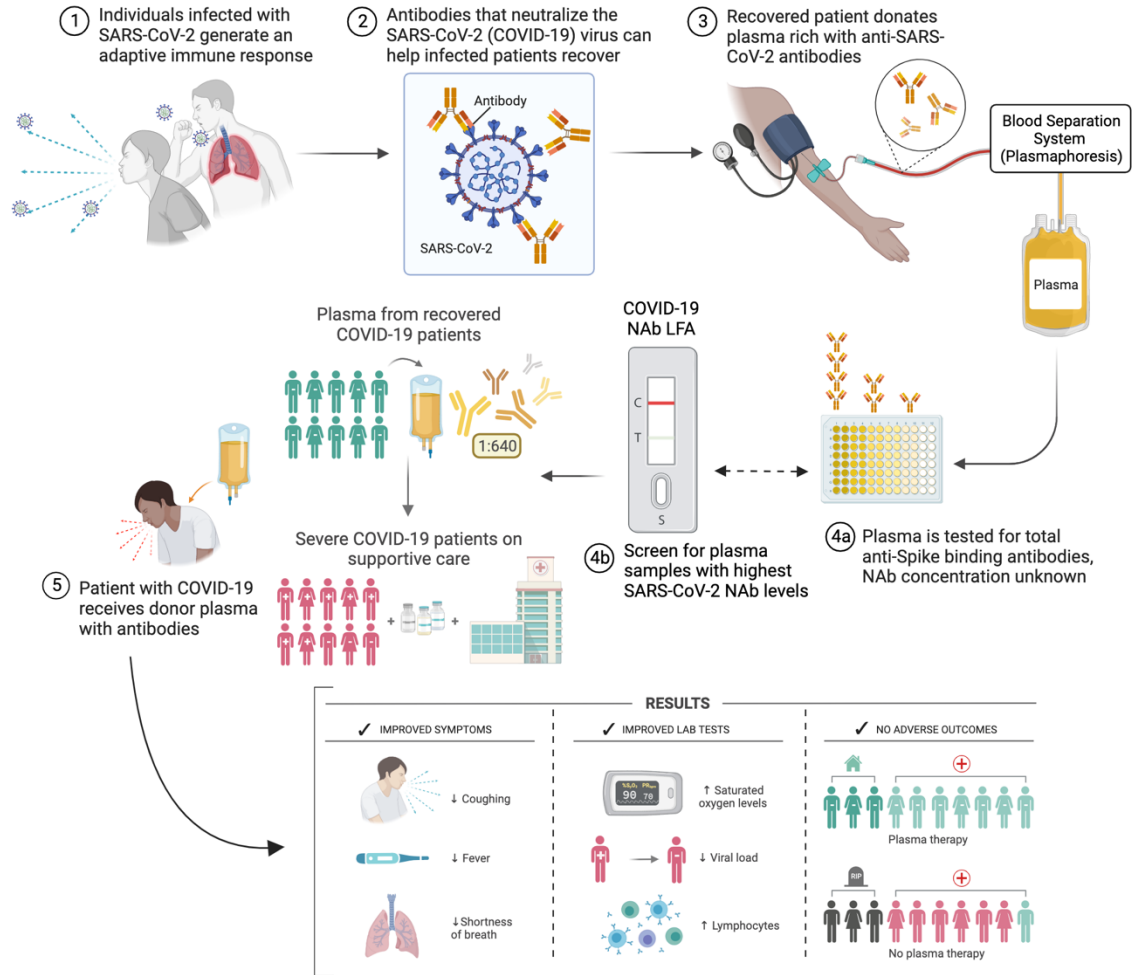


Figure 1. COVID-19 convalescent plasma as a treatment for active SARS-CoV-2 infection. Flowchart infographic diagram demonstrating COVID-19 convalescent plasma (CCP) generation from: **(1)** infection and immune response, **(2)** recovered individuals generate antibodies that can neutralize viral infection, however, binding antibodies perform functions that are different to that of neutralizing antibodies (NAbs), a critical component of CCP. **(3)** Patients recovered from COVID-19 donate plasma, a component of blood rich in antibodies using a blood separation system known as plasmapheresis. **(4)** Plasma is tested for SARS-CoV-2-specific anti-spike antibodies. **(4a)** Total anti-Spike antibodies are quantified according to approved diagnostic assays and guidelines per an Emergency Use Authorization (EUA) issued by FDA. **(4b)** COVID-19 NAb lateral flow assay (LFA), developed with the intention to be utilized as a screening tool for selection of CCP samples with highest titer NAbs, such that these CCP units may be allocated to the most severely ill patients. **(5)** Representative study demonstrating CCP with 1:640 NAb titer administered to severe COVID-19 patients on supportive care in hospital, and the associated results.²⁰ Results shown here are for figurative demonstration only, and are not formally a part of this dissertation, although we applaud authors for their NAb

quantitation prior to CCP administration and resulting work. This figure was generated using BioRender.com and adapted from template figures made by Daniel Smith and Lisa Vrooman.

SARS-CoV-2 pathogenesis and transmission

SARS-CoV-2, like many other coronaviruses, can infect a variety of host species.²¹ Zoonotic diseases (zoonoses) are those that infect humans and animals, most commonly via animal-to-human transmission,²² although case reports have documented human-to-animal transmission in rare circumstances (reverse-zoonoses).²³ Seasonal coronaviruses often infect multiple different host species prior to infecting humans. For example, human coronavirus (HCoV)-NL63, and HCoV-229E are found in bats as a natural reservoir, with camelids being an intermediate host of 229E, prior to inducing mild infection in humans (**Figure 2**).²¹ Additional seasonal CoVs include HCoV-OC43 and -HKU1. Although these viruses are primarily found in rodents as a natural reservoir, -OC43 has been observed to infect cattle as a host intermediate to humans. ^{21, 24}

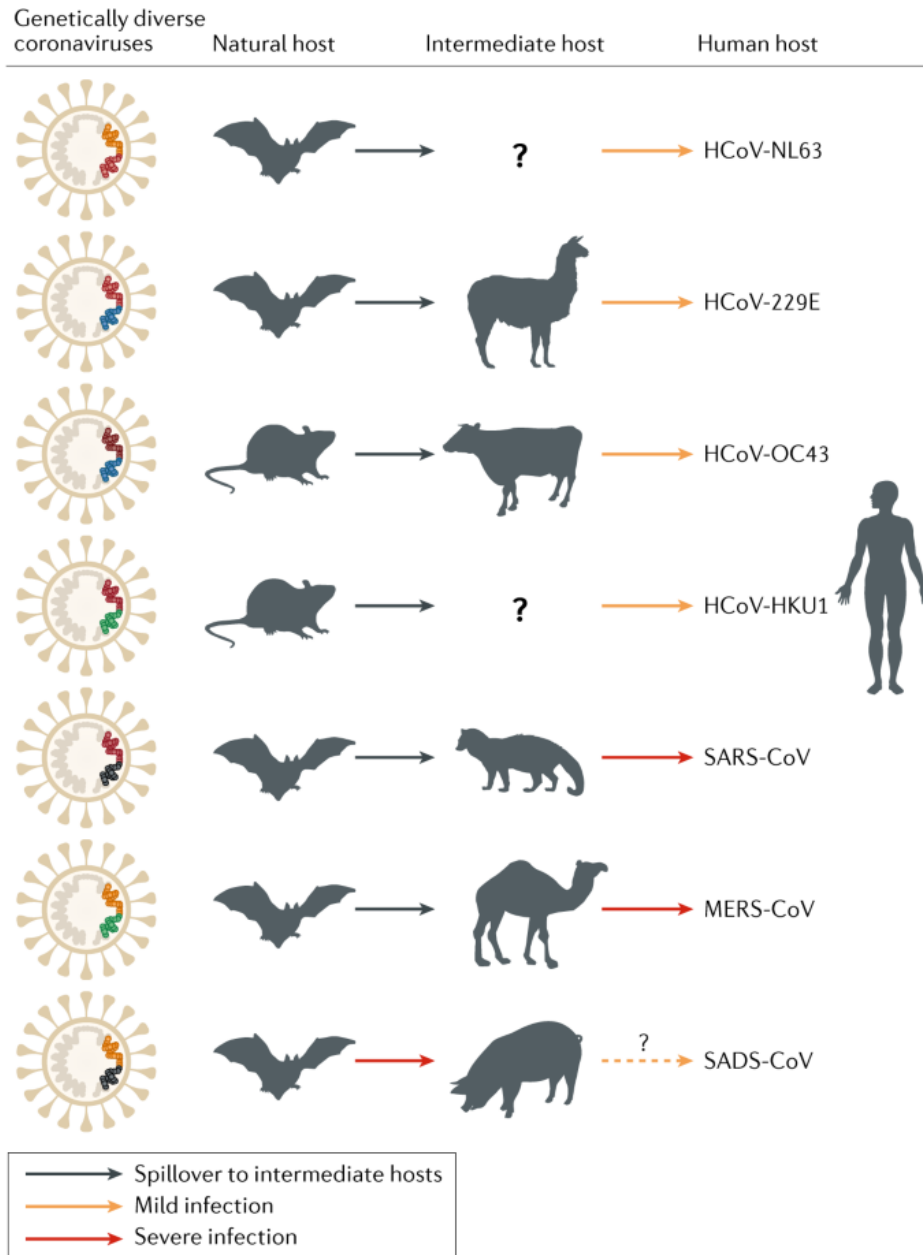


Figure 2. Animal origins of human coronaviruses. Demonstration of zoonotic transmission and interspecies spillover events for major human pathogenic coronaviruses. Seasonal CoVs, HCoV-NL63, 339E, OC43, and HKU1 all cause similar-phenotype mild infections (yellow arrow) in humans, are genetically distinct and have differing transmission lineage. HCoV-NL63 and 229E viral progenitors have been both been found in African bats, and while camelids are the most likely intermediate host for 229E, the intermediate host for HCoV-NL63 is unclear. HCoV-OC43 and HKU1 likely originated in rodents, and OC43 is also known to infect cattle, although the transmission lineage is unclear. SARS-CoV emerged through a recombination of bat SARS-related coronaviruses that led to infection of civets, and causes severe infection in humans (red

arrow). MERS-CoV, also originally found in bats, is prevalent in dromedary camel populations (likely intermediary host), and causes severe infection in humans. Severe acute diarrhea syndrome coronavirus (SADS-CoV) is of recent emergence in piglets and is caused by a novel strain of *Rhinolophus* bat coronavirus HKU2; there is no current evidence of SADS in humans. Image taken from: Cui, J., Li, F. & Shi, ZL. (2019) Origin and evolution of pathogenic coronaviruses. *Nature Reviews Microbiology* **17**, 181–192.²⁵ Image used in accordance with the Springer Nature Copyright license.

SARS-CoV and MERS-CoV both cause severe upper respiratory disease in humans and have mortality rates higher than that of SARS-CoV-2.²⁶ Although not depicted in Figure 2, SARS-CoV-2 was shown to have high sequence similarity with horseshoe bat-derived SARS-like viruses,²⁷ but is more genetically distant from SARS-CoV, hence the original classification as 2019 novel coronavirus (2019-nCov).²⁸ SARS-CoV-2 has been documented to infect a variety of animals,²¹ and abundant evidence supports the originating reservoir as the horseshoe bat.^{29,30} However, identification of an intermediate host remains unclear, despite some evidence suggesting pangolin etiology.³¹ In addition to various experimental animal models of infection, several other species have been naturally infected with SARS-CoV-2 consequent to reverse-zoonosis events (human-to-animal transmission) (**Figure 3**).²¹ Given the relative recent emergence of SARS-CoV-2, it is likely that many cross-species spillover recombination events have yet to come.

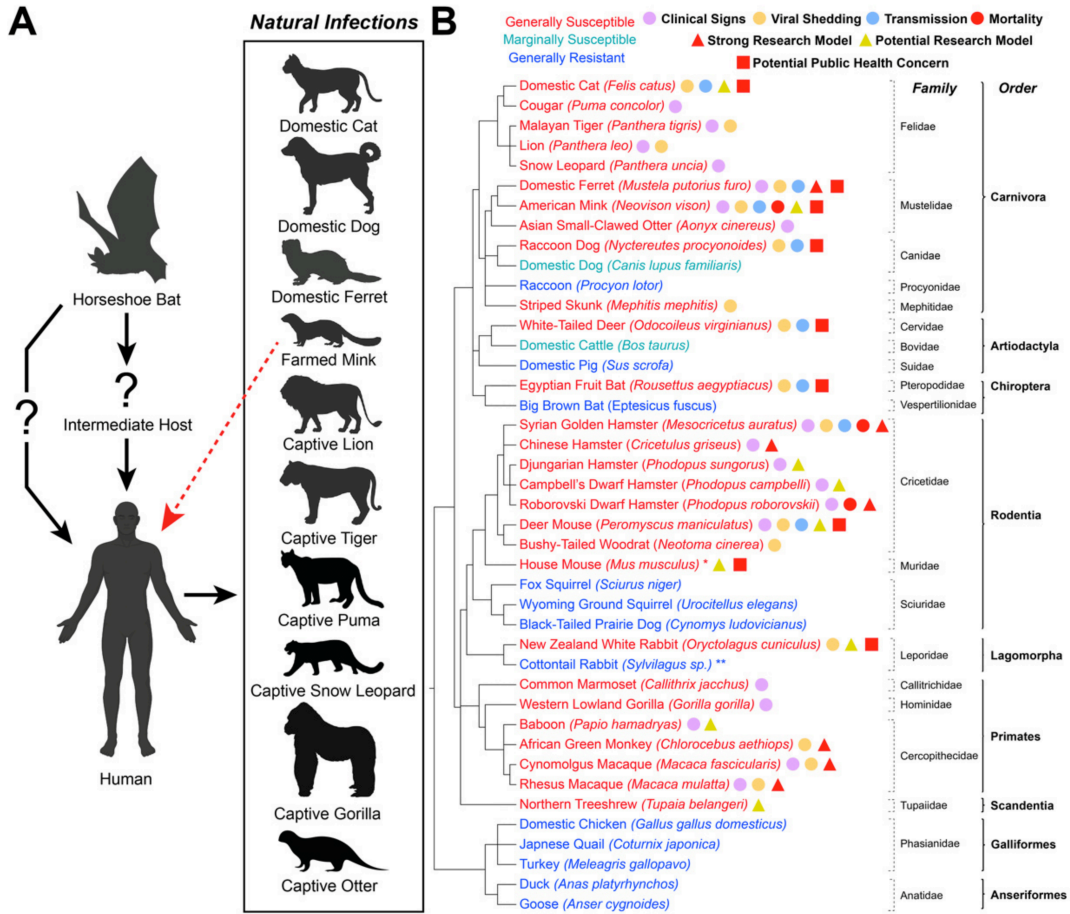


Figure 3. SARS-CoV-2 in Domestic and Wild Animals. (A) Disease ecology of SARS-CoV-2. Available evidence suggests that SARS-CoV-2 originated in a horseshoe bat and was then either transmitted directly to humans or through an unidentified intermediate host. Species with documented human-to-animal natural SARS-CoV-2 infections (reverse zoonosis events) are listed, as is the documented mink-to-human transmission of SARS-CoV-2 (red arrow). Created with BioRender.com. (B) List of documented species that have either been experimentally or naturally infected with SARS-CoV-2 as of August 2021. Species that are generally susceptible to SARS-CoV-2 are listed in red, marginally susceptible species are listed in cyan, and generally resistant species are listed in blue. Clear evidence of outwardly observable clinical signs (violet circle), shedding of infectious virus (orange circle), animal-to-animal transmission (blue circle), and mortality (red circle) upon infection is shown for each species. Species considered strong (red triangle) or potential (yellow triangle) research models are noted, as well as species with a potential public health concern (red square). Phylogenetic tree was produced using the phyloT v2 server (<https://phyloT.biobyte.de>, accessed on 26 June 2021) based on the NCBI taxonomy database. Image and legend taken from: D. A. Meekins, N. N. Gaudreault, and Juergen A Richt. (2021). Natural and Experimental SARS-CoV-2 Infection in Domestic and Wild Animals, *Viruses*.²¹ Image used in accordance with the Creative Commons Attribution license.

Rapid Lateral Flow Assay to Detect SARS-CoV-2 Neutralizing Antibodies

In May of 2020, with the goal to provide hospitals and blood centers with a rapid test that could quantify SARS-CoV-2 neutralizing antibodies (NAbs), we developed a 10-minute functional lateral flow assay (LFA) that quantitatively measures SARS-CoV-2 NAbs using a 10 μ L drop of blood or 6 μ L of plasma/serum (**Figure 4**) (Chapter II).³² The original intention of this project was to develop a rapid, quantitative, COVID-19 NAb LFA for use in a point-of-care setting using plasma or whole blood, such that convalescent donors, or units of plasma, could be screened prior to selection for use as COVID-19 convalescent plasma (CCP).

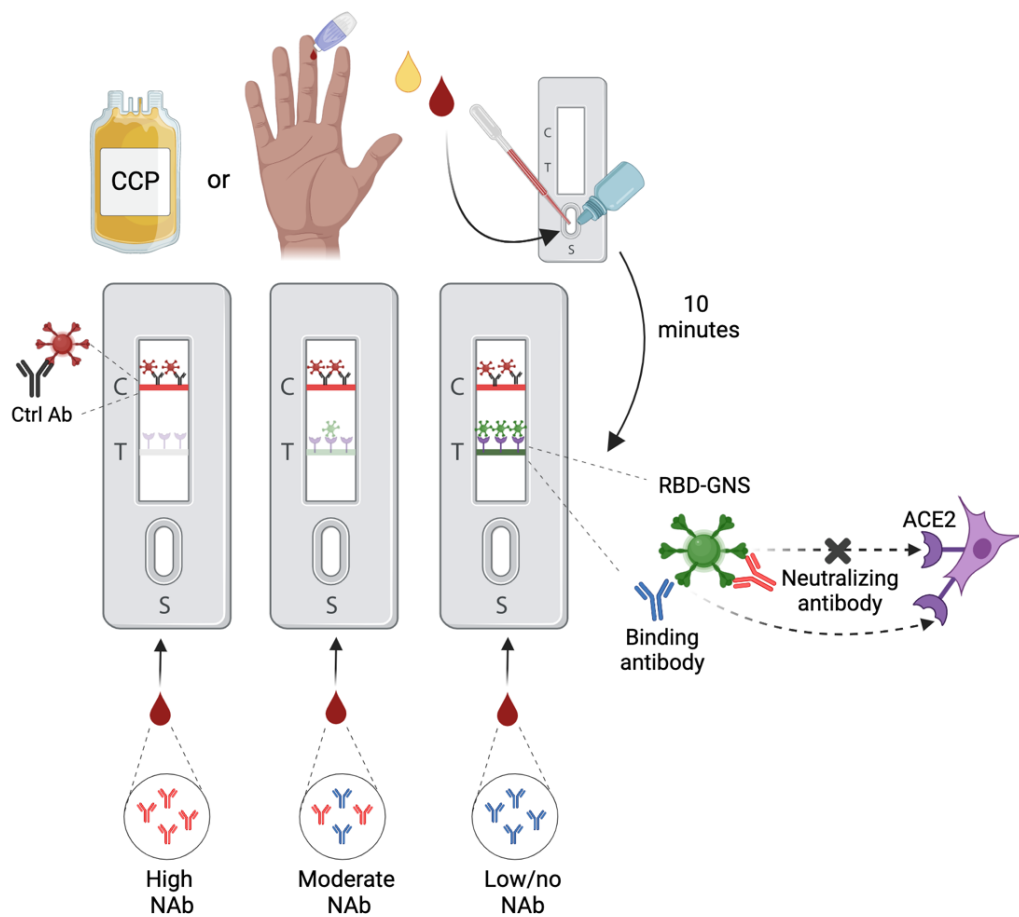


Figure 4. Rapid lateral flow assay to detect SARS-CoV-2 NAb. COVID-19 convalescent plasma (CCP), serum, or whole blood from a finger-stick can be transferred to the sample pad, followed by chase buffer, and let run for ten minutes undisturbed. The test was developed to be used with plasma, serum, or whole blood.³² Methods include transfer of 10 μ L whole blood or 6 μ L plasma or serum, followed by 50 μ L (two drops) of chase buffer, and 10 minutes run time. Results may be visually interpreted or quantified via portable densitometer, RDS-2500 (Detekt Biosciences, REF). Visual results are most simply interpreted on a tertiary scale – high NAb (faint/absent test line), moderate NAb (weak/visible test line), and low/no NAb (strong/dark test line). Assay mechanics are described in subsequent figures.

SARS-CoV-2 emergence, expansion, and evolution

In early December of 2019, a viral pneumonia of unknown etiology emerged in a small group of patients in Wuhan, China.³³ It wasn't until the end of December that Chinese Center for Disease Control (CDC) informed the World Health Organization (WHO) of the novel pneumonia. The following week, Chinese officials activated a Level 2 emergency, just days prior to the first isolation of severe acute respiratory syndrome coronavirus-2 (SARS-CoV-2). By early January of 2020, the first genomic sequence of SARS-CoV-2 was shared publicly.³⁴ The first laboratory confirmed case in the United States (US) was isolated in Washington State on January 18th,³⁵ and additional cases were reported in Illinois, California, and Arizona later that week, increasing the US case total to five individuals.³⁶

In the last week of January, as Wuhan was placed under lockdown and documented case reports approached 300, the WHO declared a 'public health emergency of international concern' on January 30th, 2020.³⁶ As global deaths resulting from SARS-CoV-2 infection surpassed 1,000, WHO published the official name for the disease

associated with the novel viral outbreak,³⁷ Coronavirus Disease 2019 (COVID-19). Late February, just one month after WHO declared an international emergency, more than 82,000 cases had been reported in at least 47 countries.³⁶ The first death in the US was reported days later.³⁸

March of 2020 was a pivotal moment for the US, as case numbers approached 100 for the first time, and were reported across several states, spanning the US coasts.³⁶ In the days following, the Grand Princess cruise ship became stranded along the northern California coastline, and at least 21 confirmed infections were noted upon arrival.³⁹ On March 11th, 2020, WHO formally declared COVID-19 a pandemic as infections surpassed 118,000 and deaths neared 4,300 in 114 countries.⁴⁰ As state-implemented shutdowns began on March 16th, the first human clinical trials of mRNA vaccines designed against SARS-CoV-2 spike protein,⁴¹ directed by Moderna Therapeutics and the National Institute of Health (NIH) were initiated. This vaccine, mRNA-1273, alongside many others that were developed at the same time using similar molecular platforms, revolutionized and modernized immunization. Although a human experiment so grandiose had yet to be conducted with respect to the mRNA vaccination platform, it certainly was not the first introduction of mRNA, DNA, or recombinant protein vaccines to the scientific and healthcare communities.^{42,43,44}

As vaccine companies raced to demonstrate safety and efficacy of their COVID-19 vaccines, researchers around the world began development of new diagnostic platforms, and therapeutics such as antivirals and monoclonal antibodies. Meanwhile, therapeutic options were limited, but included at the time the use of IV corticosteroids, interferons, monoclonal antibodies, various repurposed and experimental antivirals,^{45,46}

intravenous immunoglobulin (IVIG),⁴⁷ mechanical ventilation, and extracorporeal membranous oxygenation (ECMO). Notably, for a period from approximately March through July of 2020, the use of COVID-19 Convalescent Plasma (CCP) was mainstreamed by several major hospitals throughout the US as a first-line treatment for COVID-19,⁴⁸ as monoclonal antibodies had not yet been developed or approved by regulatory agencies. However, available therapeutics were failing for many patients, and personal protective equipment (PPE) availability was exhibiting a national shortage.³⁶ As May of 2020 approached, infections and hospitalizations continued to rise, while deaths in the US surpassed 100,000.³⁶ Early in our NAb LFA development and validation phases, we conducted several experiments using the rapid test that demonstrated a vast heterogeneity of NAb responses to SARS-CoV-2 natural infection, as is supported extensively in the current literature.^{49,50,51}

In collaboration with Mayo Clinic Hospital of Phoenix, Arizona, we used our NAb LFA to measure the titer of neutralizing antibody contained within a small volume of leftover CCP IV tubing segments. In line with literature at the time, our data from this study supported the observation that approximately 30% of naturally infected individuals failed to generate detectable NAbs during early convalescence.⁵² Most notably, these data demonstrated that only a small portion of plasma samples contained highly neutralizing antibodies (**Figure 5**), although the term ‘highly neutralizing’ is relative and dependent on the neutralization test. The remaining majority of convalescent plasma samples contained moderate and low levels of SARS-CoV-2 receptor binding domain (RBD) NAbs. Nonetheless, samples possessing either high, moderate, or low neutralization capacity were equally used for transfusion of hospitalized COVID-19 patients, as the

anti-Spike antibody thresholds, determined by approved diagnostic standards implemented by an EUA issued at the time,⁵³ had been met. Follow-up clinical studies with this sample set were not performed in our laboratory.

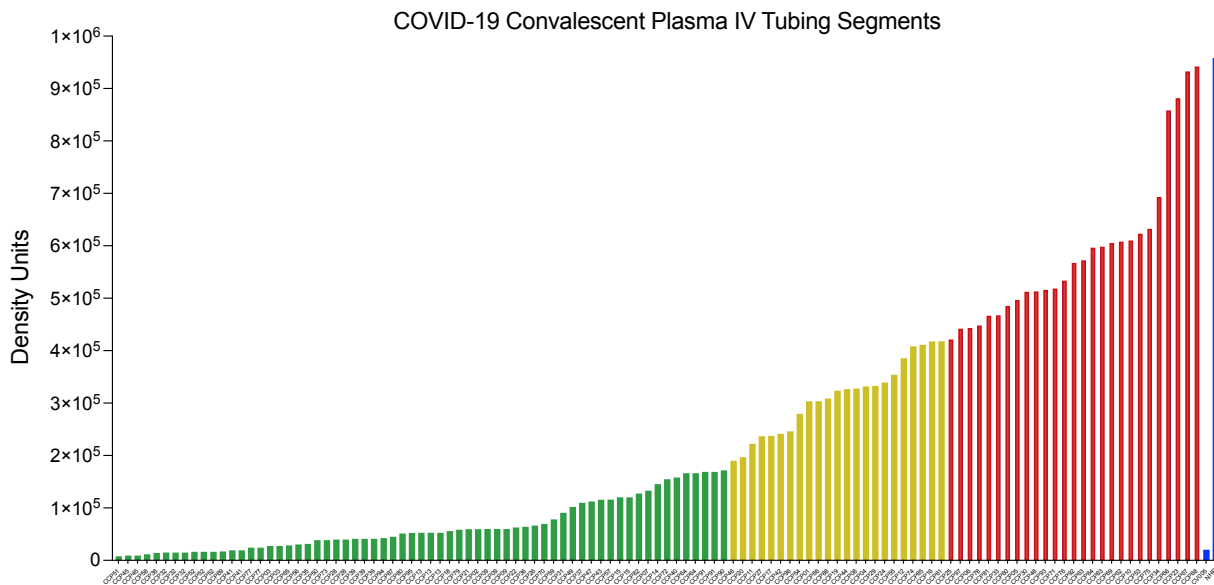


Figure 5. NAb LFA Evaluation of COVID-19 Convalescent Plasma. De-identified IV tubing segments leftover from clinical transfusion protocols were frozen following CCP administration for allocation to research facilities. Convalescent sera ($N = 97$) were run on the COVID-19 NAb LFA developed previously in our laboratory.³² Six microliters of serum were used per sample, followed by two drops ($50 \mu\text{L}$) of chase buffer. All tests ran undisturbed on a flat surface for ten minutes prior to reading. Tests were read on a RDS-2500 (Detekt Biomedical) portable densitometer for quantitation of control and test line densities. De-identified CCP tubing segments (x-axis) are graphed by test line density units (y-axis) in ascending order. Samples are grouped by high titer ($\geq 1:320$, green, $n = 47$), moderate ($< 1:160$, $\geq 1:80$, yellow, $n = 23$), and low ($< 1:80$, red, $n = 27$) titer NAb, in addition to a highly neutralizing and non-neutralizing control (blue).

COVID-19 Convalescent Plasma (CCP)

Administration of CCP was both highly political and experimental in the context of SARS-CoV-2 and COVID-19 treatment. Historically, dating back to the late 19th and early 20th century, convalescent serum or plasma has been used to treat infectious disease

in the context of tetanus, diphtheria, influenza (1918 pandemic), measles, SARS-CoV, H1N1, MERS-CoV, Ebola virus, and recently, SARS-CoV-2.¹⁴ Metanalyses comparing studies from the past 150 years have found associations between CP transfusion and reduced mortality rates in infectious disease ranging from 10-100%.^{54,55} Altogether, therapeutic efficacy of CP transfusion varies depending on the virus, disease, donor, and recipient.

While there are transfusion-associated risks that have been identified such as circulatory overload and acute lung injury,⁵⁶ convalescent plasma, particularly in the setting of novel infectious disease, is regarded as an empiric therapeutic, that may temporally bridge the gap between preventative vaccine and/or therapeutic monoclonal antibody development in a future pandemic setting.¹⁴ Emergency Use Authorization (EUA) was issued for CCP use in hospitalized patients with COVID-19 by the Food and Drug Administration (FDA) on August 23, 2020.⁵³ However, it is important to note that CCP administration without the widescale and standardized quantification of SARS-CoV-2 NAb in each sample prior to transfusion, given the technology is available beyond our lateral flow assay, likely contributes to the variable efficacies reported in retrospective metanalyses.^{57,58} Unsurprisingly, one COVID-19 retrospective analysis demonstrated a reciprocal dose-dependent relationship between mortality rate and level of NAb levels in the CCP transfused into the SARS-COV-2-infected patient,⁵⁹ highlighting a critical need for widescale quantitation of SARS-CoV-2 NAb in sero-banked CCP units, for example.

To quantify NAb titers by traditional methodology, live virus must be used under high-containment biosafety level 3 (BSL-3) conditions by highly trained, skilled

laboratory personnel. The current gold-standard assay used for NAb titer quantitation is a viral focus forming assay (FFA), or focus-reduction neutralization test (FRNT), a more high-throughput version of the viral plaque reduction test (PRNT).⁶⁰ The protocol for these assays (Appendix C, FRNT Protocol), while sufficiently optimized, is time-consuming, laborious, expensive, requires specialized BSL-3 facilities, highly trained personnel, and requires extensive incubation time (**Figure 6**). Briefly, convalescent or vaccinated serum is incubated with virus, prior to plating serum and virus on permissive and susceptible cells. Virus not neutralized by antibodies then infects cells and nearby neighboring cells, forming viral foci or groups of virally infected cells. After incubation, viral inactivation, decontamination, and several rounds of washing, the plates are transported to BSL-2 laboratory conditions for immunostaining. An additional day is required for staining, and plates can be read the following day prior to data analysis and curation. In total, these experiments require a minimum of four consecutive hands-on laboratory days, the majority of which is spent in high-containment facilities. A goal of developing the rapid COVID-19 NAb LFA was to provide a surrogate to these gold-standard assays, which could provide quantitative and accessible SARS-CoV-2 NAb data in a laboratory, point-of-care clinical, or at-home setting in a cost-effective and accessible manner, without the need for high-containment facilities.

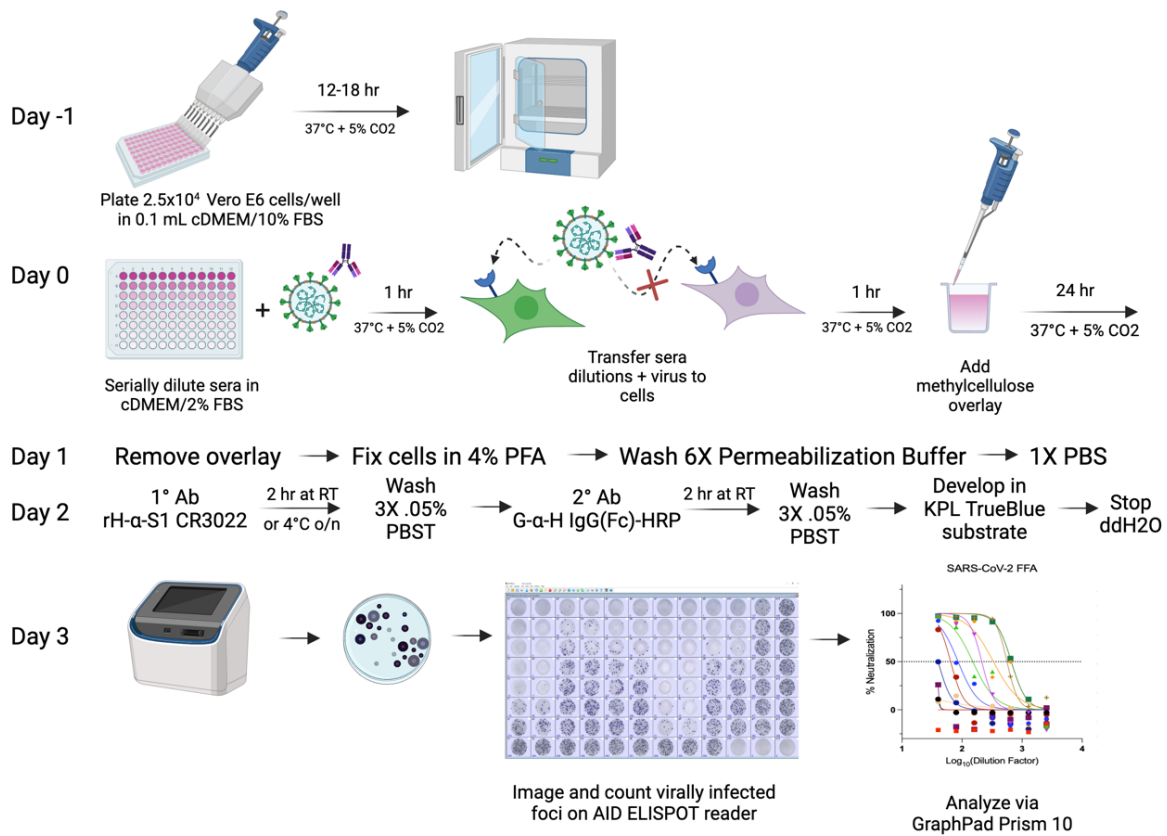


Figure 6. Focus Reduction Neutralization Test (FRNT) methodology. Graphical representation of methods required for FRNT or FFA experiments. On the day prior to infection (Day -1), Vero-E6 (REF ATCC) cells must be plated at a density of 2.5×10^4 cells/well in 0.1 mL of cDMEM containing 10% FBS. On the day of infection (Day 0), serum is serially diluted in duplicate wells of a 96-well V-bottom plate in infection medium (See Appendix C for protocol and reagents). In the BSL-3 facility, virus is added to diluted sera and incubated for one hour at 37°C/5% CO₂ to allow for antibody binding. After one hour, virus and sera are transferred to Vero-E6 cells, then incubated for another hour at 37°C/5% CO₂ to allow for initiation of infection. All wells are then overlay with equivalent volumes of 2% methylcellulose in 2X minimal essential medium (MEM) containing 4% FBS. After methylcellulose overlay is applied, plates are incubated at 37°C/5% CO₂ for 24 hours. Following incubation (Day 1), overlay is aspirated, and cells with virus are fixed in 4% paraformaldehyde (PFA) for 20 minutes at room temperature. All plates are washed six times in permeabilization buffer (See Appendix C), covered in PBS, and thoroughly decontaminated prior to removal from BSL-3 facilities. Plates are then transferred to a BSL-2 laboratory for immunostaining of virally infected cells. On multi-infection weeks, we applied primary antibody on the evening of Day 1 and incubated overnight at 4°C. On Day 2, fixed cells are probed with secondary antibody, washed, and developed with KPL TrueBlue substrate for 15 minutes at room temperature.

Plates are stopped in deionized water, let dry by inverting on paper towel, and stored away from light. On Day 3, dry plates are imaged on an AID ELISPOT reader for quantification of virally infected foci per well. Data are exported to Microsoft Excel and transferred to GraphPad Prism v10 for further analysis. A maximum of five donors per plate (and one positive and negative control) can be included. A maximum of four plates per (20 donors total) were allowed per infection. In ideal circumstances, it is possible to perform two infections per week (8 plates, 40 donors total).

The first therapeutic monoclonal antibody (mAb), Bamlanivimab was issued EUA on November 9th of 2020 (subsequently revoked),⁶¹ just days after the US broke records with 100,000 new cases within 24 hours.³⁶ Mid-November, Moderna SARS-CoV-2 mRNA vaccine, mRNA-1273, was reported to be 95.4% effective,⁶² per their phase III clinical data.⁶³ Two days later, Pfizer-BioNTech announced the 95% efficacy of their mRNA vaccine, BNT162b2.^{64,65} One month later, by mid-December of 2020, both vaccines had been issued EUA and were preparing for distribution to the US population.⁶⁶ While this was undoubtedly ill-perceived as an unusually brief amount of time for safe and effective vaccine development by the American public, it is important to note the profoundly rich history in molecular biology and viral immunology that precedes the development of mRNA-1273 and BNT162b2; a vast majority of which, outside the scope of this dissertation.

mRNA vaccines – prelude and present-day status

Earlier in 2019, prior to the SARS-CoV-2 pandemic, Moderna published data demonstrating phase I clinical trial of two influenza mRNA vaccine candidates.⁶⁷ Prior to that, in 2017 as a response to the Zika outbreaks in Brazil in 2015-2016,⁶⁸ a DNA-based Zika vaccine candidate entered phase-I clinical trials in August 2016 at NIAID,⁶⁹ was

optimized, and entered phase-II in March of 2017.⁷⁰ For many years prior to DNA and mRNA vaccination, recombinant surface antigen (protein) vaccines were used as an alternative option for immunocompromised individuals, as many live-attenuated vaccines can be replication competent or may contain infectious material.^{71,72} Recombinant antigen vaccines were first used in 1986 when Merck commercialized a recombinant hepatitis B surface-antigen subunit vaccine made using recombinant DNA technology,⁷³ and have become increasingly used since.^{74,75} Additional examples of recombinant vaccines for infectious disease includes: Lyme disease, Varicella Zoster virus/Shingles, human papilloma virus, malaria, influenza A and B, hepatitis E, and most recently, SARS-CoV-2.⁷⁵

Vaccines developed specifically for SARS-CoV-2 come in many forms. Most notably, the mRNA vaccines developed by Moderna and Pfizer, mRNA-1273 and BNT162b2, respectively, although many candidates were evaluated in early trials.⁷⁶ Pseudotyped viral vector vaccines use an unrelated virus to deliver SARS-CoV-2 genetic material to host cells, such as Ad26.COV2.S, an adenovirus vector-based vaccine developed by Johnson and Johnson,⁷⁷ and ChAdOx1-S adenoviral vector-based vaccine developed by AstraZeneca/Oxford.⁷⁸ Several recombinant protein vaccines using full-length spike protein or spike receptor binding domain (RBD) were also developed.⁷⁹ Notably, a recombinant stabilized spike-protein vaccine, Novavax,⁸⁰ in addition to numerous other novel vaccine platforms that were developed during this mid- to late-2020 time period.⁸¹

As our NAb LFA clinical agreement and validation studies were nearing completion at the end of 2020 (See Appendix B, Clinical Agreement and Validation),

convalescent plasma had become controversial and near obsolete after the development of neutralizing monoclonal antibody therapies. After mRNA-1273 and BNT162b2 were issued EUA by FDA, vaccine distribution began in the final weeks of December 2020.³⁶ Although we intended our rapid NAb LFA to be used as a tool for blood centers to evaluate CCP, we anticipated that it could also be used to assess NAb responses in vaccine recipients. In the US, the first 50 million doses of COVID-19 mRNA vaccine were administered by February of 2021, and the first 100 million doses by March 2021.³⁶ However, while many people in the US waited in line for their chance at vaccination, SARS-CoV-2 variant B.1.617.2 (Delta) emerged, expanded, became the dominant variant in circulation in early July of 2021, peaking in early September, 2021.⁸²

We conducted an 18-month longitudinal study of COVID-19 mRNA vaccine recipients which measured vaccine-induced NAb levels in more than 500 individuals. Study participants were tested prior to and after first, second, and third vaccine doses. All subjects included within the formal analyses presented in this dissertation were immunized with mRNA-1273 (Moderna) or BNT162b2 (Pfizer) vaccines. If subjects were clinically diagnosed with COVID-19 (natural infection), the data from that subject were excluded thereafter, for the remainder of the mRNA vaccine study.

Our longitudinal study (Chapter IV) identified three distinct NAb response groups that exhibited strong, moderate, and poorly neutralizing antibody responses following COVID-19 mRNA vaccination. These groups are hereinafter referred to as vaccine strong responders (VSRs), moderate (VMRs), and poor responders (VPRs) (**Figure 7**). Following a two-dose mRNA vaccination regimen, VSRs generated the highest NAb titers and maintained these titers longer than VMRs. VMRs initially mounted a high titer

NAb response, however, their titers waned more rapidly than VSRs. Most VPRs developed only low titer NAb responses, if any, typically demonstrating less than 50% neutralization (<1:160 NAb titer). In December of 2021, we submitted for publication an article demonstrating that some of the individuals categorized as VPRs after a two-dose mRNA vaccine regimen could be rescued by a third mRNA vaccine dose, regardless of vaccine manufacturer (Chapter III). Individuals for whom vaccine-induced NAb failed to exceed 50% neutralization after both second and third doses, and/or NAb declined below 50% neutralization \leq three months post-3rd vaccination dose, were categorized as VPRs in all subsequent analyses.

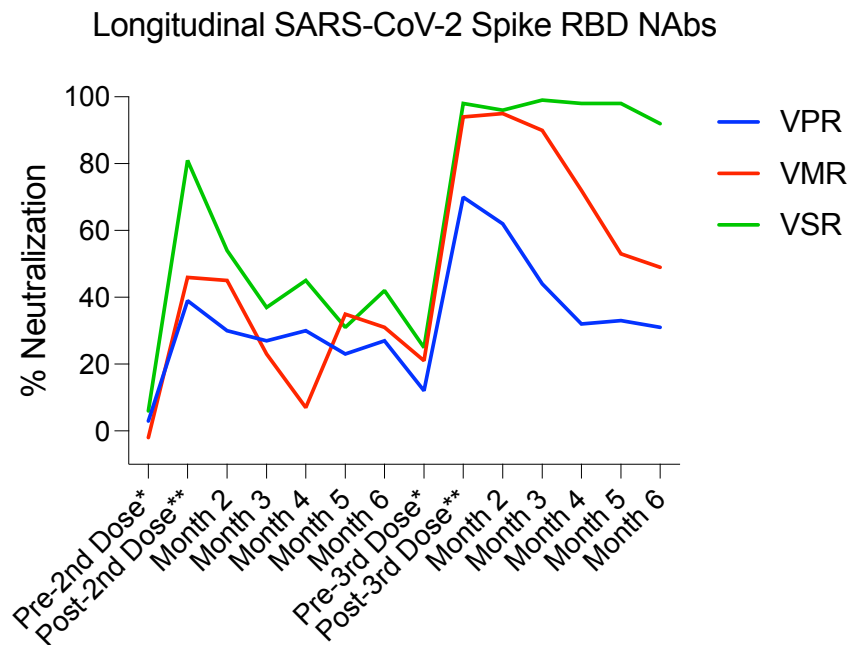


Figure 7. Longitudinal SARS-CoV-2 NAb quantitation in VPR, VMR, and VSR groups. Data are represented as mean percent neutralization over time, for each respective group. Blue line denotes vaccine poor responders (VPRs), red line denotes vaccine moderate responders (VMRs), and green line denotes vaccine strong responders (VSRs). Timepoints include pre-2nd dose, post-2nd dose, and months 2-6 following 2nd dose. The same timepoints were used for data collection and analysis following 3rd dose. *Pre-2nd and pre-3rd dose timepoint data were collected \leq 7 days prior to vaccination

dose. ** Post-2nd and post-3rd dose timepoint data were collected 2-4 weeks after vaccination dose. Data used to generate this graph were selected only from VPR ($n=11$), VMR ($n=5$), and VSR ($n=7$) individuals included in subsequent analyses (Chapter VI).

Throughout the entirety of our longitudinal study, as illustrated by the publications described in Chapters II—IV, there remained a small population of otherwise healthy individuals (independent of sex and age), that failed to generate high titer mRNA-vaccine induced NAb; true VPRs. We first questioned if spike-specific CD4⁺ and CD8⁺ T cell responses were intact in these individuals, and if so, was there evidence of compensatory activation in either VPR T cell compartment, as compared to VMRs and VSRs? We hypothesized that discordant T cell abundance and activation would be evident between groups, in CD4⁺ and/or CD8⁺ T cell compartments following 24-hour stimulation with spike-peptide megapools (Chapter VI).

The culminating work of this dissertation aimed to investigate T cell responses in individuals with impaired NAb responses to SARS-CoV-2 mRNA vaccination, relative to those with strong NAb responses. Using activation induced marker (AIM) assays and multicolor flow cytometry, we quantified SARS-CoV-2 specific CD4⁺ and CD8⁺ T cell responses in VPRs, VMRs, and VSRs. Additionally, we compared T cell responses of our cohort to naturally infected individuals (NIs) and normal donors (NDs). We also sought to investigate T follicular helper cells (Tfh) within these NAb response groups, as Tfh cells are known helpers in the overarching antibody response to immunization.⁸³ We hypothesized that VPRs could be identified by discordant frequencies of activated CD4⁺

and CD8⁺ T cells, as well as frequency of CD4⁺ Tfh cells by phenotype, in comparison to VMRs and VSRs.

Finally, Chapter VII, entitled “*Discussion*” will discuss broader impacts and potential implications of the findings presented in Chapters II-VI, as well as remaining questions and future experiments elicited by the project that may be addressed should a curious lab mate find inspiration in this dissertation following my departure.

CHAPTER II

DEVELOPMENT OF A RAPID POINT-OF-CARE TEST THAT MEASURES NEUTRALIZING ANTIBODIES TO SARS-COV-2

Reprinted with permission from Elsevier publishers.
Originally published in
Journal of Clinical Virology, Dec. 2021, vol. 145, issue 1.

Douglas F. Lake, Alexa J. Roeder, Erin J. Kaleta, Paniz Jasbi, Kirsten M. Pfeffer, Calvin Koelbel, Sivakumar Periasamy, Natalia Kuzmina, Alexander Bukreyev, Thomas E. Grys, Liang Wu, John R. Mills, Kathrine McAulay, Maria Gonzalez-Moa, Alim Seit-Nebi, and Sergei S. Svarovsky

Abstract

Background: After receiving a COVID-19 vaccine, most recipients want to know if they are protected from infection and for how long. Since neutralizing antibodies are a correlate of protection, we developed a lateral flow assay (LFA) that measures levels of neutralizing antibodies from a drop of blood. The LFA is based on the principle that neutralizing antibodies block binding of the receptor-binding domain (RBD) to angiotensin-converting enzyme 2 (ACE2). *Methods:* The ability of the LFA was assessed to correctly measure neutralization of sera, plasma or whole blood from patients with COVID-19 using SARS-CoV-2 microneutralization assays. We also determined if the LFA distinguished patients with seasonal respiratory viruses from patients with COVID-19. To demonstrate the usefulness of the LFA, we tested previously infected and non-infected COVID-19 vaccine recipients at baseline and after first and second vaccine doses. *Results:* The LFA compared favorably with SARS-CoV-2 microneutralization

assays with an area under the ROC curve of 98%. Sera obtained from patients with seasonal coronaviruses did not show neutralizing activity in the LFA. After a single mRNA vaccine dose, 87% of previously infected individuals demonstrated high levels of neutralizing antibodies. However, if individuals were not previously infected, only 24% demonstrated high levels of neutralizing antibodies after one vaccine dose. A second dose boosted neutralizing antibody levels just 8% higher in previously infected individuals, but over 63% higher in non-infected individuals. *Conclusions:* A rapid, semi-quantitative, highly portable and inexpensive neutralizing antibody test might be useful for monitoring rise and fall in vaccine-induced neutralizing antibodies to COVID-19.

Introduction

Severe Acute Respiratory Syndrome Coronavirus-2 (SARS-CoV-2) causes COVID-19 and originated in Wuhan, China in December 2019.^{84,85,86} Vaccines continue to be tested^{65,87} with the goal of preventing COVID-19 via induction of neutralizing antibodies (NAbs) and anti-viral T cells. Vaccine trials show that RNA vaccines elicit protective immunity, but durability of natural and vaccine-induced immunity is not fully known.⁸⁷ Several groups reported that up to one-third of serum samples from individuals who recovered from COVID-19 do not neutralize SARS-CoV-2.^{88,89,52} Whether previously infected or vaccinated, it is informative for individuals to learn if they generated high levels of NAbs so that they can resume normal activities without fear of re-infection and transmitting the virus.^{90,91,92}

Viral neutralization assays measure antibodies that block infection of host cells. The gold standard of neutralization for SARS-CoV-2 measures reduction of viral plaques

or foci in microneutralization assays. These assays are slow, laborious, require highly trained personnel and a BSL3 facility. Another challenge is that neutralization assays require careful titration of virus and depend on host cells for infection, both of which add variability to the assay. These limitations prevent use of SARS-CoV- 2 neutralization assays for clinical applications.

SARS-CoV-2 uses receptor binding domain (RBD) on spike protein to bind angiotensin converting enzyme 2 (ACE2) on host cells; RBD appears to be the principal neutralizing domain.^{93,94} Using this knowledge, we developed a lateral flow assay (LFA) that measures levels of NAbS which block RBD from binding to ACE2. Other groups have developed RBD-ACE2-based competition ELISAs,⁹⁵ but none have developed a rapid, highly portable, semi-quantitative test that can easily be incorporated into clinical settings or research studies where traditional laboratory or neutralization tests are not practical.

Materials and Methods

Human subjects and samples

Serum and finger-stick blood samples were collected for this study under an Arizona State University institutional review board (IRB) approved protocol #0601000548 and Mayo Clinic IRB protocol #20-004544. Serum samples obtained from excess clinical samples at Mayo Clinic were left over from normal workflow. COVID-19 samples ranged from 3 to 84 days post PCR positive result.

Twenty-seven control serum samples from patients with non-COVID- 19 respiratory illnesses as determined by the FilmArray Respiratory Panel 2 (Biofire

Diagnostics) were collected from patients from 2/14/17 – 4/6/20 as part of routine clinical workflow. All residual clinical samples were stored at 2–8 °C for up to 7 days, and frozen at -80°C thereafter.

SARS-CoV-2 microneutralization assay

A microneutralization assay was performed using a recombinant SARS-CoV-2 expressing mNeonGreen (SARS-CoV-2 ng) as previously described.⁹⁶ Inhibitory concentrations for which 50% of virus is neutralized by serum antibodies (IC₅₀ values) were obtained on a set of 38 COVID-19 sera. Sixty µL aliquots of SARS-CoV-2 ng were pre-incubated for 1 h in 5% CO₂ at 37 °C with 60 µL 2-fold serum dilutions in cell culture media, and 100 µL were inoculated onto Vero-E6 monolayers in black polystyrene 96-well plates with clear bottoms (Corning) in duplicate. The final amount of the virus was 200 PFU/well, the starting serum dilution was 1:20 and the end dilution was 1:1280 unless an IC₅₀ was not reached in which case serum was diluted to 1:10, 240. Cells were maintained in Minimal Essential Medium (ThermoFisher Scientific) supplemented by 2% FBS (HyClone) and 0.1% gentamycin in 5% CO₂ at 37 °C. After 2 days of incubation, fluorescence intensity of infected cells was measured at 488 nm using a Synergy 2 Cell Imaging Reader (Biotek). Signal was normalized to virus alone with no serum added and reported as percent neutralization. IC₅₀ was calculated with GraphPad Prism 6.0 software. Work was performed in a BSL-3 biocontainment laboratory of the University of Texas Medical Branch, Galveston, TX.

Serologic antibody assay

The Ortho Vitros Anti-SARS-CoV-2 IgG test (Ortho Vitros test) was performed on an Ortho Clinical Diagnostics Vitros 3600 Immunodiagnosics System at the Mayo Clinic. This assay is approved for clinical testing under FDA Emergency Use Authorization to qualitatively detect antibody to the S1 subunit of SARS-CoV-2 spike protein. Results are reported as reactive ($S/CO \geq 1.0$) or nonreactive ($S/CO < 1.0$). Specimens were tested within 7 days of collection and stored at 2–8 °C. The same 38 serum samples were run in the Ortho Vitros test, microneutralization assay, and the LFA.

Lateral flow neutralizing antibody assay

The Lateral Flow NAb assay was developed to measure levels of antibodies that compete with ACE2 for binding to RBD. The LFA single port cassette (Empowered Diagnostics) contains a test strip composed of a sample pad, blood filter, conjugate pad, nitrocellulose membrane striped with test and control lines, and an absorbent pad (Axim Biotechnologies Inc). The LFA also contains a control mouse antibody conjugated to red gold nanospheres and corresponding anti-mouse IgG striped at the control line.

LFAs were run at room temperature on a flat surface for 10 min prior to reading results. To perform the test, 6.7 μL of serum or 10 μL whole blood were added to the sample port followed by 60 μL of chase buffer. After 10 min, densities of both test and control lines were recorded in an Detekt RDS-2500 density reader.

The test leverages the interaction between RBD-conjugated green-gold nanoshells (Nanocomposix) that bind ACE2 at the test line when RBD-neutralizing antibodies

(RBD-NAbs) are absent or low. Test line density is inversely proportional to RBD-NAbs present within the sample. As a semi-quantitative test, the results of the LFA can be interpreted using a scorecard or a densitometer. A red line across from the “C” indicates that the test ran properly. An absent or faint test line indicates high levels of RBD-NAbs, whereas a dark test line suggests low or lack of RBD-NAbs.

Precision testing was performed using sera from one highly, and one non-neutralizing donor in replicates of 10. Density values were recorded as above and %CVs calculated using the formula: (Standard Deviation/ Mean) * 100%.

Data analysis

Pearson’s correlation (r) was conducted to assess the strength and significance of associations between the LFA, the Ortho Vitros test and IC₅₀ values. Regression analysis using IC₅₀ values evaluated consistency while Bland-Altman plots assessed agreement and bias.^{97,98} Correlation analysis was conducted using IBM SPSS. For two-group analysis, IC₅₀ values corresponding to >240 were categorized as titer of $\geq 1:320$ (neutralizing), whereas IC₅₀ values ≤ 240 were categorized as $\leq 1:160$ (low/non-neutralizing). Receiver operating characteristic (ROC) analysis was performed to assess accuracy, sensitivity, and specificity of the LFA and Ortho Vitros tests in assessing neutralization; optimal cutoffs for each method were established to maximize area under curve (AUC).^{99,100} ROC analysis was conducted using R language in the RStudio environment (version 3.6.2; RStudio PBC). All analyses were conducted using raw values; data were not normalized, transformed, or scaled.

Results

As shown at the bottom in **Figure 8A**, serum containing high levels of NAb results in a weak or ghost test line because NAb bind RBD on green-gold beads, preventing RBD from binding to the ACE2 receptor at the test line. Serum with low levels of NAb results in a strong test line because little to no antibodies prevent RBD on beads from binding to ACE2. **Figure 8B** demonstrates results of the test using COVID-19 sera with different levels of NAb.

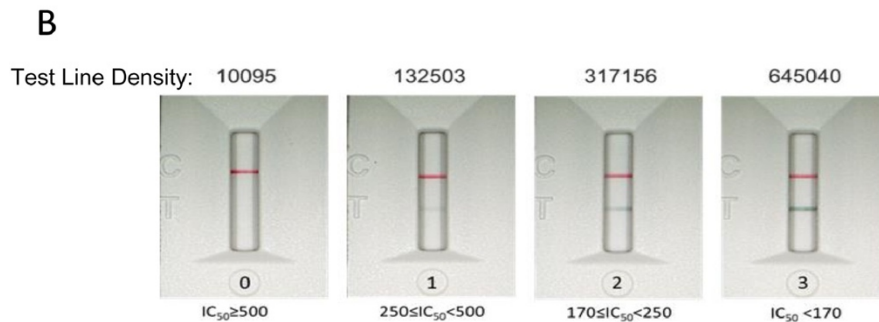
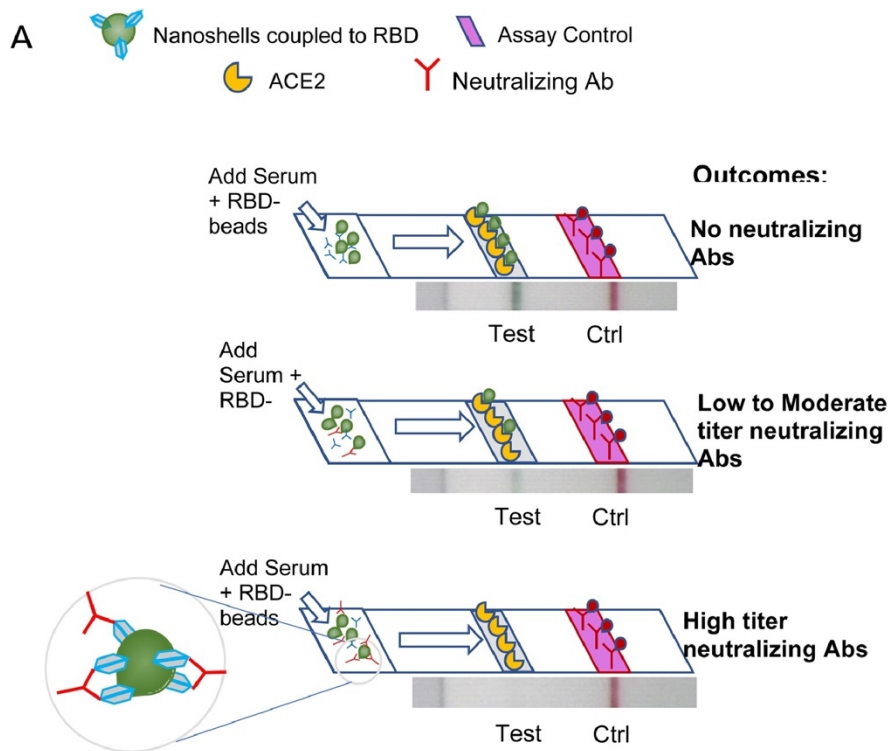


Figure 8. Principles of SARS-CoV-2 NAb LFA. (A) Schematic of SARS-CoV-2 Neutralization LFA. Below each graphic is a representative image of a lateral flow strip

demonstrating actual line density. Addition of non-COVID-19-immune serum or plasma (*top*) does not block binding of RBD-beads (green particles) to ACE2 resulting in the RBD-bead–ACE2 complex creating a visible line. Addition of patient serum with moderate titer NAbs to the sample pad creates a weak line (*middle*). Addition of patient serum with high titer NAbs ($> 1:640$) blocks binding of RBD-beads to ACE2 such that no line is observed at the test location on the strip (*bottom*). Red control line represents capture of a mouse monoclonal antibody coupled to red beads. **(B)** Scorecard for measuring levels of NAbs. Red control line across from the “C” on the cassette indicates that the test ran properly and the green test line across from the “T” can be used to measure the ability of plasma or serum to block RBD on gold nanoshells from binding to ACE2. **(0)** represents patient serum producing a visually non-existent line with density units of 10,095 and an $IC_{50} > 500$ ($IC_{50} = 1151$); **(1)** represents patient serum with a line density of 132,503 and an IC_{50} of 396; **(2)** represents patient serum with a line density of 317,156 and an IC_{50} of 243; **(3)** represents patient serum with a line density of 645,040 and an IC_{50} of 96.

To support the application of the LFA to measure NAb levels to SARS-CoV-2, we tested 38 serum samples that were assigned IC_{50} values in a SARS-CoV-2 microneutralization assay.⁹⁶ The experiment was performed in a blinded manner such that personnel running either the LFA or the microneutralization assay did not know the results of the comparator test. When line densities from the LFA were plotted against IC_{50} values determined in the microneutralization assay, serum samples with strong neutralization activity demonstrated low line densities; this indicates that NAbs inhibited RBD from binding to ACE2 (**Figure 9**).

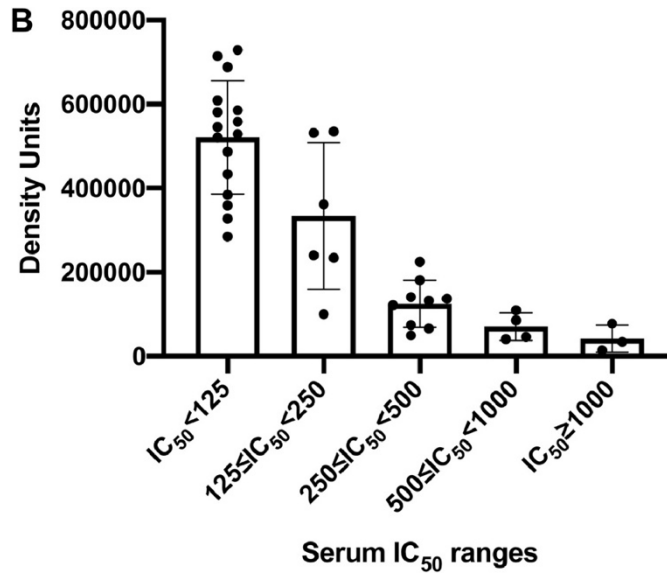


Figure 9. RBD-ACE2 competition LFA density and IC₅₀ value comparison. LFA density value and IC₅₀ value comparison determined in a SARS-CoV-2 microneutralization assay on 38 samples (collected 3 to 90 days after PCR positive result). Ranges of IC₅₀ values are shown on the X-axis plotted against LFA line density units on the Y-axis.

Next, we determined if the LFA detected neutralization activity in serum samples collected from patients with other PCR-confirmed respiratory viruses including seasonal coronaviruses (**Figure 10A**) and for serum samples collected prior to December 2019 (**Figure 10B**). Neither seasonal respiratory virus sera, nor pre-December 2019 samples showed neutralizing activity.

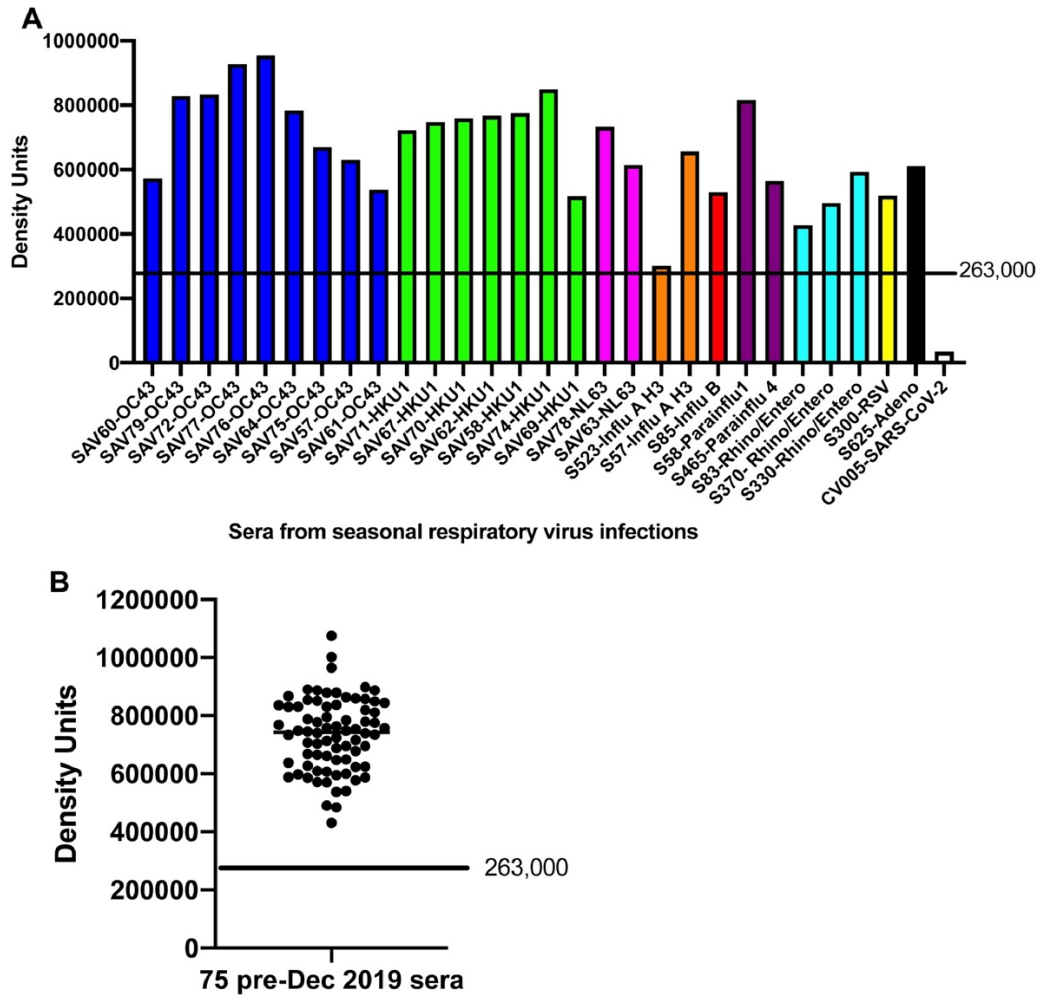


Figure 10. Cross-reactivity evaluation using seasonal respiratory virus convalescent sera. A) Serum samples collected with PCR-confirmed diagnosis of seasonal respiratory viruses (Coronavirus OC43, blue; Coronavirus HKU-1, green; Coronavirus NL-63, pink; influenza A, orange, influenza B, red; parainfluenza, purple; rhinovirus, teal; respiratory syncycial virus, yellow; and adenovirus, black) were run on the LFA as described in Methods. A positive control serum from a convalescent COVID- 19 patient is shown on the far right of the bar graph in white. **B)** Serum samples collected pre-December 2019. Cutoff value of 263,000 density units was calculated based on receiver operating characteristic curves (see Fig. 13).

We then compared both the Ortho Vitros test and our LFA to sera with IC_{50} values determined in the SARS-CoV-2 microneutralization assay using 38 COVID-19 sera. To assess agreement between our LFA and the Ortho Vitros test, density units from the LFA and values from the Ortho test were regressed onto IC_{50} values (**Figure 11**).

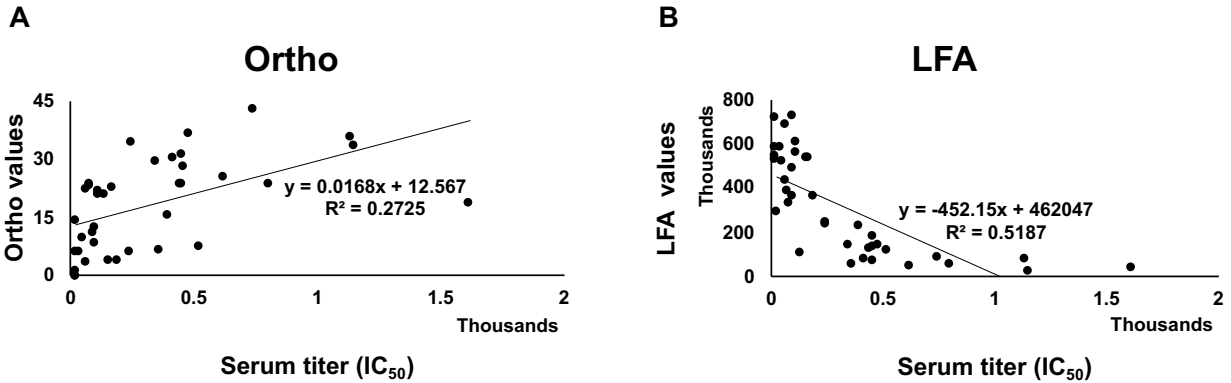


Figure 11. Regression analyses of serum NAb titers. (A) Ortho Vitros SARS-CoV-2 IgG test and serum titer (IC₅₀) **(B)** LFA values and serum titer (IC₅₀). Regression plots show explained variance (R^2) between compared methods. Thirty-eight samples were tested.

LFA values accounted for roughly 52% of observed variance in IC₅₀ values, while the Ortho Vitros test accounted for approximately 27% of IC₅₀ variance. LFA showed significant negative correlation with IC₅₀ values ($r = -0.720$, $p < 0.001$), while the Ortho Vitros test values showed a significant positive correlation to IC₅₀ values ($r = 0.522$, $p = 0.001$). Additionally, the LFA and Ortho Vitros test values correlated with each other ($r = -0.572$, $p < 0.001$).

To evaluate bias, mean differences and 95% confidence intervals (CIs) were calculated and plotted alongside limits of agreement (**Figure 12**). Both LFA and Ortho Vitros test values showed strong agreement with titer, although the Ortho Vitros test showed a tendency to underestimate neutralizing capacity while the LFA method showed no bias.

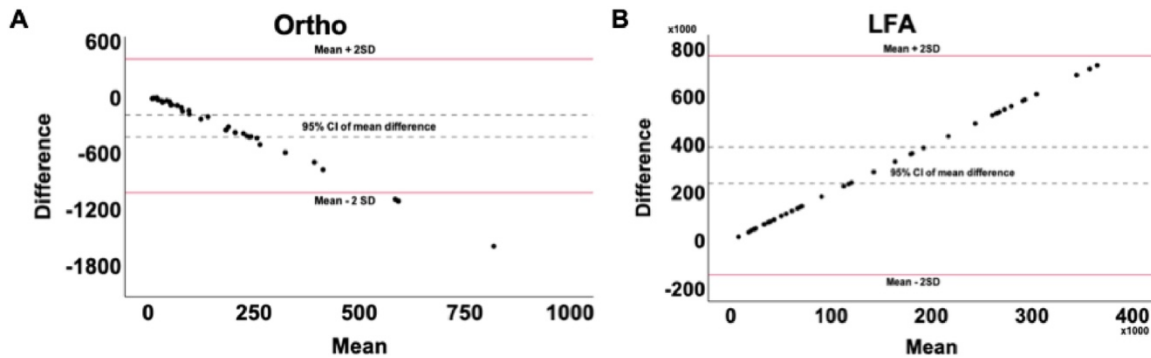


Figure 12. Bland-Altman analyses of Ortho Vitros and NAb LFA. Bland-Altman plots showing bias (mean difference and 95% CI) and computed limits of agreement (mean difference \pm 2SD) between (A) Ortho Vitros Anti- SARS-CoV-2 IgG test and IC₅₀ values and (B) our LFA and IC₅₀ values. Thirty-eight samples were tested.

ROC analysis was performed to assess the ability of the LFA and the Ortho Vitros test to classify low/non-neutralizing (Neg, <1:160), and highly neutralizing groups (\geq 1:320) (**Figure 13**). As shown in **Fig. 13B** and **13D**, the LFA misclassified one non-neutralizing sample (Neg, <1:160) as neutralizing (\geq 1:320) which the Ortho Vitros test also misclassified as neutralizing. The Ortho test also incorrectly classified five additional neutralizing samples as non-neutralizing.

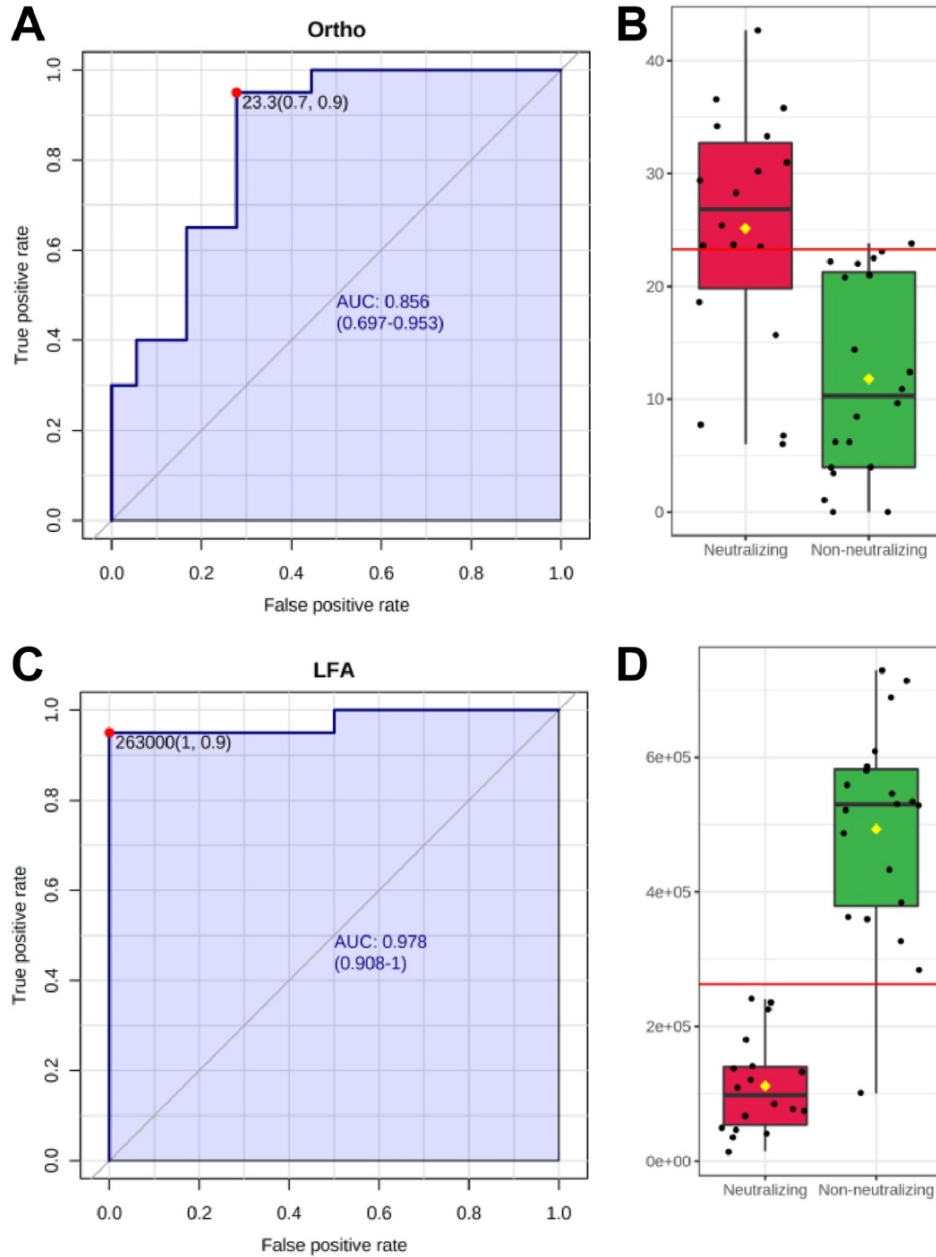


Figure 13. Univariate ROC analyses of Ortho Vitros and NAb LFA. (A) Univariate ROC analysis of Ortho Vitros Anti-SARS-CoV-2 IgG test for discrimination of neutralizing samples ($\geq 1:320$) [AUC: 0.856, 95% CI: 0.697–0.953, sensitivity = 0.9, specificity = 0.7]. **(B)** Box plot of Ortho Vitros Anti-SARS-CoV-2 IgG test values between neutralizing ($\geq 1:320$) and non-neutralizing (Neg—1:160) groups. **(C)** Univariate ROC analysis of LFA for discrimination of neutralizing samples ($\geq 1:320$) [AUC: 0.978, 95% CI: 0.908–1.0, sensitivity = 0.9, specificity = 1.0]. **(D)** Box plot of LFA values between neutralizing ($\geq 1:320$) and non-neutralizing (Neg—1:160) groups.

Our LFA showed high accuracy for classification of neutralizing samples (AUC = 0.978), while the Ortho Vitros test showed modest accuracy (AUC = 0.856). Notably, while both methods showed roughly 90% sensitivity, the Ortho Vitros test showed only 70% specificity. In contrast, the LFA showed perfect specificity (100%) in this analysis of 38 samples.

Optimal cutoffs were computed to maximize AUC. For the LFA, density unit values below 263,000 classify samples as neutralizing and correspond to titers $\geq 1:320$. Density values above this LFA cutoff classify samples in the non-neutralizing group. For the Ortho Vitros test, values between 0 and 23.3 were representative of non-neutralizing capacity, whereas values above 23.3 were reflective of the neutralizing group.

Precision studies were performed on replicate samples ($n = 10$) and showed a CV of ~9% from a serum sample in the high neutralizing range and ~6% CV in a serum sample from the low neutralizing range (**Table 1**).

A

Low Neutralizing Range			
10 min	C	T	T/C Ratio at 10 min
1	503764	932173	1.850416068
2	484316	944154	1.949458618
3	509424	902070	1.770764628
4	441318	840951	1.905544301
5	484558	990076	2.043255916
6	472319	906922	1.920147189
7	519936	971429	1.868362645
8	495254	992223	2.00346287
9	467545	816303	1.745934616
10	534262	941643	1.762511652
Average	491269.6	923794.4	1.88198585
STD Dev	25849.98843	55966.17114	0.096780674
%CV	5.26	6.06	5.14

B

High Neutralizing Range			
10 min	C	T	T/C Ratio at 10 min
1	415421	232022	0.558522559
2	404845	286183	0.706895232
3	419873	261146	0.621964261
4	417475	248141	0.594385293
5	409970	263808	0.64348123
6	397812	294120	0.739344213
7	409681	237096	0.578733209
8	412275	242082	0.587185738
9	373751	222959	0.596544223
10	373339	224335	0.600888201
Average	403444.2	251189.2	0.622794416
STD Dev	16097.74032	23457.01668	0.055137744
%CV	3.99	9.34	8.85

Table 1. SARS-CoV-2 NAb LFA precision study using one (A) Low Neutralizing Range serum sample and one (B) High Neutralizing Range serum sample in replicates of ten. Low range neutralization is defined as densities from 370,000 – 800,000. The used for precision analysis was from an individual who recovered from COVID-19 but did not neutralize virus in the microneutralization assay ($IC_{50} < 20$). High neutralization range samples are defined as densities from 10,000 – 369,999. This sample has an IC_{50} of 248.

Since NAb levels may be considered correlates of protection, we tested sera from RNA vaccine recipients (mRNA-1273 and BNT162b2) in “previously infected” and “not previously infected” individuals using finger-stick blood in the rapid LFA (**Figure 14**). In

previously infected individuals at baseline (within 3 months of PCR-based diagnosis), 38% demonstrated high levels of NAb. After the first vaccine dose, 87% of *previously infected* individuals demonstrated high NAb levels, while only 24% of *not previously infected* individuals developed high levels of NAb. After the second vaccine dose, levels of NAb increased to 95% in the *previously infected* cohort, while NAb levels increased to 87% in the *not previously infected* cohort. This data suggests that a second vaccine dose is important for highest levels of NAb.

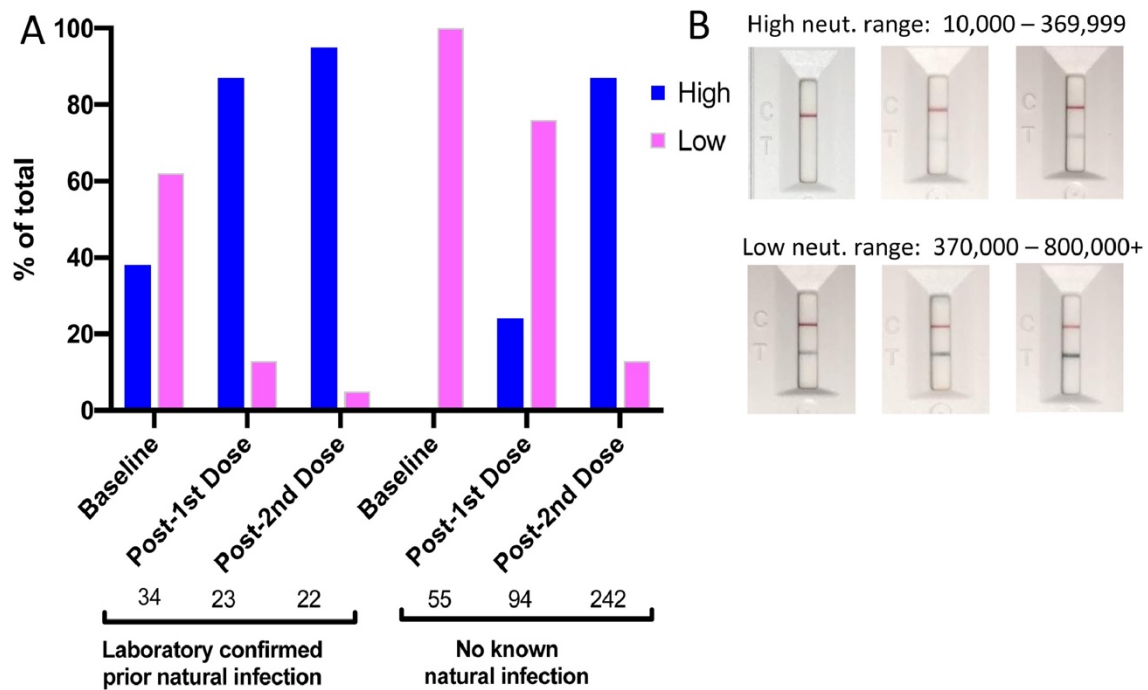


Figure 14. NAb levels in prior infection and vaccine-induced individuals. (A) Baseline indicates within one week of first vaccine dose; Post-1st Dose indicates within one week of 2nd vaccine dose; Post 2nd Dose indicates 10–20 days after 2nd vaccine dose. High and Low indicates density ranges of Test lines shown in (B). Densities were read in a reader as described in Methods. Serum titers that correspond to high range densities are $>1:1280$ to $\geq 1:160$. Serum titers corresponding to low range densities are $<1:160$.

Discussion

We developed a rapid test that measures levels of NAbs in serum and whole blood. As shown in **Figure 9**, the LFA correlates well with serologic titers determined using a SARS-CoV-2 microneutralization assay, especially when serum sample IC_{50} values are >250 . Advantages of the LFA test are that it can be inexpensively and rapidly deployed to determine levels of NAbs in vaccine recipients. Moreover, the test can be used longitudinally to evaluate duration of protective immunity in naturally infected and vaccinated individuals—many more than could ever be evaluated using BSL2 or BSL3-based neutralization assays.

The LFA and Ortho Vitros test showed a significant correlation with each other ($r = -0.572, p < 0.001$), displaying good linear relation ($r = -0.720, p < 0.001$).¹⁰¹ The LFA accounts for 52% of observed IC_{50} variance ($R^2 = -0.5187$), while the Ortho Vitros test accounts for 27% ($R^2 = -0.2725$). Although absolute quantitation demands an excellent coefficient of determination ($R^2 \geq 0.99$),¹⁰² variables with $R^2 \geq 0.5$ are highly predictive in univariate regression models while measures with $R^2 < 0.5$ are recommended for use in multivariate models with complementary measures to increase predictive accuracy.^{103,104} Bland-Altman analysis (**Figure 12**) showed the Ortho Vitros test to be prone to underestimation of IC_{50} values, while the LFA method did not exhibit over- or underestimation bias. Furthermore, across mean values for both methods, the LFA showed discrete differential values while the Ortho Vitros test struggled to differentiate high neutralizing samples.

Using our rapid test to measure NAb in previously infected vaccine recipients and those who were not infected agrees with other studies in BSL3 facilities using serum from venipuncture blood.^{87,105,106,107,108,109} Natural infection may not elicit high levels of NAb,^{88,89,52} but a first dose of vaccine induces high levels of NAb in the majority of recipients similar to 2 doses of vaccine in non-previously infected individuals, suggesting natural infection primes the immune system.¹¹⁰ In naïve individuals, a single dose of vaccine elicits high NAb levels (Titers >1:160) in only 24% of vaccine recipients, leaving 76% of vaccine recipients with titers lower than 1:160 which would not qualify for convalescent plasma donation according to FDA memo of March 9, 2021. After a second vaccine dose, the LFA indicated high levels of NAb in 87% of recipients, identical to levels observed in previously infected individuals after the first vaccine dose. These findings might suggest that a booster (3rd vaccine dose) in non-infected individuals could induce the highest levels of NAb in the most people.

Limitations of the LFA are that it uses only the RBD portion of spike protein. Although the vast majority of reports indicate that the principle neutralizing domain is the RBD portion of spike protein, mAbs have been reported that neutralize SARS-CoV-2 by binding to the N-terminal domain of spike protein.^{111,112} Also, since the spike protein assumes multiple conformations during viral binding and entry,¹¹³ neutralizing epitopes exist on the quaternary structure of spike.¹¹² Although RBDs on the nanoparticles may associate, it is not known if they assume a native conformation.

Other limitations are the binary nature of this data analysis (high and low neutralizing) of a continuous assay. NAb levels should be evaluated longitudinally to assess rise and fall in NAb levels; this rapid test is well-suited for that role. Another

limitation is that the LFA does not differentiate high affinity anti-RBD NAbs from an abundance of lower affinity anti-RBD NAbs.

This test may prove useful in monitoring COVID-19 vaccine recipients as a correlate of protection. It would be logistically difficult to obtain a tube of blood from every vaccine recipient for BSL3 work. However, since this LFA requires only a drop of blood, individual use of this test might lead to more comprehensive longitudinal monitoring of protective humoral immunity and indicate when boosters might be required.

CHAPTER III

THIRD COVID-19 VACCINE DOSE BOOSTS NEUTRALIZING ANTIBODIES IN POOR RESPONDERS

Reprinted with permission from Springer Nature publishers.
Originally published in
Nature Communications Medicine, July. 2022, vol. 2, article 89.

Douglas F. Lake, Alexa J. Roeder, Maria J. Gonzalez-Moa, Megan Koehler, Erin Kaleta,
Paniz Jasbi, John Vanderhoof, Davis McKechnie, Jack Forman, Baylee A. Edwards,
Alim Seit-Nebi, and Sergei Svarovsky

Abstract

Background: While evaluating COVID-19 vaccine responses using a rapid neutralizing antibody (NAb) test, we observed that 25% of mRNA vaccine recipients did not neutralize >50%. We termed this group “vaccine poor responders” (VPRs). The objective of this study was to determine if individuals who neutralized <50% would remain VPRs, or if a third dose would elicit high levels of NAbs.

Methods: 269 healthy individuals ranging in age from 19 to 80 (Average age = 51; 165 females and 104 males) who received either BNT162b2 (Pfizer) or mRNA-1273 (Moderna) vaccines were evaluated. NAb levels were measured: (i) 2–4 weeks after a second vaccine dose, (ii) 2–4 months after the second dose, (iii) within 1–2 weeks prior to a third dose and (iv) 2–4 weeks after a third mRNA vaccine dose.

Results: Analysis of vaccine recipients reveals that 25% did not neutralize above 50% (Median neutralization = 21%, titers <1:80) within a month after their second dose.

Twenty-three of these VPRs obtained a third dose of either BNT162b2 or mRNA-1273

vaccine 1–8 months (average = 5 months) after their second dose. Within a month after their third dose, VPRs show an average 5.4-fold increase in NAb levels (range: 46–99%).

Conclusions: The results suggest that VPRs are not permanently poor responders; they can generate high NAb levels with an additional vaccine dose. Although it is not known what levels of NAbs protect from infection or disease, those in high-risk professions may wish to keep peripheral NAb levels high, limiting infection, and potential transmission.

Introduction

COVID-19 mRNA vaccines prevent serious clinical disease requiring hospitalization in ~95% of vaccine recipients. This suggests that 5% of vaccinated individuals remain susceptible to potentially severe disease.^{63,65} If 300 million people receive two doses of the COVID-19 mRNA vaccines, then approximately 15 million people may not be fully protected. Although T cells are important in anti-viral immunity, their activity is difficult to rapidly evaluate at scale. Furthermore, if T cells are engaged, the host is already infected. After natural infection with SARS-CoV-2 or vaccination against COVID-19, anti-viral antibodies are generated by the host. Antibodies of primary importance are neutralizing antibodies (NAbs) because they prevent infection. However, non-neutralizing antibodies may also play an important role in the host's humoral response.^{114,115} NAbs block the spike protein on SARS-CoV-2 from binding to the host cell receptor, angiotensin converting enzyme 2 (ACE2). In particular, the portion of the spike protein that binds to ACE2 is the receptor binding domain (RBD)^{93,94} and there have been many reports of natural, vaccine-induced^{116,117,118,119} and therapeutic antibodies¹²⁰ that neutralize the virus by binding to the RBD.

After 2 doses of either BNT162b2 or mRNA-1273, antibodies to spike protein and neutralizing antibodies have been quantified in vaccine recipients.^{63,65,105,107} Durability of those responses has been reported.^{87,109} Although NAb titers as a correlate of protection remain undefined and are complicated by evolving variants, titers that provide protection from disease likely differ from titers that prevent infection. Both are also largely dependent on the dominant variant in circulation. Even when vaccinated, immunosuppressed individuals are at increased risk of infection and disease if exposed.^{121,122} As such, caregivers for high-risk individuals may want to measure or monitor their NAb levels after their last vaccination or natural infection, to lessen the possibility of asymptomatic infection which may result in transmission to vulnerable patient populations. Since the vaccines do not elicit protective immunity in everyone, many vaccine recipients may want to know how well their vaccine induced protective antibodies, and how long they circulate in peripheral blood. NAb levels have been modeled as correlates of protection from infection and/or disease.¹¹⁷ Here we report the results of a study in which NAb levels were measured in finger-stick whole blood from mRNA vaccine recipients at 2–4 weeks and 2–4 months after their second dose, and then again pre- and post-3rd mRNA vaccine dose.

Our results demonstrate 25% percent (n = 67) of 2-dose vaccine recipients' (n = 269) NAb levels show <50% neutralization 2–4 weeks after their second dose and are therefore classified as vaccine poor responders (VPRs). Twenty-three of the 67 VPRs received a third mRNA vaccine as a booster dose. Sixty-five percent of these VPRs received three doses of BNT162b2 (Pfizer), 4% had 3 doses of mRNA-1273 (Moderna), and 30% had 2 doses of BNT162b2 followed by a third dose of mRNA-1273 (booster).

Within a month after receiving a third dose, NAb levels in the 23 VPRs increased an average of 5.4-fold, suggesting the importance of a third dose for high levels of peripheral protection.

Materials and Methods

Rapid test to detect SARS-CoV-2 neutralizing antibody

Since performing neutralization assays with authentic SARS-CoV-2 is time-consuming, expensive and requires high containment facilities with specially trained laboratory personnel, we previously developed a rapid test that semi-quantitatively measures levels of neutralizing antibodies in whole blood or serum. The rapid test utilizes lateral flow technology and is based on the principle that NAbs prevent the receptor binding domain (RBD) on spike protein from binding to ACE2 (**Figure 15**).^{93,94} Interpretation of the test is counter-intuitive: the weaker the test line, the stronger the neutralizing activity. Test and control line densities can be quantified with a lateral flow reader and recorded electronically.

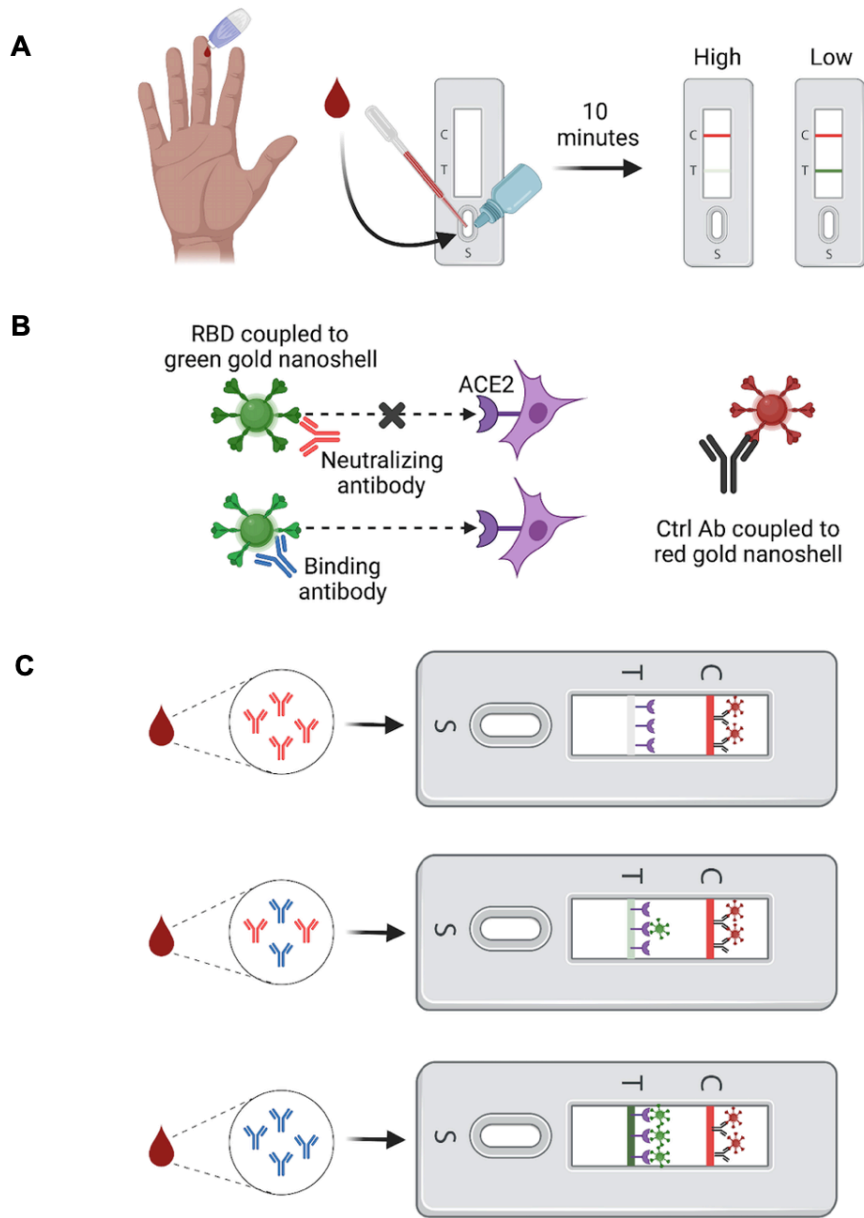


Figure 15. Lateral Flow Assay to Detect SARS-CoV-2 Neutralizing Antibody. Interpretation of the rapid test is counter intuitive. **A)** Methodology overview. Fingerstick blood is transferred to the sample port and followed by two drops chase buffer. Ten minutes later results can be interpreted. Absent or faint test line indicates high NAB levels, while dark or intense test line indicates low/no NABs. **B)** Mechanistic schematic. NABs bind RBD coupled to a green gold nanoshell (GNS) and *prevent* the RBD/ACE2 interaction from occurring. Abs that bind RBD but do not neutralize *allow* the RBD/ACE2 interaction to occur, shown as increasingly dark signal as more RBD-GNS/ACE2 binds at the test line. **C)** Example tests showing highly neutralizing (top), moderately neutralizing (middle), and poorly neutralizing antibodies (bottom) using either

finger-stick whole blood. A monoclonal control antibody coupled to a red-GNS runs laterally with the sample/buffer mixture and binds at the control line, seen as a red line.

Study design and population

Male and female adults ranging in age from 18 to 80 years old were recruited with informed consent to measure their NAb levels using the rapid test after vaccination with either BNT162b2 or mRNA-1273. The study was approved as an observational study by the institutional review board (IRB) at Arizona State University (IRB# 0601000548). In this cohort, no participant ever tested positive by PCR or was diagnosed with COVID-19 prior to the study. NAb levels were measured in all participants 2–4 weeks after a second dose of either BNT162b2 or mRNA-1273 vaccine, then measured 2–4 months after dose 2. In those participants who informed us that they had decided to get a third vaccine dose, NAb levels were measured within 2 weeks of receiving dose 3 of either BNT162b2 or mRNA-1273, and then measured again 2–4 weeks after dose 3.

Ethical approval

All data generated in this study used finger-stick peripheral blood collected under an Arizona State University institutional review board (IRB) approved protocol #0601000548. Subjects were assigned a vaccine study de-identification number (VAC-ID) at the time of enrollment and all subsequent collections were conducted in compliance with the Collaborative Institutional Training Program (CITI) Human Subjects Research (HSR) regulatory guidance.

Assay design and implementation

The LFA cassette contains a test strip composed of a blood filter overlapped with a conjugate pad, nitrocellulose membrane striped with test and control lines, and an absorbent pad to wick excess moisture. Test strips are secured in a plastic cassette that contains a single sample port. Recombinant ACE2-6xHis protein (Axim Biotechnologies, Inc) is striped onto the nitrocellulose membrane as a test line and an anti-mouse antibody is striped onto nitrocellulose as a control line. Recombinant SARS-CoV-2 Wuhan RBD-6xHis protein (Axim Biotechnologies, Inc) is coupled by carbodiimide chemistry to the surface of 150 nm carboxyl-functionalized gold nanoshells (Nanocomposix Inc). The LFA also contains a control mouse monoclonal antibody (Axim Biotechnologies, Inc) conjugated to the surface of 40 nm carboxyl-functionalized gold nanospheres (Nanocomposix, Inc) and corresponding anti-mouse IgG (Lampire Biological Laboratories) at the control line to ensure the test was performed properly. A mixture of RBD modified gold nanoshells and a mouse IgG-modified gold nanospheres is dried on the conjugate pad. Linearity of the assay was determined by serial dilutions of strongly neutralizing plasma (reciprocal titer 640-1280) into non-neutralizing (negative) plasma. The assay response is linear up to ~8x dilution of neutralizing serum into non-neutralizing serum. At higher dilutions the test signal approaches levels comparable to a negative sample. Limit of quantitation was adjusted to a reciprocal titer of ~40 using a series of NAb-positive samples with titers assigned by live Wuhan virus FRNT assay. The precision of the test was determined by T-line/C-line ratio to be 4.75%, 8.5% and 15% low (high signal), medium and high (low signal) Nab levels, respectively,

with each level run in 20 replicates. Determining NAb levels using the rapid test. To determine NAb titers, 10 μL of finger-stick blood was transferred via micropipette to the sample port in the LFA cassette. After 10–30 s, 60 μL (2 drops) of chase buffer was added to the port. Ten minutes after addition of chase buffer, control and test line densities were quantified using a Detekt RDS-2500 density reader (Detekt, Austin, TX). Higher titers of NAb in blood will cause the test line to be weak or absent because they prevent RBD-gold-nanoshells from binding to ACE2 at the test line, while lower titers of NAb allow RBD-gold nanoshells to bind ACE2 so that a test line is visible. Test line density is inversely proportional to RBD-NAb present within the sample as previously reported¹⁸

Focus reduction neutralization test (FRNT)

To support the application of the rapid test to measure NAb levels to SARS-CoV-2, we correlated LFA test line densities with IC_{50} values obtained in a Focus Reduction Neutralization Test (FRNT) from 38 serum samples.³² Test performance was evaluated using a correlation regression analysis of IC_{50} values and LFA line densities to obtain the equation, $Y = -0.7698 * X + 24.14$ when $X = \log_2 \text{IC}_{50}$ as shown in **Figure 16**.

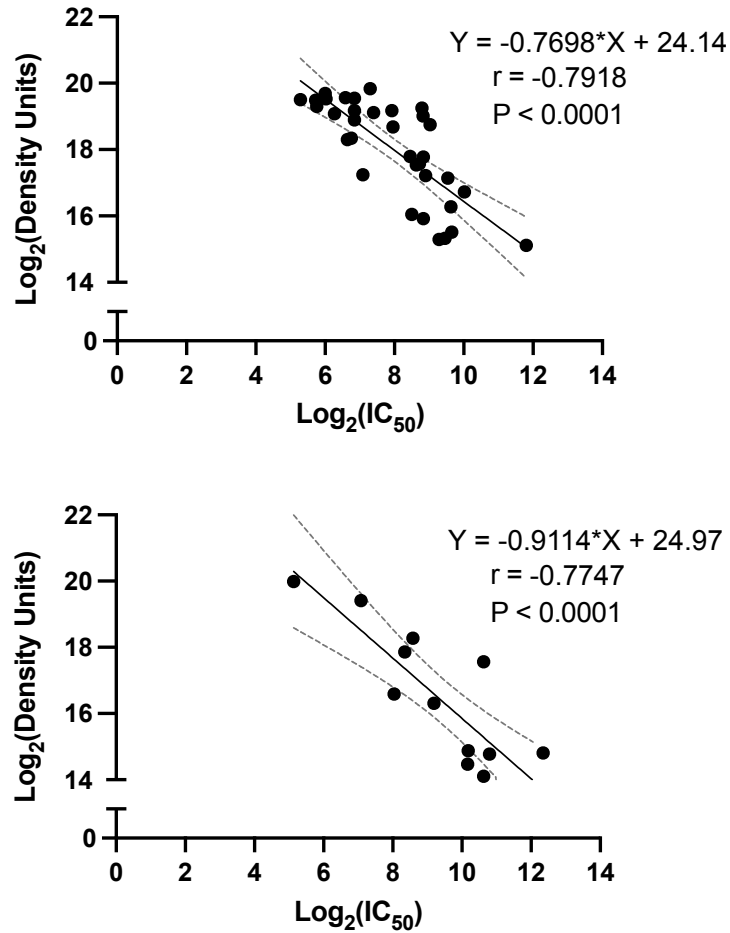


Figure 16. Regression analysis of LFA density and neutralization IC_{50} values. Comparison between LFA density units and IC_{50} values obtained using (top graph) convalescent sera isolated from 36 recovered COVID-19 patients and (bottom graph) mRNA-1273 or BNT162b2 vaccinated sera. Neutralization was tested on LFA using 6 μL serum and a dilution series was performed by authentic SARS-CoV-2 FRNT assay to obtain IC_{50} values. To calculate IC_{50} , data were analyzed in GraphPad Prism 9.0 using methods described by Ferrara and Temperton. Density values and IC_{50} values were Log_2 -transformed and analyzed using a simple linear regression and nonparametric Spearman correlation with two-tailed P value and a 95% confidence interval (CI). Regression analysis with 95% CI boundaries is indicated in solid black and grey dotted lines. Spearman's rho and two-tailed P value are labeled.

Statistical Analyses

Levene's test was used to assess homoscedasticity between groups prior to significance testing (IBM SPSS Statistics for Macintosh, Version 26.0; Armonk, NY). To account for unequal variances resulting from unequal sample sizes, Welch's t test with Benjamini-Hochberg false discovery rate (FDR) correction was performed using Microsoft Excel (Version 16.55; Redmond, WA) to evaluate significant differences in mean neutralization between BNT162b2 (n = 180) and mRNA-1273 (n = 89) 2-4 weeks post-2nd dose. Cohen's d was calculated using Microsoft Excel. Post-hoc power analysis was computed using G*Power 3.1 software¹⁹.

Results

Correlation of test line densities to serum IC₅₀ values

To support the application of the LFA to measure NAb levels to SARS-CoV-2, we previously reported¹⁸ correlation of LFA test line densities with IC₅₀ values obtained in a Focus Reduction Neutralization Test (FRNT). The rapid test accurately and semi quantitatively measures levels of NABs directed against SARS-CoV-2. Serum samples with strong neutralizing activity demonstrate low test line densities while sera with weak neutralizing activity demonstrate high test line densities.

Armed with IC₅₀ values, LFA densities and neutralizing serum titers from the FRNT, we calculated % neutralization as: $1 - (\text{Test Line Density} / \text{Limit of Detection}) * 100\%$. **Table 2** shows percent neutralization ranges that correlate to serum titers, FRNT₅₀ values and test line densities. Percent neutralization was used throughout

the study to measure NAb levels in study participants. **Figure 17** shows actual LFA tests with density values and corresponding IC₅₀ values, NAb titers, and percent neutralization.


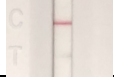
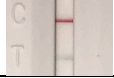
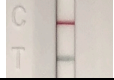
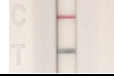
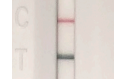
Image of NAb test result	Test line density unit ranges (thousands)	IC ₅₀ ranges	Reciprocal NAb titer ranges	% Neutralization ranges
	10-99	17,530 to 880.54	<1280, ≥640	99 to 90
	100-199	880.53 to 357.847	<640, ≥320	89 to 80
	200-369	357.845 to 160.927	<320, ≥160	79 to 61
	370-599	160.927 to 85.88	<160, ≥80	60 to 36
	600-799	85.88 to 59.102	<80, ≥40	35 to 15
	800-1000	59.101 to 44.23	≤ 40	≤ 15

Table 2. SARS-CoV-2 NAb LFA density unit conversion to IC₅₀, reciprocal NAb titer, and percent neutralization. Correlation of IC₅₀ values from a Focus Reduction Neutralization Test (FRNT) using authentic SARS-CoV-2 with serum titers using 17 PCR-confirmed samples with IC₅₀ values <125, six samples with IC₅₀ values ≥125 and <250, nine samples with IC₅₀ values ≥250 and <500, four samples with IC₅₀ values ≥500 and <1000 and three samples with IC₅₀ values ≥1000. Reciprocal NAb titers were derived using the highest dilution that did not exceed each serum IC₅₀ value. Percent neutralization was calculated using the following formula: 1-(Test sample line density/Limit of Detection)*100% where LoD for non-neutralizing sera for the rapid test was 942,481. Limit of detection (LoD) was calculated based on the method of Armbruster and Pry,¹²³ using a convalescent serum sample containing the lowest detectable concentration of analyte (neutralizing antibodies) still distinguishable from a blank. Due to the competitive format of the LFA, the operand was changed to reflect subtraction from limit of blank (LoB) rather than addition: LoD= limit of blank (LoB) – (1.65* SD_{low conc sample}): LoD=1,047,382- (1.65 * 63,769)= 942,481 Test Line Density Units. A lower LoD was not applicable, as polyclonal antisera was used in this study, rather than an individual Mab. Alternatively, the average line density observed for the top 10 donors who demonstrated the strongest ability to prevent RBD from binding to ACE2 was 20,706.

	VAC-93	VAC-81	VAC-77	VAC-82	VAC-74	VAC-99
TLD	1,007,231	765,297	477,787	295,032	156,481	14,212
IC₅₀	43.8	62.6	115.4	215.9	492.2	11,103.9
NAb Titer	≤ 40	≥40, <80	≥80, <160	≥160, <320	≥320, >640	≥640
% Neut	0	19	49	69	84	99

Figure 17. NAb LFA with Density, IC₅₀, Titer, and Percent Neutralization Values. LFA densitometer images with corresponding Test Line Density (TLD), IC₅₀ value, reciprocal NAb titer, and percent neutralization. TLD is reported as unmodified, discrete values. IC₅₀ values are derived from the regression equation shown in Supplementary Figure S1. Reciprocal NAb titer is derived from IC₅₀, such that titer is equal to the last dilution factor (DF) (DF = 20*2⁻ⁿ) for which IC₅₀ is ≥ the lower threshold range for a given titer. For example, IC₅₀=43.8 is classified as an NAb titer of 40. Further, a hypothetical IC₅₀=158 would classify as NAb titer ≥80 and <160. Percent neutralization was calculated using the equation: 1-(TLD/LoD) when LoD=942,481 as described in Table 1 legend.

Evaluation of COVID-19 mRNA vaccine NAb response

NAb levels were measured using our semi-quantitative rapid test in 269 healthy individuals who ranged in age from 19 to 80 (Average age = 51; 165 females and 104 males) who received 2 doses of either BNT162b2 (Pfizer) or mRNA-1273 (Moderna) vaccines¹⁸. Twenty-three of the 269 were VPRs (neutralized < 50%) and independently received a third dose of either BNT162b2 or mRNA-1273 vaccines. Demographics of the third dose cohort are shown in **Table 3**.

Age / Sex	RT-PCR Results	1 st and 2 nd Dose Vaccine	3 rd Dose Vaccine	Months Post-2 nd Dose, Prior to 3 rd
70-75 / M	Negative [^]	BNT162b2	BNT162b2	1
30-35 / M	Negative [*]	BNT162b2	BNT162b2	7
60-65 / M	Negative [*]	BNT162b2	BNT162b2	8
50-55 / M	N/A	BNT162b2	BNT162b2	5
56-60 / F	Negative [*]	BNT162b2	BNT162b2	6
60-65 / M	Negative [^]	BNT162b2	BNT162b2	7
50-55 / F	Negative [*]	BNT162b2	BNT162b2	7
60-65 / M	N/A	BNT162b2	BNT162b2	6
66-70 / F	Negative [*]	BNT162b2	BNT162b2	6
60-65 / F	Negative [^]	BNT162b2	mRNA-1273	1
56-60 / F	Negative [*]	BNT162b2	BNT162b2	7
70-75 / F	Negative [~]	BNT162b2	BNT162b2	5
70-75 / F	N/A	BNT162b2	BNT162b2	6
76-80 / M	Negative [*]	BNT162b2	BNT162b2	7
70-75 / F	Negative [*]	BNT162b2	mRNA-1273	6
76-80 / F	N/A	BNT162b2	mRNA-1273	6
60-65 / F	Negative [*]	BNT162b2	mRNA-1273	5
66-70 / M	Negative [^]	BNT162b2	BNT162b2	6
40-45 / M	Negative [^]	BNT162b2	mRNA-1273	6
70-75 / M	Negative [^]	mRNA-1273	mRNA-1273	5
50-55 / F	N/A	BNT162b2	mRNA-1273	3
70-75 / F	Negative [*]	BNT162b2	BNT162b2	6
36-40 / F	Negative [*]	BNT162b2	mRNA-1273	4

[^] = TaqPath (Thermo Fisher)

^{*} = Abbott Real Time SARS-CoV-2

[~] = PerkinElmer SARS-CoV-2 Real-Time RT-PCR assay

NA= Not Available; participants denied having COVID-19 or being exposed.

Table 3. Demographic information for 3rd mRNA vaccine dose recipients. Twenty-two individuals received two doses of BNT162b2 and one individual received two mRNA-1273 doses initially. 15 of the 22 individuals that were originally vaccinated with BNT162b2 obtained a 3rd dose of BNT162b2, and 8 received mRNA-1273 (100 μ g) as their 3rd dose. One individual originally vaccinated with mRNA-1273 received a 3rd, 100 μ g dose of mRNA-1273. All participants had either confirmed negative RT-PCR results or no known history of infection prior to enrollment. RT-PCR platform indicated using symbols defined below Table 3. Age ranges are provided to protect the identities of the individuals in the study.

NAb levels in vaccine recipients were measured at: (i) 2–4 weeks after a second vaccine dose, (ii) 2–4 months after the second dose, (iii) within 1–2 weeks prior to a third

dose and (iv) 2–4 weeks after a third mRNA vaccine dose. Several observations were made during this study. Percent neutralization ranged from 0 to 99% 2–4 weeks after a second dose (**Figure 18A**). Although our LFA is a surrogate neutralization test, our results agree with previous findings in which the majority (75%) of vaccine recipients demonstrate NAb levels at $\geq 50\%$ 2–4 weeks after their second dose^{14,15}. Our study also revealed that 25% of vaccine recipients did not neutralize above 50% (Median neutralization = 21%) within a month after their second dose (**Figure 18B**). Twenty-three VPRs ranging in age from 31 to 79 (10 males, 13 females, average age = 62.5, Table 2) independently obtained a third dose of either BNT162b2 or mRNA-1273 vaccine 1-8 months (average = 5 months) after their second dose. Two to four weeks after their third dose, VPRs showed a 5.4-fold increase in NAb levels (range 46%–99%) (**Figure 18B**), when comparing average percent neutralization at post-2nd dose and post-3rd dose timepoints, suggesting that most VPRs are not permanently poor responders; they are capable of generating high NAb levels with an additional vaccine dose.

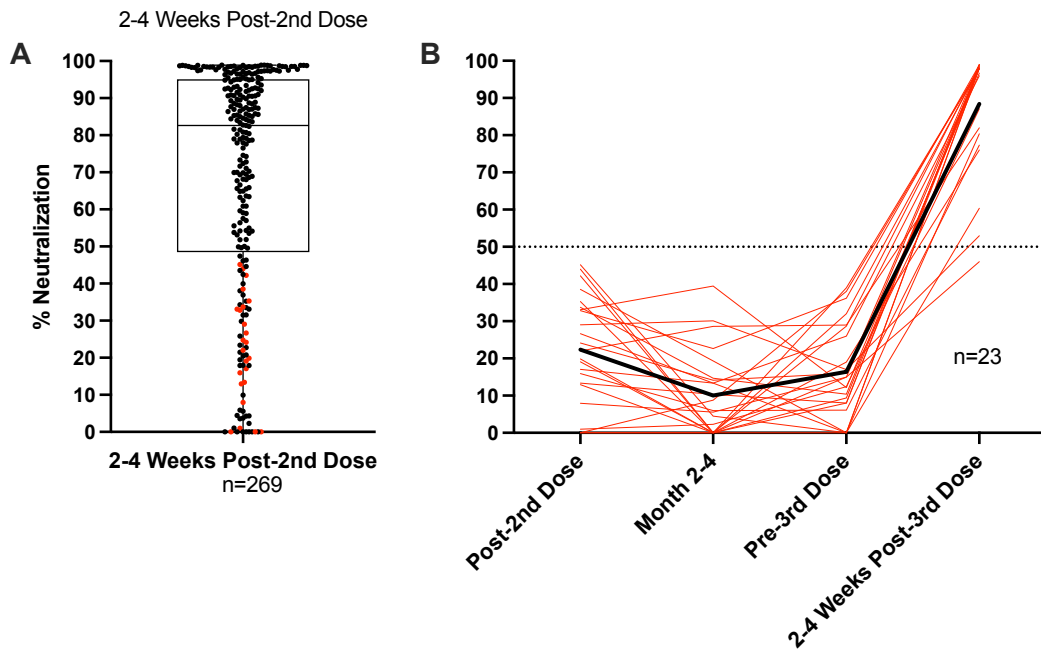


Figure 18. NAb Profile of RNA Vaccine Recipients Pre- and Post-3rd Vaccine Dose.

A) Spectrum of NAb levels 2-4 weeks post 2nd RNA vaccine dose (180 BNT162b2 combined with 89 mRNA-1273 vaccine recipients=269) ranging from 0% neutralization to 99% neutralization. Horizontal line within second and third quartile box denotes median at 83%. Sixty-nine participants in the lower quartile neutralized at <50%. Red dots in lower quartile indicate participants who received 3rd vaccine doses as shown in panel B. **B)** Vaccine Poor Responder Third Dose Recipients Red lines indicate NAb levels in poor responders (<50% neutralization) at 2-4 weeks post second dose, 1-2 weeks prior to a third vaccine dose and two to four weeks after a third dose of either BNT162b2 or mRNA-1273. Solid black line is the average % Neutralization of 3rd vaccine dose recipients at each time point. At 2-4 weeks post 3rd dose the average neutralization was 88%.

Separating VPRs in **Fig. 18A** into mRNA-1273 and BNT162b2 vaccine recipients unexpectedly revealed that 14% of mRNA-1273 recipients were VPRs, while 31% of BNT162b2 recipients were VPRs. Only one of twelve mRNA-1273 VPRs chose to receive a third dose of vaccine. In contrast, 23 of 58 BNT162b2 VPRs chose to receive a third dose of either vaccine (see Table 2) as shown in **Figure 19**. Statistically, Levene's test indicated heteroscedasticity ($p < 0.001$), while Welch's t test showed significant

differences in mean neutralization between groups 2–4 weeks post-2nd dose ($q < 0.001$) with medium effect ($d = 0.537$) and observed power nearing unity ($1-\beta = 0.981$).

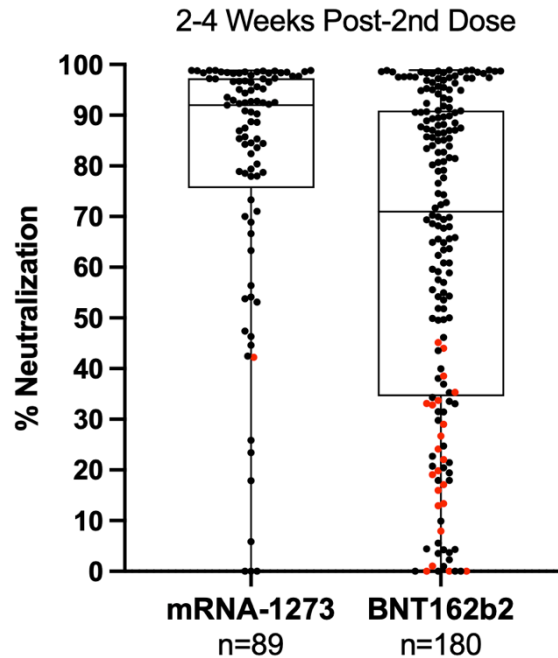


Figure 19. Comparison of NABs after 2nd dose of mRNA1273 or BNT162b2. % Neutralization (y-axis) indicates NAB levels ranging from 0% to 99% neutralization. Data shown as box and whisker plots with black vertical lines that denote upper and lower extremes, and horizontal lines that denote upper and lower quartiles with median at the midline. Median neutralization of mRNA1273 (n=89) and BNT162b2 (n=180) is 92% and 71%, respectively. Mean neutralization for mRNA1273 and BNT162b2 groups is 80% and 63%, respectively. Red dots indicate VPRs that received a 3rd vaccine dose as shown in **Figure 18B**, demographics in **Table 3**.

Discussion

Some considerations about our findings include the following. We were surprised to observe that 67/269 (25%) of participants in our study did not demonstrate neutralization >50%. It is not known if poor NAb responders are at increased risk of

infection or severe disease. However, anti-viral T cells and antibodies that mediate ADCC are also important components of immunity and prevent disease once a host is infected. Although 50% neutralization corresponds to titers <1:160, it is not known if titers of 1:80, for example, would protect an individual from infection and disease. Likewise, it is not known if individuals with highly neutralizing antibodies corresponding to titers of $\geq 1:320$ would not be protected from infection and disease. However, some models and reports have predicted that NAb levels can serve as a correlate of protection.^{117,124,125}

The debate about whether a vaccinated individual can transmit virus depends in part on their levels of neutralizing antibodies. NAbs prevent infection and are used therapeutically to treat COVID-19 patients¹¹. T cells are crucially important for eliminating infected cells,^{126,127,128} but if anti-viral T cells are engaged, the host is already infected. As NAb levels decrease with time after vaccination, there is an increased likelihood that exposure to SARS-CoV-2 could lead to infection which could potentially lead to transmission.¹²⁹ This may be an important point since a significant portion of the population has not been vaccinated and could be infected by a vaccinated individual whose NAb levels are low, such that they do not prevent infection and asymptotically shed virus just prior to reactivation of immune memory.

Twenty-five percent of total participants ($n = 269$) in our study did not generate NAb levels stronger than 50% after a 2-dose regimen. These VPRs ranged in age from 19 to 80 with an average age of 57, median age of 60 ($n = 67$). The age range of non-VPRs was 20–80 with an average age of 50, median age of 51 ($n = 202$). Further studies could be performed to determine the relationship of age and NAb levels <50% after COVID-19

vaccination. Our data suggest that COVID-19 vaccine strategies might follow at least a multiple-dose regimen to keep peripheral NAb levels high, limiting infection, asymptomatic viral replication, and potential transmission. It also suggests that NAb levels in vaccine recipients could be evaluated with a rapid test on an individual basis to indicate when an additional dose might be indicated.

Although healthcare policy may recommend that a population should receive a third COVID-19 vaccination at a particular timepoint, an inexpensive rapid test could provide personalized NAb levels on an individual basis to indicate who might or might not require a third dose. Not only would this conserve vaccine, but vaccinating individuals who already have elevated levels of NABs may not provide benefit since spike protein could be cleared by circulating NABs as fast as it is made by cells.

Previous reports indicate that NAb levels decline much more rapidly than protection from hospitalization and disease,^{87,130} but that does not account for vaccine recipients who never generated high levels of NABs after two doses. Moreover, it is possible that VPRs could be a source of breakthrough infections. Although it is not known what levels of NABs protect from infection or disease, many vaccine recipients in high-risk professions may wish to keep peripheral NAB levels high, limiting infection, asymptomatic viral replication, and potential transmission.

Although vaccine durability studies indicate an average neutralization geometric mean titer (GMT) of ≥ 320 during the peak period after 2nd dose,^{105,131} the distribution among individual serum samples obtained during the observed peak neutralization period (4 to 30 days post-2nd dose) varies greatly.¹³¹ It is unclear what percentage of a population falls below a given GMT or IC_{50} during the peak neutralization period

following 2nd dose. Our study supports other findings that majority of healthy individuals generate a NAb response $\geq 75\%$ neutralization ($IC_{50} \geq 160$ and < 320).

However, we highlight a VPR population that, despite healthy status at the time of vaccination, fail to mount a NAb response $> 50\%$ ($IC_{50} < 160$) after two doses.

Poor NAb titers have been reported in special populations such as patients with ongoing cancer therapies,¹³² solid organ transplant patients,^{133,134,135} and individuals on systemic immunosuppressive regimens for various immune-mediated inflammatory diseases.¹³⁶ However, current literature is lacking regarding protective antibody responses to COVID-19 in a healthy population. Finally, it is not unprecedented in other vaccine settings such as influenza to observe poor or non-neutralizing responses in healthy individuals.^{137,138} Due to the urgency to develop vaccines to slow the COVID-19 pandemic, we are still learning the parameters of mRNA vaccine dose, frequency, timing and durability in the human population.

This study has several limitations. First, it is still unknown what levels of neutralizing antibodies correlate with protection against infection and potential disease. It is possible, but unlikely, that NAb levels as low as 20% could protect against infection.⁸ Second, although antibodies directed against the N-terminal domain of spike protein have also been shown to neutralize SARS-CoV-2, it is currently characterized as a minor component of neutralizing antibodies^{118,111} and our test does not detect them. Although we measured NAb levels for twice as many BNT162b2 vaccine recipients as mRNA-1273 recipients, we examined homogeneity of variance using Levene's test and, upon confirming unequal variances, assumed Welch's t-test as a conservative and robust alternative to parametric comparisons of means. Importantly, potential for type I error

was mitigated using FDR-adjustment of calculated significance, and Cohen's *d* showed appreciable effect size between groups. Moreover, posthoc power analysis showed exceptional sensitivity and low chance of type II error, further supporting the significantly lower percent neutralization observed in Pfizer recipients 2–4 weeks post-2nd dose.

Finally, the Omicron variant(s) became widespread since the submission of this manuscript. Although vaccines based on the ancestral Wuhan sequence may not be as effective at preventing infection as an Omicron-based vaccine if it becomes available, additional boosters have been shown in recent publications to be partially effective against virus with Omicron-like mutations and pseudotyped Omicron, as boosting with ancestral-spike encoding mRNA vaccines promotes antibody affinity maturation in previously naturally infected or vaccinated individuals, contributing to increased protection against infection with Omicron variant(s) and subsequent disease.¹³⁹

In conclusion, our findings suggest that 14% of mRNA-1273 and 31% of BNT162b2 two-dose vaccine recipients ranging in age from 19 to 80 with an average age of 57 (median age of 60) may not have generated levels of NAb $\geq 50\%$, and that additional COVID-19 vaccine doses might be indicated for these individuals. Longitudinal studies are ongoing to determine if high NAb levels in recipients of a third vaccine dose are more durable than NAb levels after two doses.

CHAPTER IV
LONGITUDINAL COMPARISON OF NEUTRALIZING ANTIBODY RESPONSES
TO COVID-19 MRNA VACCINES AFTER SECOND AND THIRD DOSES

Reprinted with permission from MDPI publishers.
Originally published in
Vaccines, Aug. 2022, vol. 10, issue 9.

Alexa J. Roeder, Megan A. Koehler, Paniz Jasbi, Davis McKechnie, John Vanderhoof,
Baylee A. Edwards, Maria J. Gonzalez-Moa, Alim Seit-Nebi, Sergei A. Svarovsky, and
Douglas F. Lake

Abstract

COVID-19 mRNA vaccines protect against severe disease and hospitalization. Neutralizing antibodies (NAbs) are a first-line defense mechanism, but protective NAb responses are variable. Currently, NAb testing is not widely available. This study employed a lateral flow assay for monitoring NAb levels postvaccination and natural infection, using a finger-stick drop of blood. We report longitudinal NAb data from BNT162b2 (Pfizer) and mRNA-1273 (Moderna) recipients after second and third doses. Results demonstrate a third dose of mRNA vaccine elicits higher and more durable NAb titers than the second dose, independent of manufacturer, sex, and age. Our analyses also revealed that vaccinated individuals could be categorized as strong, moderate, and poorly neutralizing responders. After the second dose, 34% of subjects were classified as strong responders, compared to 79% after the third dose. The final months of this study coincided with the emergence of the SARS-CoV-2 Omicron variant and symptomatic breakthrough infections within our study population. Lastly, we show that NAb levels

sufficient for protection from symptomatic infection with early SARS-CoV-2 variants were not protective against Omicron infection and disease. This work highlights the need for accessible vaccine response monitoring for use in healthcare, such that individuals, particularly those in vulnerable populations, can make informed vaccination decisions.

Introduction

COVID-19 mRNA vaccines BNT162b2 (Pfizer) and mRNA-1273 (Moderna) dramatically reduced the incidence of severe disease and hospitalization due to SARS-CoV-2 infection.^{63,65} One goal of all COVID-19 vaccines is to induce neutralizing antibodies (NAbs), which prevent the virus from infecting host cells.^{126,127,128} Vaccines also induce antiviral T cells that kill infected cells, but when cytotoxic T cells are engaged, the host is already infected and virus is actively replicating, creating the potential for transmission. In individuals vaccinated with the ancestral SARS-CoV-2 spike protein-encoding mRNA, breakthrough infections likely occur due to waning levels of neutralizing antibodies^{140,141,142,143,144} or infection with a variant of concern, such as one of the Omicron variants.^{145,146} The principle neutralizing domain of SARS-CoV-2 spike glycoprotein is the receptor binding domain (RBD),⁹⁴ although additional NAbs have been observed that target the N-terminal domain (NTD) of spike.¹¹¹ Antibodies that target the RBD of spike have potent neutralizing activity,¹¹² but are particularly prone to loss of efficacy as variants arise. RBD has been shown to be highly mutated in several variants of concern (VOCs), most significantly in the Omicron variant and subvariants.¹⁴⁷ The assay employed in this study uses the RBD of SARS-CoV-2 USA-WA1/2020 spike for

detection of Nabs that inhibit RBD binding to host the cellular receptor, angiotensin-converting enzyme 2 (ACE2). For the purposes of this study, NAbs that obstruct the RBD-ACE2 interaction are quantitatively measured (**Figure 20**) using a rapid lateral flow assay (LFA), previously described.³² The RBD-NAb LFA has been shown to detect vaccine-induced NAbs as well as those induced by natural infection.¹⁴⁸

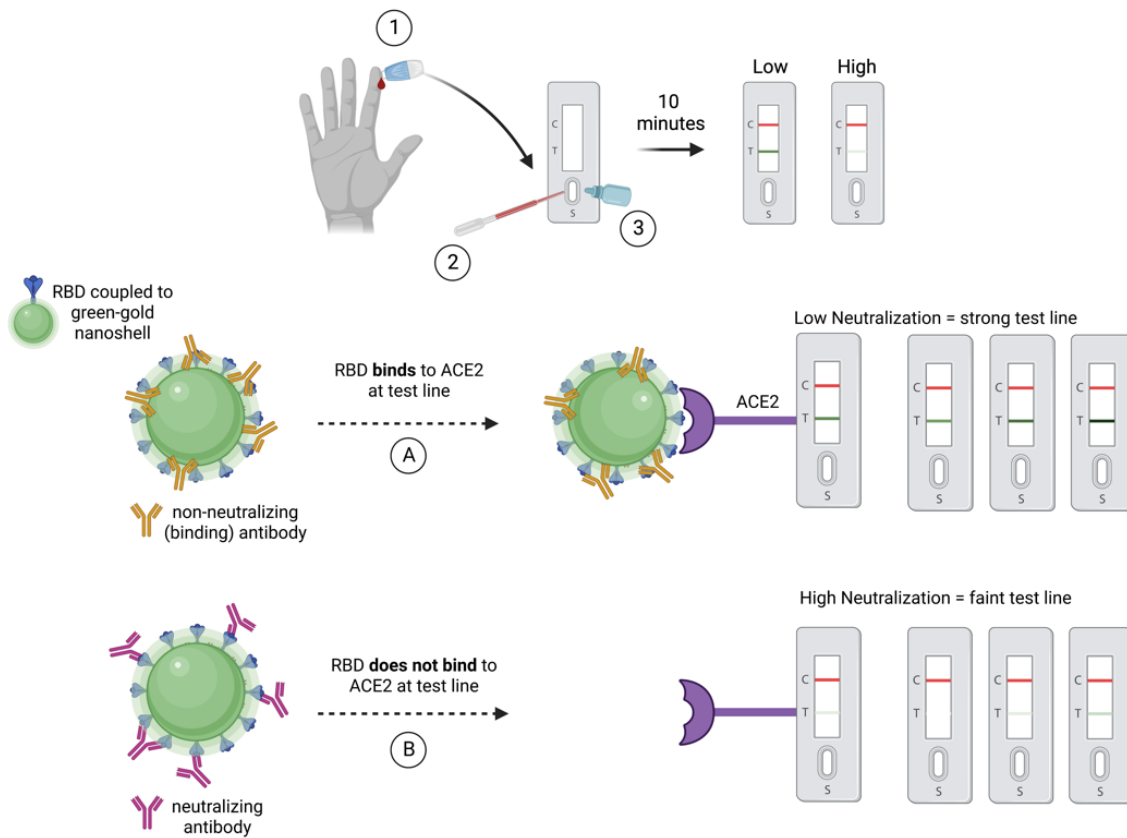


Figure 20. Schematic diagram of NAb LFA principle/mechanism. (1) Fingerstick blood is obtained using a pressure-activated safety lancet. (2) Ten microliters of blood are transferred to the sample port on a test cassette. (3) Buffer is applied to the sample port. (Left to right) RBD of spike (blue) is shown coupled to a green-gold nanoshell (green-GNS). Non-neutralizing antibodies (gold) are shown to bind outside of the RBD, such that in outcome (A) RBD-GNS is available to bind ACE2, seen as a strong test line. Neutralizing antibodies (maroon) are shown binding to RBD, obstructing the interaction between antigen and receptor, such that in outcome (B) RBD does not bind to ACE2, observed as a faint or absent test line.

As the COVID-19 pandemic transitions into an endemic phase with potential surges occurring in different geographic locations at certain times of year, monitoring vaccine-induced immunity may be an important component of healthcare. Specifically, monitoring NAb titers may also allow individuals and their healthcare providers to gauge when a booster might be warranted as NAb titers wane, especially in vulnerable and immunosuppressed populations. Prevention of SARS-CoV-2 infections could reduce opportunities for the virus to mutate into more infectious or pathogenic VOCs, as has been demonstrated throughout the pandemic.^{149,150} Although measuring NAb titers has been suggested as a correlate of protection,^{124,125,117} it is not known what the risk of infection is, as NAb titers wane after both vaccination and natural infection. In addition to waning titers, it is known that natural infection alone may not elicit measurable levels of NAb titers,⁸⁸ especially when infections are mild.¹⁵¹ However, breakthrough infections have been reported to boost NAb titers in vaccinated individuals.¹⁵²

We undertook this study to learn the durability of RBD-NAb titers in previously uninfected COVID-19 vaccine recipients after second and third vaccine doses. Here we report longitudinal second- and third-dose data from 302 healthy individuals and demonstrate the importance of a third dose for RBD-NAb longevity, independent of mRNA vaccine manufacturer. Since Omicron-variant infections became widespread during the final few months of our study, we present breakthrough infection data pre- and post-Omicron surge in the United States, specifically Arizona. This is the first report that employs a rapid NAb test to longitudinally measure levels of neutralizing antibodies after a second and third mRNA vaccine dose.

Materials and Methods

Experimental Design

The purpose of this study was to quantify RBD-NAb levels prior to and post-mRNA vaccination using a rapid lateral flow assay developed previously in our laboratory.³² Participants were tested at variable timepoints prior to the second vaccine dose, then monthly for the remainder of their enrollment. Finger-stick blood samples were obtained within one week prior to 2nd dose, and 2–4 weeks post-2nd-dose. Longitudinal data were collected monthly according to the date of participants' post-2nd-dose test ($n = 265$). As third vaccine doses (boosters) became available, we began monitoring third-dose recipients' RBD-NAbs in the same manner ($n = 142$). Some of the individuals in the 3rd-dose cohort were newly enrolled, although many continued from prior enrollment in the 2nd-dose study ($n = 105$), such that paired longitudinal data were collected from 105 participants.

Participant Recruitment

Male and female adults ranging in age from 18–80 years old upon entry into the study were recruited and enrolled with informed consent under a protocol approved by the institutional review board at Arizona State University (IRB #0601000548). Participants were enrolled at various times throughout vaccination and returned for monthly testing until the study completed. Reasons for termination of enrollment prior to completion of the study included breakthrough infection and participant dropout.

Inclusion/Exclusion Criteria

Individuals under the age of 18 and older than 80 years old at the time of enrollment were excluded from this study, as well as individuals with PCR-confirmed natural infection prior to vaccination. Individuals with symptomatic and laboratory-confirmed breakthrough infections as well as those that were asymptomatic but detected due to routine testing were excluded from data analyses; however, subjects were not required to test routinely for the purpose of the study. Patients actively undergoing cancer therapies or treatment for severe autoimmune disease with systemic immunosuppressive therapy were also excluded. The study population included healthy individuals between 18 and 80.

Longitudinal NAb Monitoring Using a Rapid RBD-NAb LFA

Longitudinal monitoring was conducted using ten microliters of blood obtained from a finger stick using a 28-gauge, 1.8 mm pressure-activated safety lancet. Blood was transferred to the test cassette by volumetric micro transfer pipette and chased with two drops (50 μ L total) of buffer. The test ran undisturbed on a flat surface for ten minutes, then read using a portable densitometer (Detekt RDS-2500) to quantify control and test line densities. Data were exported to Microsoft Excel using the Detekt Data Manager software (Detekt Biomedical, Austin, TX, USA) and recorded as de-identified participants in a master file.

Data analysis

Raw data were converted to percent neutralization by normalizing values according to the limit of detection previously defined for the rapid test.³² The equation used to calculate percent neutralization was: $1 - (\text{test line density} / \text{limit of detection}) * 100\%$. Limit of detection of least neutralizing serum was a density of 942,481 density units. Normalized data were subsequently analyzed using GraphPad Prism 9.0 (GraphPad Software, San Diego, CA, USA). Unsupervised hierarchical clustering, principal component analysis (PCA), and significance testing with correction for false discovery rate (FDR) were performed and results were visualized using R version 4.1.2. Percent neutralization graphs were made using Microsoft Excel version 16.6.1. Post hoc power analysis was performed and critical R2 visualized using G*Power version 3.1.9.6. Missing values were imputed using a subject-wise k-nearest-neighbor algorithm. Conversions between test line density, percent neutralization, and NAb ranges are demonstrated in **Figure 21**. All normalized or raw de-identified data can be made available upon request to the corresponding author.


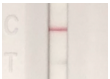
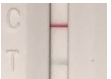
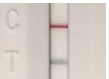
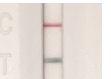

NAb LFA Test Image						
Test Line Density Units (thousands)	10-99	100-199	200-369	370-599	600-799	800-1000
Neutralization (%)	99-90	89-80	79-61	60-36	35-15	≤15
NAb Titer Ranges	<1:1280 ≥1:640	<1:640 ≥1:320	<1:320 ≥1:160	<1:160 ≥1:80	<1:80 ≥1:40	≤1:40

Figure 21. NAb LFA density units correspond to percent neutralization and NAb titer. Validation of the rapid NAb test using gold standard focus reduction neutralization

test (FRNT₅₀) with authentic SARS-CoV-2 Wuhan isolate and correlation/regression analyses are previously described. Percent neutralization was calculated as 1-Test line density/Limit of Detection (942,481) *100%. Titers are based on the last dilution of a serum sample that inhibited 50% of infectious foci in a Focus Reduction Neutralization test.^{32,148}

Results

We previously developed a rapid test to measure levels of neutralizing antibodies to SARS-CoV-2 using 10 μ L of finger-stick peripheral blood.³² The test quantitatively measures antibodies that inhibit spike protein RBD-GNS from binding to ACE2 (neutralizing antibodies) in a lateral flow assay. Test line density is quantified in a lateral flow assay reader, and converted to percent neutralization and NAb titers compared to a live-virus focus reduction neutralization test, as previously reported.¹⁴⁸ The rapid test has been shown to measure NAbs induced after a natural infection and after mRNA vaccination.³² In this study, we monitored 302 individuals' NAb responses after they received a second and/or third dose of COVID-19 mRNA vaccine. All study participants were healthy with no reported current comorbidities. We evaluated the durability of RBD-NAbs in COVID-19 mRNA vaccine recipients monthly for 6–8 months after the second dose, and for 6–8 months after the third dose. Study participants in whom breakthrough infections occurred were discontinued from the study at the time of the PCR-confirmed SARS-CoV-2 infection.

The study began in December 2020 after participants began to receive their first dose of either BNT162b2 or mRNA-1273. If participants were available, NAb levels were measured within seven days prior to the second and third vaccine doses. At the

height of recruitment, 2–4 weeks after the second vaccine dose, 234 participants were enrolled. Nabs were measured 2–4 weeks after the second or third dose, then monthly for 6–8 months. If a participant missed a month, they remained in the study until months 7 or 8 or until the study was completed. The number of vaccinated participants in the second- and third-dose groups and corresponding demographics are shown in **Table 4**. A flowchart demonstrating sample sizes of the second- and third-dose groups is shown in **Figure 22**.

Variable *	Total (N = 265) n (%)		Total (N = 142) n (%)	
	2nd Dose		3rd Dose	
	BNT162b2	mRNA-1273	BNT162b2	mRNA-1273
Sex				
Female	107 (40)	54 (20)	33 (23)	47 (33)
Male	65 (25)	39 (15)	30 (21)	32 (23)
Age (Median [range])	55 [20–82]	50 [19–73]	61 [26–81]	58 [20–79]
Female				
<65	87 (33)	47 (18)	21 (15)	34 (24)
≥65	20 (8)	7 (3)	12 (8)	12 (8)
Male				
<65	46 (17)	30 (11)	18 (13)	17 (12)
≥65	19 (7)	9 (3)	12 (9)	16 (11)

Table 4. Population demographics of COVID-19 mRNA vaccine study participants. Data shown as 2nd- and 3rd-dose population size (*N*). Sample sizes (*n*) are shown for sex and age subgroups with percentage of total population size (i.e., females < 65 years old that received a 2nd dose of BNT162b2 [*n* = 87] compose 33% of the total 2nd-dose population [*N* = 265]). All subjects included in analyses presented in this manuscript related to vaccine-induced NAb were SARS-CoV-2 RT-PCR-negative at the time of enrollment and had no known breakthrough infections throughout the remainder of their enrollment. Subjects for which breakthrough infections did occur were included in vaccine-induced NAb data until the timepoint prior to infection, after which data were excluded. Such individuals are included in sample and population sizes above.

Figure 22 demonstrates annexation of sample size with respect to dose and vaccine manufacturer. This flowchart is provided for clarity of sample sizes discussed throughout the manuscript. **Figures 24B and 24C** in the main text reference “mixed” and “non-mixed” 3rd vaccine doses.

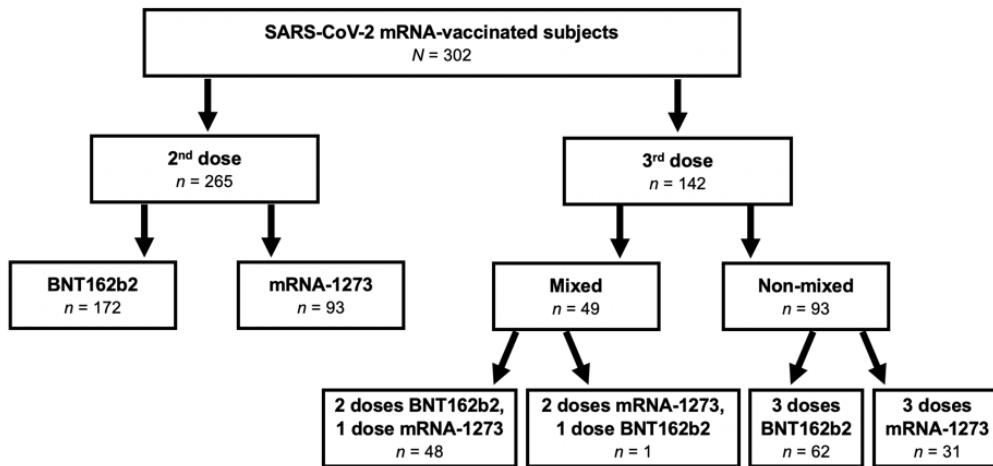


Figure 22. Flowchart of mRNA-vaccinated subjects. Sample sizes for the second dose group are divided into BNT162b2 and mRNA-1273 recipients. The third dose group is first divided into mixed and non-mixed vaccine recipients, and subsequently by number of doses per vaccine manufacturer.

Longitudinal NAb Titers

The range of individuals’ NAb titers is shown at <1 week prior to a second vaccine dose, 2–4 weeks after dose two, and then monthly for 6–8 months for recipients of either BNT162b2 or mRNA-1273 vaccine (**Figure 23A**). Two to four weeks after the second dose, mean NAb titers increased from between 1:40 and 1:80 (35% neutralization) to between 1:160 and 1:320 (71% neutralization). However, 28% (65/234)

of second-dose recipients' NAb titers did not reach 50% neutralization 2–4 weeks after the second vaccine dose, when antibody titers are typically at their peak. Between months two and three after a second dose, mean titers declined to between 1:80 and 1:160 (56% mean neutralization), and remained relatively constant between titers of 1:80 and 1:160.

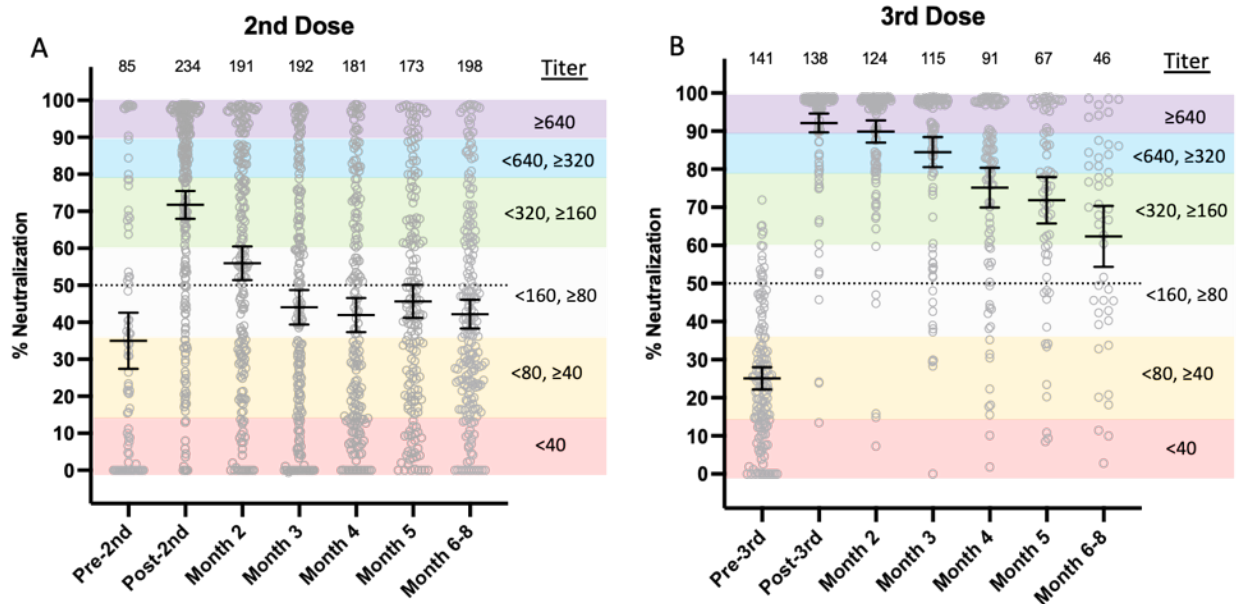


Figure 23. Comparison of 2nd and 3rd mRNA vaccine-induced NAb durability. (A) Second dose; (B) third dose. Gray circles represent percent neutralization from each study participant vaccinated with either BNT162b2 or mRNA-1273 within one week prior to vaccination (Pre-2nd), 2–4 weeks postvaccination (Post-2nd), then monthly after either second or third doses. The horizontal black lines with error bars represent mean with 95% confidence intervals. Dotted line is 50% neutralization. Numbers above each x-axis time point indicate the number of participants. Reciprocal titer ranges corresponding to % neutralization are shown on the graphs as shaded purple ($\geq 1:640$), blue ($< 1:640, \geq 1:320$), green ($< 1:320, > 1:160$), light grey ($< 1:160, \geq 1:80$), orange ($< 1:80, \geq 1:40$), and red ($< 1:40$) as reported in [18]. Percent neutralization was calculated as $1 - (\text{test line density} / \text{limit of detection}) \times 100\%$ (limit of detection test line density = 942,481), as detailed previously.¹⁴⁸

Study participants received their third vaccine dose an average of 7 months after their second dose, when mean titers were between 1:40 and 1:80 (~25% neutralization).

Two to four weeks after a third dose, mean NAb titers increased to $\geq 1:640$ (92% neutralization; **Figure 23B**). In contrast to the second dose of mRNA vaccine in which mean titers declined rapidly, NAbs remained elevated in third-dose vaccine recipients and did not drop below 50% mean neutralization, even at 6–8 months.

Homologous and Heterologous mRNA Vaccination

Our study design allowed for comparison of longitudinal NAb data between homologous booster vaccine recipients (i.e., those who received two or three doses from the same manufacturer) versus heterologous booster vaccine recipients, or those who received two or three doses from different manufacturers (mixed vaccines). After a second dose, recipients of mRNA-1273 elicited significantly stronger NAb responses at the post-second-dose timepoint through month 5 ($p < 0.05$ - 0.0005 ; **Figure 24A**). There were no significant differences in the NAb responses to different vaccines after the third dose (**Figure 24B**). It should be noted that all but one individual in the BNT162b2 group ($n = 62$) shown in **Figure 24B** had previously received two BNT162b2 vaccine doses. However, in the mRNA-1273 third dose group ($n = 80$), 31 individuals received mRNA-1273 previously, while 48 individuals previously received BNT162b2. Further, we found that receiving a third dose of either mRNA vaccine was more important than adherence to one particular manufacturer (i.e., “mix and match”, **Figure 24C**), although at month 5, we observed a significant increase in percent neutralization of the mixed vaccine population, relative to the group that received three BNT162b2 doses ($p < 0.05$). The difference was resolved at months 6–8 post-third vaccination, and mean titers remained in the $\geq 1:160$, $< 1:320$ range, independent of vaccine manufacturer or mixed vaccines.

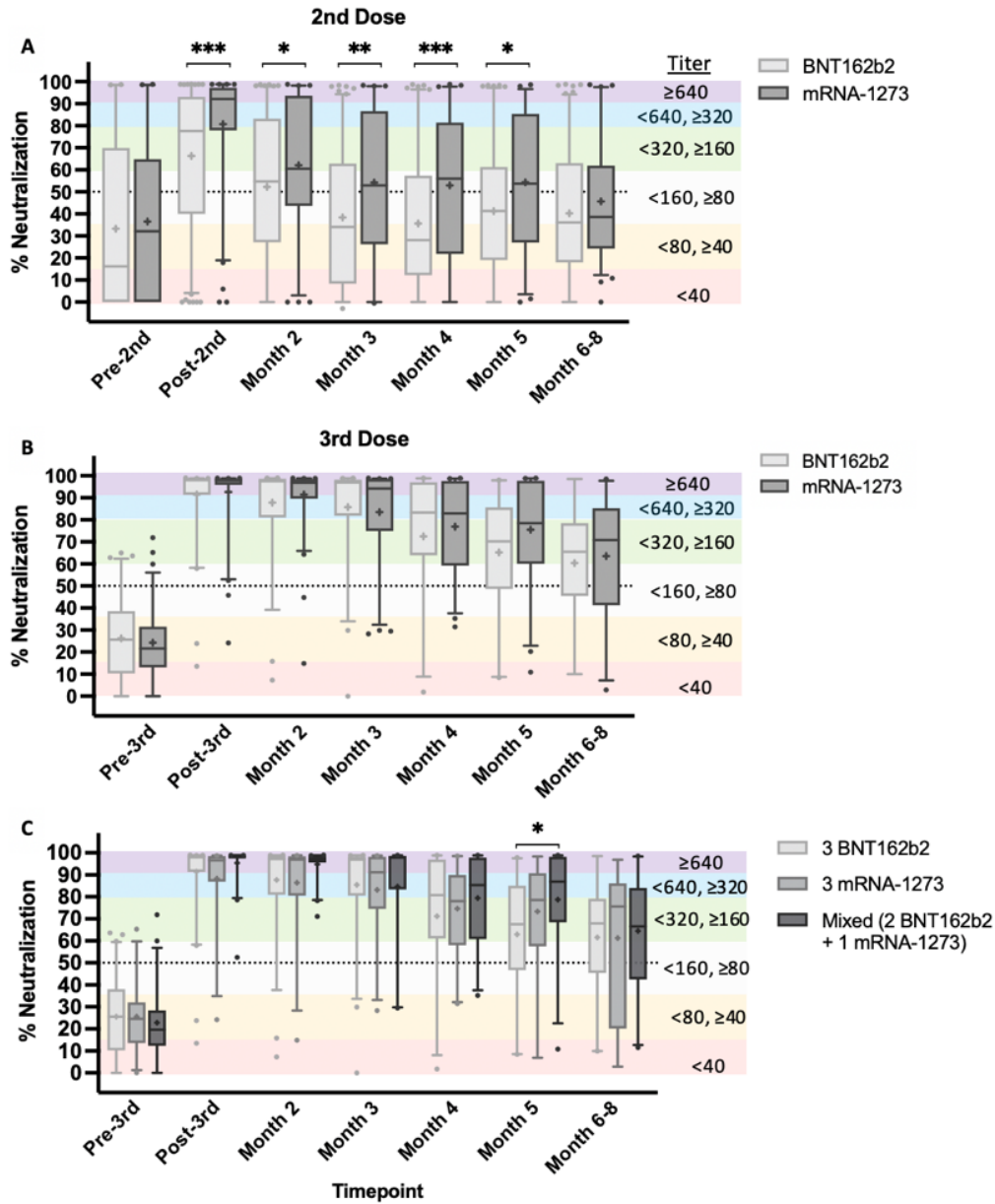


Figure 24. NAb durability of second and third mRNA vaccine doses by manufacturer. NAb test timepoints represented as percent neutralization are pre-2nd/3rd (within one week), post-2nd/3rd (2–4 weeks after second or third dose), and monthly for 6–8 months after vaccination. (A) Longitudinal 2nd-dose data of BNT162b2 (Pfizer) in comparison to mRNA-1273 (Moderna). (B) Longitudinal 3rd-dose data. (C) Longitudinal 3rd-dose data of individuals that received the same vaccine type for all three vaccine doses, in comparison to individuals that received two Pfizer doses and a Moderna booster dose. Data are shown as grouped box and whisker plots with error bars representing 5th–95th percentile of each population. Outliers outside of the 5th–95th percentile are shown as circular symbols above or below error bars. Graphs A and B data were analyzed using nonparametric Mann–Whitney test to evaluate mean rank between groups with a two-

tailed p-value ($p < 0.05$) and 95% confidence interval (CI). Graph C data were analyzed using a nonparametric Kruskal–Wallis test to evaluate mean rank between groups using multiple comparisons (two-tailed $p < 0.05$ and 95% CI). Titers corresponding to percent neutralization ranges are described (see **Figure 23** legend). * $p < 0.05$, ** $p < 0.005$, *** $p < 0.0005$.

Sex-Based Differences

Sex and age have previously been implicated as factors in COVID-19 vaccine efficacy.¹⁵² Although reports of sex-based differences with respect to humoral immunity elicited by mRNA vaccination have yielded conflicting results,^{153,154} antibody responses to other viral vaccines have been shown to be more robust in females.¹⁵⁵

We evaluated NAb levels in male and female vaccine recipients who were <65 and those who were ≥ 65 after second and third doses. No sex-based differences were observed after second dose (**Figure 25A**) and we observed only a slight increase in mean titers of females ($p = 0.05$) 2–4 weeks post-third-dose (**Figure 25B**), although both males and females had means of $\geq 90\%$ neutralization (NAb titer $>1:640$), 2–4 weeks post-third-dose.

Age-Based Differences

When evaluating age, differences were observed only after the second dose, and when grouped as ≥ 65 or <65 years old (**Figure 25C**). Significant age-based differences were observed at post-second-dose and month 3 timepoints only ($p < 0.05$ and $p < 0.005$, respectively). When grouped at other age ranges, such as above and below 50 years, no differences were observed (data not shown). In vaccine recipients younger than 65, mean titers declined from between 1:320 and 1:160 (76% neutralization, mean + SEM) to

between 1:160 and 1:80 (44% neutralization, mean + SEM) at 2 and 6–8 months after the second dose, respectively (**Figure 25C**). However, by month 3 following the second dose in the 65-and-older cohort, mean titers declined to between 1:80 and 1:40 at 35% neutralization (mean + SEM), compared to 51% neutralization (mean + SEM) in the younger cohort ($p < 0.005$). Significant differences disappeared after month 4. In contrast, for both age groups after the third dose (**Figure 25D**), mean titers were sustained between 1:160, and 1:320 at 6–8 months, or $\geq 64\%$ neutralization (mean + SEM), further strengthening the value of a third vaccine dose in a population 65 and older.

Sex and Age-Based Differences

When evaluating sex and age together, females < 65 had a slight tendency for higher mean titers compared to females ≥ 65 , after both the second and third vaccine doses (**Figure 25E**). Statistically significant differences were observed when comparing females ≥ 65 and < 65 only at the month 3 timepoint after the second dose ($p < 0.005$), and differences disappeared by month 4. Additionally, only a modest significant difference in mean NAb levels was observed between females ≥ 65 and < 65 ($p < 0.05$), within one week prior to their third dose (**Figure 25F**). No additional differences were observed at subsequent timepoints following a third vaccine dose when comparing sex and age together.

Figure 25 demonstrates longitudinal analysis of NAb titers with respect to sex, age, and sex/age concurrently using unpaired 2nd and 3rd dose data sets.

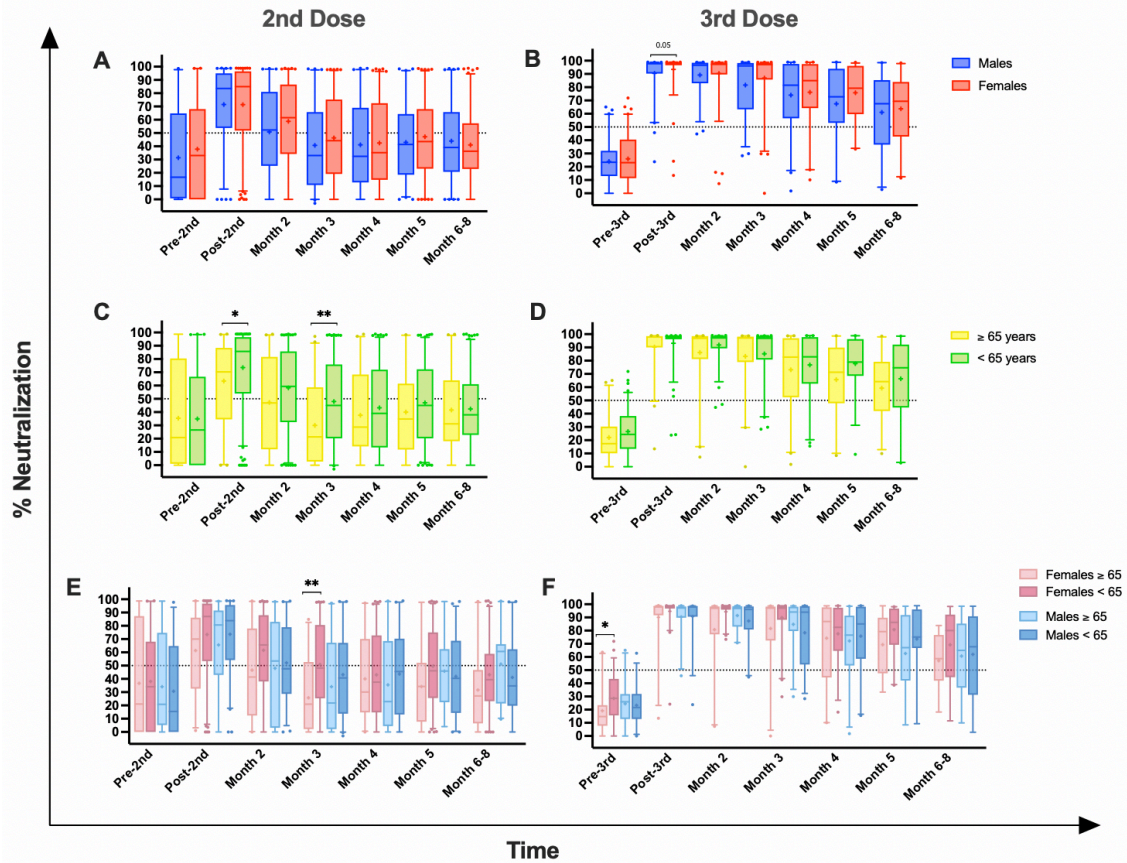


Figure 25. Comparison of 2nd and 3rd Dose NAb Durability by Sex and Age. Graphs are grouped by column and row. Graphs in the left column represent 2nd dose data, grouped by sex (top row), age (≥ or < 65 years old, middle row), and combined sex and age analyses (bottom row). Graphs in the right column demonstrate 3rd dose data, grouped by row as detailed previously. **A)** Evaluation of sex-based differences after 2nd dose, and **B)** after 3rd dose. **C)** Evaluation of age-based differences after 2nd dose, and **D)** after 3rd dose. **E)** Evaluation of sex and age combined differences after 2nd dose, and **F)** after 3rd dose. Data are shown as grouped box and whisker plots with error bars representing 5th-95th percentile of each population. Outliers outside of the 5th-95th percentile are shown as circular symbols above or below error bars. Data corresponding to graphs in top and middle rows were analyzed using non-parametric Mann-Whitney test to evaluate mean rank between groups with a two-tailed P-value ($p < 0.05$) and 95% confidence interval (CI). Bottom row graphs were generated from data analyzed using a

non-parametric Kruskal-Wallis test to evaluate mean rank between groups using multiple comparisons (two-tailed $p < 0.05$ and 95% CI). Axes are labeled as time (X) and percent neutralization (Y). Pre- and post-vaccine dose timepoints are defined in the (*see* **Figure 23** legend).

Classification of Vaccine-Induced NAb Responses Using Unpaired Data

Unpaired samples were analyzed by second and third doses. Unsupervised hierarchical clustering was performed on 265 subjects using percent neutralization data collected pre-second- and post-second-dose, as well as at months 2–8, and the associated dendrogram was analyzed for optimum grouping. As shown in **Figure 26A**, data were best arranged into two groups. The same analysis was performed using percent neutralization of 142 subjects collected similarly at pre-third- and post-third-dose, and at months 2–8. These data advocated most strongly for classification as two groups as well (**Figure 26B**).

Subjects were grouped as indicated by unsupervised clustering. Percent neutralization was graphed at each timepoint and then analyzed by dose. Following both the second and third doses, some subjects exhibited a strong neutralization response to vaccination while others exhibited a relatively tempered response in comparison (**Figure 26C,D**). As such, the former group was labeled vaccine strong responders (VSRs) and the latter termed vaccine moderate responders, or VMRs. After the second dose, 201 subjects were classified as VMRs (~76%), while 64 subjects were classified as VSRs; interestingly, this observation was reversed following the third dose, with 112 subjects (~79%) classified as VSRs by immune response and only 30 subjects classified as VMRs. Percent neutralization of VSR and VMR groups was significantly different at all

timepoints for both second (**Figure 26C**) and third (**Figure 26D**) doses; both groups showed significant differences in percent neutralization at the $q = 0.001$ level for all timepoints except pre-third-dose, which was significant at $q = 0.05$.

PCA was performed for the second- and third-dose data and respective score plots were analyzed for separation and percent variance (**Figure 26E,F**). Using percent neutralization data from pre-second-dose to months 6–8, VSR and VMR groups showed appreciable separation and accounted for 63.3% of between-group variance (**Figure 26E**). Using third dose data, even greater separation between VSR and VMR groups was noted, while PC1 and PC2 accounted for 70.3% of observed variance (**Figure 26F**). Cumulatively, PCA results confirm major differences in percent neutralization across time between VSR and VMR groups indicated by unsupervised clustering (**Figure 26A,B**) and identified by significance testing (**Figure 26C,D**).

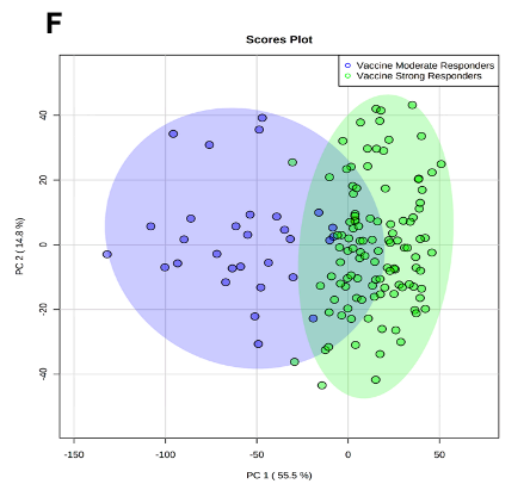
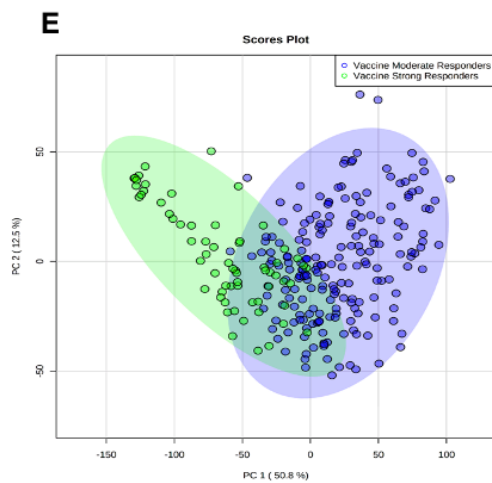
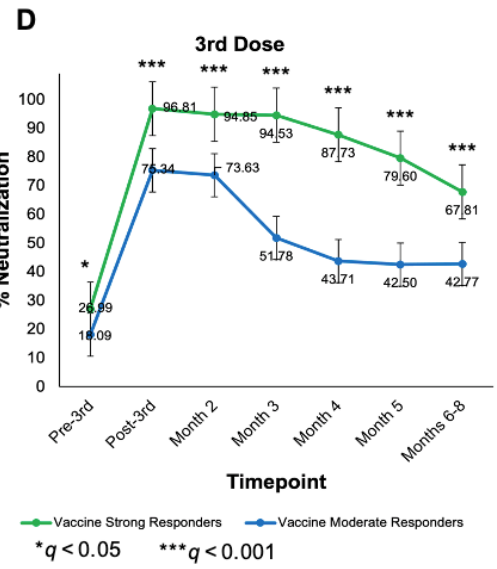
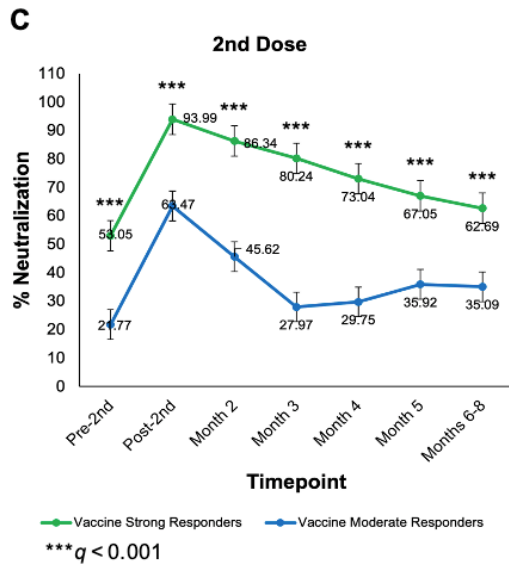
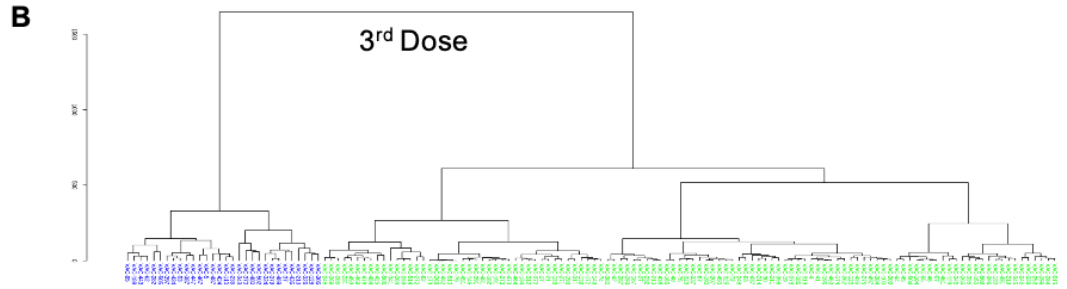
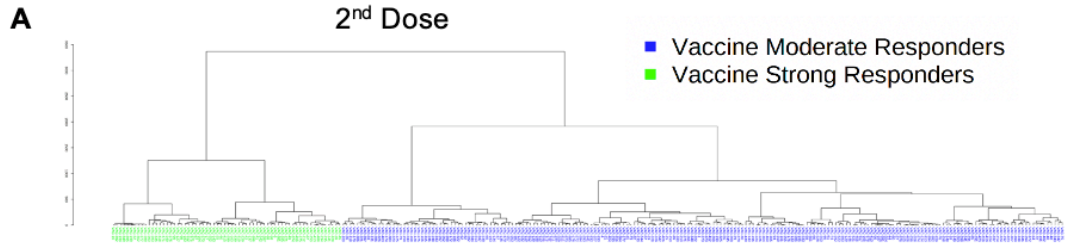


Figure 26. 2nd and 3rd vaccine dose cluster analyses of longitudinal NAb data. (A,B) Unsupervised hierarchical clustering analysis performed using (A) 265 s dose subjects with percent neutralization data collected at pre-2nd dose, post-2nd dose, month 2, month 3, month 4, month 5, and months 6–8, and (B) 142 third-dose subjects with percent neutralization data collected at pre-3rd dose, post-3rd dose, month 2, month 3, month 4, month 5, and months 6–8. Dendrograms from both (A,B) show that the data are best classified as two groups such that within-group covariance is greater than between-group variance. In (A), 201 subjects were grouped as “vaccine moderate responders” while 64 subjects were classified as “vaccine strong responders” (VSR), while in (B), 30 subjects were classified as “vaccine moderate responders” (VMR) and 112 subjects were classified as “vaccine strong responders” (see (C,D)). (C,D) Line graphs showing percent neutralization by time following (C) 2nd dose and (D) 3rd dose between VSR and VMR. Data were grouped as indicated by unsupervised clustering (A,B). Error bars represent standard error. Significance determined by Mann–Whitney U test; FDR-controlled q values shown. * $q < 0.05$, *** $q < 0.001$. (E,F) PCA performed using percent neutralization values from (E) pre-2nd dose to months 6–8, and (F) pre-3rd dose to months 6–8. For both PCA score plots, subjects were classified as VSR or VMR via unsupervised clustering and significance analysis of measured differences in percent neutralization at each timepoint

Subjects were also analyzed by dose, irrespective of response group. In **Figure 27**, percent neutralization in response to second and third doses is graphed for each timepoint from pre-dose to months 6–8. At pre-second and pre-third doses, no significant difference in percent neutralization was observed ($q > 0.05$). However, at post-second and post-third doses, a significant difference in percent neutralization was observed between recipients ($q < 0.001$), a trend that continued through months 6–8.

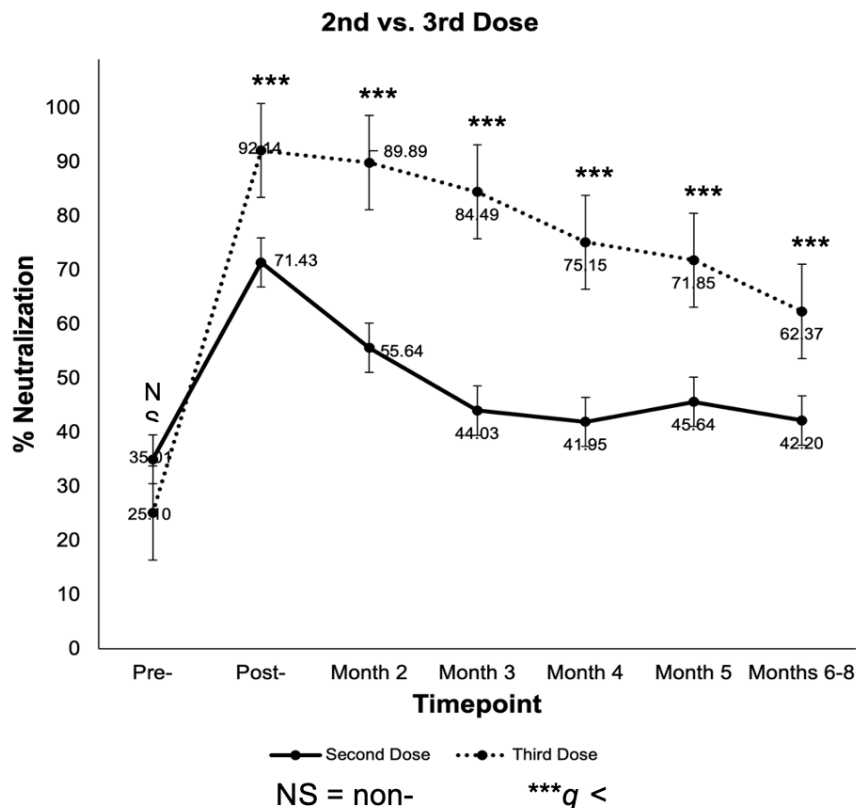


Figure 27. Percent neutralization between 2nd and 3rd vaccine dose. Error bars represent standard error. Significance determined by Mann–Whitney U test; FDR-controlled q values shown.

Classification of Vaccine-Induced NAb Responses using Paired Longitudinal Data

Unsupervised hierarchical clustering on data from 105 subjects from which we obtained concomitant second- and third-dose data across 14 timepoints revealed a tendency for two groups (**Figure 28A**). Subjects were grouped as indicated by the dendrogram, and percent neutralization across the 14 timepoints with coexistent data was graphed to assess longitudinal vaccine durability between groups. As can be seen in **Figure 28B**, two distinct trends in percent neutralization emerged when subjects were

grouped as indicated by clustering. VSRs ($n = 42$) showed the strongest response to the second dose and remained VSRs after the third dose.

The other group, VMRs, to which the majority of subjects with concurrent data were assigned ($n = 63$), showed a moderate response to vaccination in comparison to the VSR group, especially with regard to the second dose, and remained VMRs after the third dose. A Mann–Whitney U test was used to assess significant differences in percent neutralization between identified groups across measured timepoints and type I error was controlled for FDR (i.e., q values reported). Notably, no significant between-group difference was observed pre-second dose ($q > 0.05$), although both groups were significantly different from post-second dose to months 14–16. VSR and VMR groups showed significant differences in percent neutralization at the $q = 0.001$ level following the second dose as well as at months 2, 4, 5, 11, 12, 13, and 14–16. Groups were also significantly different from each other at month 3, pre-third-dose, and at month 10 ($q < 0.01$), while groups differed least significantly at months 6–8 and post-third-dose ($q < 0.05$).

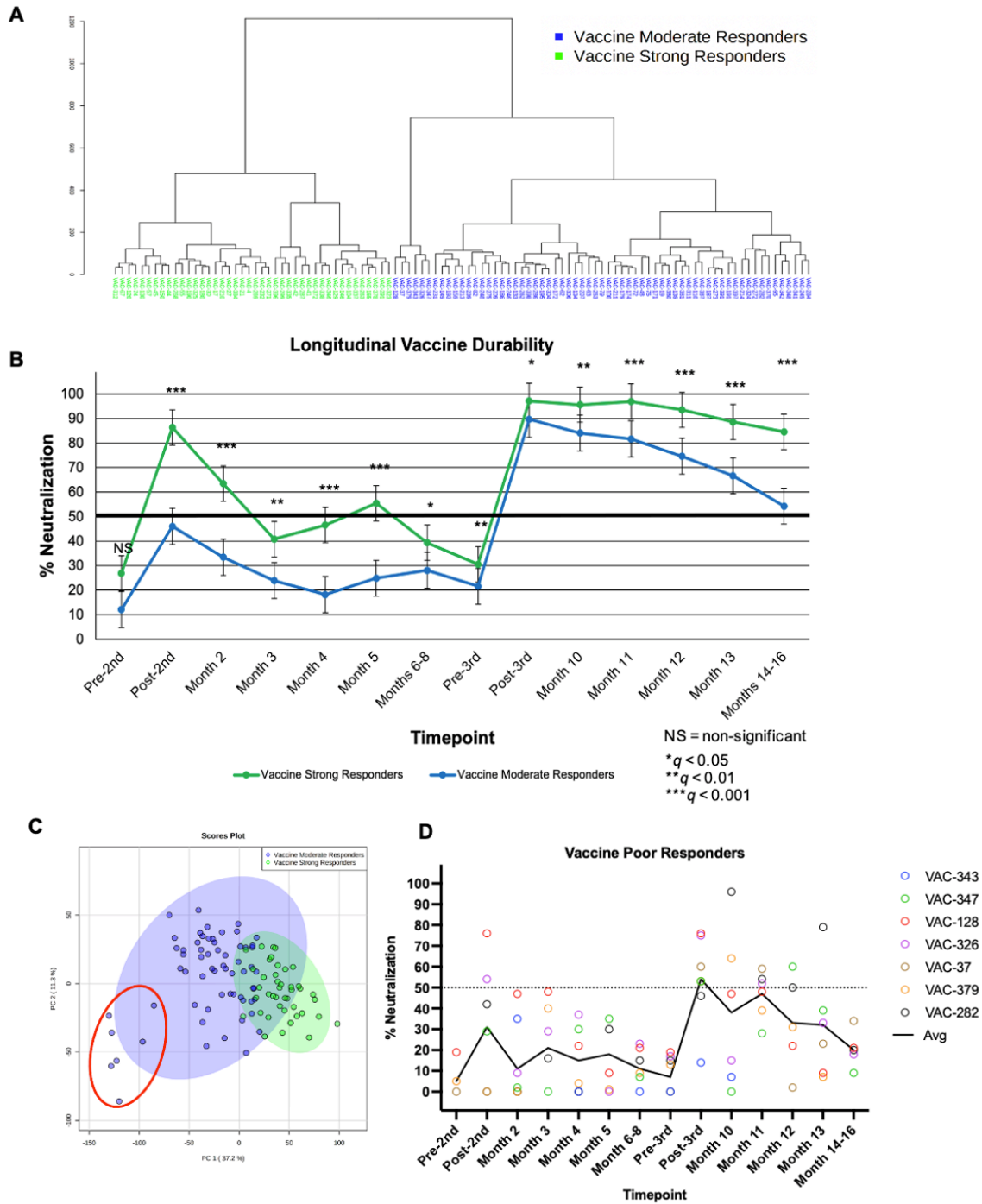


Figure 28. Grouping analyses of paired longitudinal NAb data. (A) Unsupervised hierarchical clustering analysis performed using 105 subjects with percent neutralization data collected at pre- and post-2nd dose, month 2, month 3, month 4, month 5, months 6–8, pre- and post-3rd dose, month 10, month 11, month 12, month 13, and months 14–16. Subjects were grouped as indicated by dendrogram and analysis of line graphs revealed

the nature of two distinct groups (see (B)): VSRs (n = 42), VMRs (n = 63). (B) Line graph showing longitudinal vaccine durability (i.e., percent neutralization by time in response to 2nd and 3rd doses) between VSRs (n = 42) and VMRs (n = 63). Data were grouped as indicated by unsupervised clustering (A). Error bars represent standard error. Significance determined by Mann–Whitney U test; FDR-controlled q values shown. Referent line placed at 50% neutralization. (C) PCA performed using percent neutralization values from 105 subjects with longitudinal data from pre-2nd dose to months 14–16. Subjects were classified as VSR (green) or VMR (blue) via unsupervised clustering and significance analysis of measured differences in percent neutralization at each timepoint. A subgroup of the VMR population with poor neutralizing responses to mRNA vaccination, VPRs (n = 7), are shown outlined in red and loosely clustered within the VMR group (blue). (D) Paired longitudinal 2nd- and 3rd-dose data for VPR subjects identified in (C).

PCA was performed for the paired longitudinal data between VSR and VMR subjects for which parallel second- and third-dose data were obtained (n = 105) and the two-dimensional score plot was analyzed for separation and percent variance (**Figure 28C**). Using percent neutralization data from pre-second dose to months 14–16, VSR and VMR groups showed appreciable separation and accounted for 48.5% of between-group variance. Cumulatively, PCA results confirm major differences in percent neutralization across time between VSR and VMR groups indicated by unsupervised clustering (**Figure 28A**) and identified by significance testing (**Figure 28B**).

A post hoc power analysis was performed to compute achieved β given α (0.05), sample size (N = 105), and effect size ($R^2 = 0.3$). With these parameters, power was calculated for a two-tailed, random-model linear multiple regression (exact test) with 14 predictors; power (i.e., $1 - \beta$) was calculated to be 0.974 (**Figure 29**).

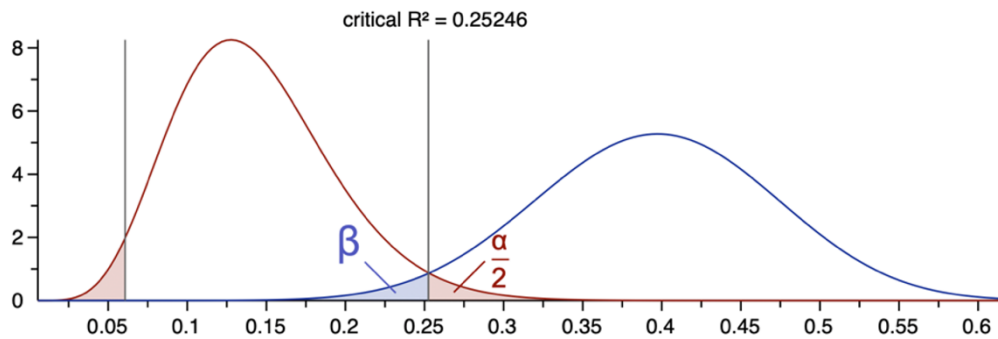


Figure 29. Post hoc power analysis of paired longitudinal data. Computation of power analysis set given α (0.05), sample size ($N = 105$) and effect size ($R^2 = 0.3$). Statistic calculated for two-tailed, random-model linear multiple regression (exact test) with 14 predictors: power ($1 - \beta$) = 0.974.

Clustering analyses of paired longitudinal data statistically favored vaccinated subjects categorized as two groups. However, a third, loosely clustered population ($n = 7$) can be visualized within the VMR group (**Figure 28C**, red circle). Although this minor subgroup is not statistically defined, all seven subjects showed a particularly weak neutralization response to vaccination and subsequent poor durability. As such, this group was identified as vaccine poor responders (VPRs). Average percent neutralization at post-second- and post-third-dose timepoints was 31% and 54%, respectively (**Figure 28D**). The seven VPRs identified in **Figure 28C** were an average age of 68 years old and were 57% male.

Breakthrough Infections

During the last 4 months of this study (December 2021–March 2022), Omicron became the dominant variant circulating in the study population. Prior to the Omicron surge in the United States and throughout the Delta variant wave, we observed only 14 PCR-confirmed breakthrough infections in our study population of mRNA vaccine recipients. Ninety-three percent (13/14) of these breakthrough infections occurred when NAb titers were <1:80 (**Figure 30**). These thirteen breakthrough infections demonstrated an average of 16% neutralization (median 17%, range 0–84%) prior to infection. Only one individual in the pre-Omicron breakthrough population had a NAb titer >1:80.

Conversely, 14 individuals that had high NAb titers ($\geq 1:640$ [$n = 9$], $\geq 1:320$ [$n = 2$] and $\geq 1:160$ [$n = 3$], average 90% neutralization) after receiving a third mRNA vaccine dose became symptomatic with a breakthrough infection, as Omicron had already become the dominant variant in circulation,¹⁵⁶ (range 67–99%, median 97%) (Supplementary Figure S5). The majority of the individuals with Omicron breakthrough infections had titers $\geq 1:320$ ($\geq 80\%$ neutralization) to the ancestral-strain RBD used in our test prior to natural infection. Population demographics, vaccination data, and time between NAb and PCR testing are shown in the Supplementary Materials (**Table 5**).

Figure 30 demonstrates NAb titers prior to breakthrough infection in a population infected prior to the emergence of the SARS-CoV-2 Omicron variant (Delta variant or earlier), compared to a population infected during the Omicron wave.

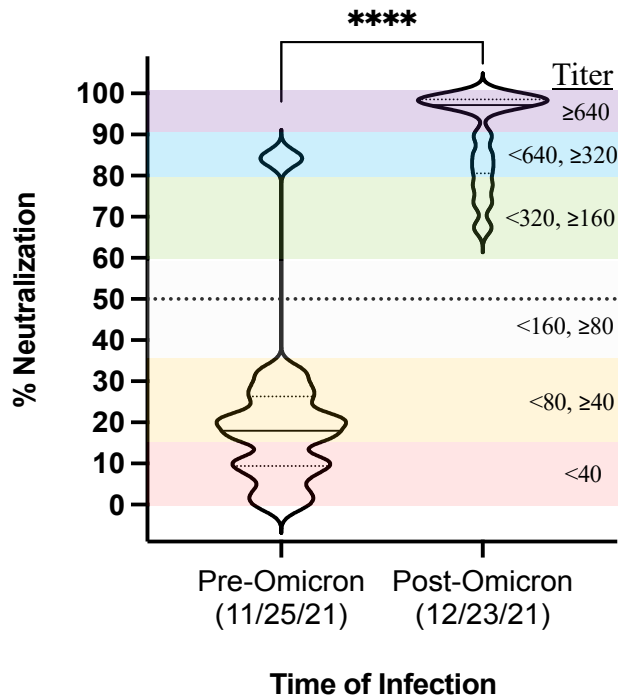


Figure 30. NAb titers of naturally infected subjects pre and post Omicron dominance. NAb data prior to infection are shown as percent neutralization violin plots where solid black lines represent median, and dotted black lines indicate upper and lower quartiles. A single outlier in the pre-December 2021 group had 84% neutralization prior to infection, however, was on the 2nd week of a 40 mg/day prednisone taper at the time of infection. Demographic information pertaining to individuals in both groups are detailed in Table 5.

Table 5A and B are provided in reference to **Figure 30**, to give readers additional information regarding the time between vaccination, NAb testing, and confirmed breakthrough infection.

A

Age	Sex	1 st /2 nd Dose mRNA Vaccine	3rd Dose mRNA Vaccine	Date of 3rd Dose	Pre-Infection NAb Test	Pre- Infection % Neut. (NAb Titer)	Date of PCR+	NAb Test to PCR+ (days)
31-35	M	mRNA-1273	mRNA-1273	Nov-2021	Dec-2021	98.9 (>1:640)	Jan-2022	26
61-65	F	BNT162b2	BNT162b2	Oct-2021	Dec-2021	98.8 (>1:640)	Dec-2021	19
56-60	F	BNT162b2	BNT162b2	Oct-2021	Jan-2022	98.8 (>1:640)	Jan-2022	17
46-50	F	BNT162b2	mRNA-1273	Sep-2021	Dec-2021	98.5 (>1:640)	Jan-2022	34
51-55	F	BNT162b2	mRNA-1273	Oct-2021	Dec-2021	98.5 (>1:640)	Jan-2022	27
51-55	F	BNT162b2	BNT162b2	Oct-2021	Dec-2021	98.4 (>1:640)	Jan-2022	20
36-40	F	BNT162b2	mRNA-1273	Nov-2021	Nov-2021	97.4 (>1:640)	Jan-2022	60
46-50	M	BNT162b2	mRNA-1273	Aug-2021	Nov-2021	96.9 (>1:640)	Jan-2022	34
46-50	M	BNT162b2	BNT162b2	Oct-2021	Dec-2021	89.7 (>1:640)	Jan-2022	27
41-45	F	BNT162b2	BNT162b2	Oct-2021	Dec-2021	85.0 (>1:320)	Jan-2022	25
66-70	M	mRNA-1273	mRNA-1273	Oct-2021	Dec-2021	81.6 (>1:320)	Jan-2022	30
61-65	M	BNT162b2	BNT162b2	Aug-2021	Dec-2021	77.6 (>1:160)	Dec-2021	18
41-45	F	BNT162b2	BNT162b2	Oct-2021	Dec-2021	73.4 (>1:160)	Jan-2022	24
36-40	F	mRNA-1273	mRNA-1273	Sep-2021	Jan-2022	67.4 (>1:160)	Jan-2022	6

B

Age	Sex	1 st /2 nd Dose mRNA Vaccine	Date of 2nd Dose	Pre-Infection NAb Test	Pre-Infection % Neut. (NAb Titer)	Date of PCR+	NAb Test to PCR+ (days)
46-50	M	BNT162b2	Mar-2021	Sep-2021	84.2 (>1:320)	Sep-2021	8
31-35	M	BNT162b2	Jan-2021	Apr-2021	32.3 (<1:80)	Oct-2021	187
26-30	F	BNT162b2	Jan-2021	Jul-2021	28.5 (<1:80)	Aug-2021	18
61-65	M	BNT162b2	Jan-2021	Aug-2021	25.6 (<1:80)	Sep-2021	20
76-80	F	BNT162b2	Jan-2021	May-2021	21.3 (<1:80)	Jul-2021	61
31-35	F	mRNA-1273	Mar-2021	Sep-2021	20.8 (<1:80)	Nov-2021	40
51-55	M	BNT162b2	Feb-2021	Sep-2021	19.4 (<1:80)	Sep-2021	8
51-55	F	mRNA-1273	Feb-2021	Aug-2021	16.6 (<1:80)	Sep-2021	21
76-80	M	BNT162b2	Feb-2021	May-2021	16.3 (<1:80)	Jul-2021	53
51-55	F	mRNA-1273	Feb-2021	Sep-2021	10.8 (<1:40)	Nov-2021	69
56-60	M	BNT162b2	Feb-2021	Oct-2021	10.1 (<1:40)	Oct-2021	3
81-85	F	BNT162b2	Feb-2021	Sep-2021	7.3 (<1:40)	Oct-2021	23
46-50	F	BNT162b2	Feb-2021	Oct-2021	2.9 (<1:40)	Nov-2021	43
41-45	F	BNT162b2	Mar-2021	Aug-2021	0.0 (<1:40)	Sep-2021	17

Table 5. Breakthrough infection population demographics. (A) Pre-Omicron and (B) Post-Omicron population demographics, vaccination status, and NAb result preceding infection. Age, sex, 1st/2nd vaccine dose and date, 3rd dose vaccine and date (if applicable), date of last NAb test prior to infection, pre-infection NAb result, date of positive PCR for SARS-CoV-2 detection, and days between NAb and PCR dates are detailed in these tables. Pre-infection NAb test result is shown as % neutralization, calculated using the limit of detection our rapid NAb lateral flow as described previously. Average age of the pre- and post-December 2021 populations were 54 and 49 (median 55 and 49.5), respectively. Populations in (A) and (B) were 57% and 64% female, respectively.

Discussion

In this manuscript, we report durability of RBD-NAb levels elicited by second and third doses of COVID-19 mRNA vaccines, BNT162b2 and mRNA-1273, using a quantitative rapid test. Our study demonstrates three main findings: (i) a third vaccine dose elicits NAb titers that are higher and more durable than a second dose; (ii) the increase in NAb titers and durability of response are independent of vaccine manufacturer; and (iii) high titer NABs elicited by a third vaccine dose for which mRNA sequences encode spike glycoprotein of the Wuhan-Hu-1 SARS-CoV-2 isolate do not protect against infection and symptomatic disease with Omicron variants, but appear to protect against severe disease and hospitalization.

One striking feature of our data is the wide range of individual NAb titers elicited by a second vaccine dose. This observation is most notable in BNT162b2 vaccine recipients compared to mRNA-1273 vaccine recipients post-second-dose (**Figure 24A**). When NAb titers should be at their highest levels, 2–4 weeks after vaccination, nearly one-quarter of BNT162b2 recipients did not reach NAb levels of 50%.¹⁴⁸ Two to four weeks after the second dose, mRNA-1273-vaccinated individuals exhibited significantly

higher NAb titers relative to BNT162b2-vaccinated individuals ($p < 0.0005$) and retained significance through month 5 ($p < 0.05$ – 0.0005). By six months after the second dose, both groups fell below 50% neutralization and no significant difference was observed. These findings demonstrate that although the vaccines elicit high-titer NABs in the majority of recipients, a large portion of a population that is currently considered to be fully vaccinated with two doses may not have mounted adequate protective NAB responses. The wide range of individual responses highlight the need for accessible NAB testing for individualized vaccine response monitoring. However, we wish to note that this study did not measure T-cell reactivity, an important component of long-term immunity postvaccination.¹⁵⁷

We observed that a third mRNA vaccine dose was highly effective in inducing NAB titers $>1:640$ at 2–4 weeks postvaccination, independent of vaccine manufacturer (Figure 3B). Both BNT162b2 and mRNA-1273 groups exhibited higher and more durable titers ($\leq 1:320$, $>1:160$) that neutralized $\geq 60\%$ 6–8 months after vaccination, although mean titers for the mRNA-1273 group were slightly higher. Interestingly, at month 5, the mixed vaccine group demonstrated a significant increase in neutralization relative to the group that received all three BNT162b2 doses (**Figure 24C**). No differences in mean titers between mixed and non-mixed vaccine groups were observed at 6–8 months; however, when comparing median titers of mixed and non-mixed groups, we observed an 8–12% neutralization increase in the group that received three mRNA-1273 doses compared to those that received three doses of BNT162b2 or mixed vaccines, respectively. The group that received all three mRNA-1273 vaccines had mean titers

more proximal to the 1:320 to 1:640 range, measured 6–8 months following their last vaccination, suggesting increased durability for mRNA-1273 vaccine recipients.

Statistical analysis of unpaired percent neutralization data revealed two distinct groups within our second- (n = 265) and third-dose (n = 142) populations (**Figure 26**), moderate responders (VMRs), and strong responders (VSRs). Analyses of paired second- and third-dose longitudinal data (n = 105) also demonstrated VMRs and VSRs as two statistically distinct groups; however, we observed a small subgroup of subjects (n = 7) statistically clustered within the VMR group that we called VPRs, shown in **Figure 28C**. Paired longitudinal data for these seven subjects demonstrated suboptimal RBD neutralization in response to vaccination, combined with poor durability of those responses, rarely neutralizing greater than 50% (**Figure 28D**). Although a minor subpopulation, VPRs highlight a group of otherwise healthy individuals that fail to mount high-titer protective antibody responses to mRNA vaccination, and likely do not know that their vaccine did not elicit high-titer protective NAbs. Ongoing investigations in our laboratory aim to investigate T-cell differences in VSR, VMR, and VPR groups, but are beyond the scope of this report.

NAbs as a correlate of protection remain undefined and are complicated by evolving variants, demonstrated by data shown in **Figure 30**. As the technology is available to rapidly measure titers of protective NAbs and is fairly easily modified to the circulating variant, it is possible to deploy variant-specific rapid tests on a large scale to establish a probability of infection based on titers of RBD-Nabs that reflect the variant(s) in circulation.

Limitations of our study include the surrogate nature of the rapid test, which detects NAb that block RBD from binding to ACE2. The test does not detect antibodies that neutralize by binding to the N-terminal domain¹¹¹ or outside the RBD-ACE2 binding site.^{94,112,118} However, the RBD is a major determinant of neutralization,¹¹⁸ and FDA approved therapeutic monoclonal antibodies block RBD from binding to ACE2.^{120,158}

Another limitation is in the cohort of mixed vaccines. Study participants who mixed vaccines received BNT162b2 as their first and second doses and mRNA-1273 as a third dose, but we had only one participant who received two doses of mRNA-1273 followed by a third dose of BNT162b2 (**Figure 22**). Although mean NAb titers declined to lower levels in BNT162b2 vaccine recipients than in mRNA-1273 recipients, they were both in the <1:160, ≥1:80 range at 6–8 months.

It is well-established that COVID-19 mRNA vaccines protect against severe disease and hospitalization, but protection wanes over time¹³¹ and a probability of infection at given NAb titers is not known, although multiple models have been reported.^{117,159} For example, is an individual with a NAb titer of 1:320 considered to be ‘twice’ as well protected from infection as someone with a NAb titer of 1:160? This question is difficult to answer and is confounded by evolving SARS-CoV-2 variants such as Omicron and its subvariants, as well as other effector functions of binding antibodies and cell-mediated immune responses.

Prior to December 2021 and throughout the Delta wave, breakthrough infections occurred almost exclusively in study participants whose NAb titers were <1:80, suggesting that titers below 1:80 might not protect against symptomatic infection. However, when Omicron displaced Delta as the dominant variant in circulation, even

individuals with high titers (>1:320) elicited by a third vaccine dose of vaccine became symptomatically infected.

To be considered fully vaccinated at the time of this writing, one must have received two doses of either mRNA vaccine or a single dose of Ad26.CoV2.S.¹⁶⁰ Our data suggest that a third dose provides a more durable NAb response than two doses and support the likely need for subsequent booster vaccines after the second and third doses.

As is evident by surges in Omicron cases across the United States,¹⁶¹ many of which are symptomatic infections in “boosted” individuals months out from their last vaccine,^{145,161} additional vaccinations containing one or more Omicron variant(s) spike encoding mRNA may be warranted. It is unclear at this time what the evolutionary space of SARS-CoV-2 will be, and what the frequency of vaccination to protect against symptomatic infection will be. Our results, along with many other reports of breakthrough infections in third-dose recipients,¹⁶¹ implicate the importance of variant-specific booster vaccines. Furthermore, individuals’ responses to variant-specific vaccines could be monitored using a rapid NAb test.

While many have called for NAb test accessibility, we acknowledge that this remains a heavily debated topic, as the implications of that knowledge are not clearly defined. We wish to highlight the importance of quantifying protective antibodies, particularly in people who have high contact with vulnerable populations, which include but are not limited to immunosuppressed and immunodeficient individuals, cancer and transplant patients, and elderly people, in addition to vulnerable individuals themselves. This is the first study that reports individual mRNA vaccine-induced NAb responses longitudinally using a rapid test. It demonstrates that an accessible NAb test may prove

useful so that individuals and their healthcare providers can make informed decisions about vaccination and boosting, based on their risk tolerance potential for infection with SARS-CoV-2.

CHAPTER V

DEVELOPMENT OF SARS-COV-2 VARIANT-SPECIFIC NEUTRALIZING ANTIBODY LATERAL FLOW ASSAYS

Introduction

Emergence of the SARS-CoV-2 B.1.1.529 (BA.1) Omicron variant began in November of 2021¹⁶² just months after the Delta wave peaked in July, and was followed by the largest waves of infection thus far in the COVID-19 pandemic. In December of 2021, we observed an increased frequency of breakthrough infections while conducting our longitudinal mRNA vaccine-induced NAb study, compared to the few we observed during Delta and prior waves. At that time, many study participants had received a third mRNA vaccine dose, either homologous or heterologous to the primary two-series vaccine received. Despite NAb titers $\geq 1:640$ induced by a third vaccine dose encoding ancestral spike protein measured just a week prior, Omicron (BA.1) infected many vaccinated individuals with high titer peripheral NAbS against ancestral spike protein. The global conversation surrounding a likely need for variant-specific vaccines began shortly after the emergence of Omicron.

NAbS have been proposed as a potential ‘correlate of protection’ (CoP)^{125,163} to assess probability of SARS-CoV-2 infection at a given time, however, the idea is heavily confounded by the emergence of evolving variants. If such a metric is to be established using NAbS as the correlate, quantification of NAbS which target ancestral spike protein encoded by initial COVID-19 mRNA vaccines is obsolete and therefore, variant-specific NAb tests are critically needed. To address this critical need, we developed a BA.1-specific NAb LFA and performed corresponding validation studies. However, by the time

these studies were completed, BA.1 had been replaced as the dominant variant in circulation, thus our utility for the BA.1 LFA was limited.

New omicron subvariants quickly evolved in the months that followed, and BA.4/5 eventually emerged as the dominant variant in the US, in July of 2022.^{164,165} With the same intention, to quantify variant-specific NAb, we began modification of the BA.1 NAb LFA to contain BA.5 spike protein, and conducted corresponding validation experiments. In this chapter, we present data generated for the development and validation of BA.1 and BA.5-specific NAb LFAs, in addition to correlation/regression analyses demonstrating the relationship between LFA density values and IC₅₀ values obtained using live virus FRNT assays in the BSL-3 laboratory. We observed a significant negative correlation for both BA.1 and BA.5 NAb LFAs, as density values are inversely proportional to NAb concentrations. Our BA.5 NAb LFA is currently being used as part of a collaborative sero-surveillance study at Arizona State University, for which we have tested more than 1,000 serum samples thus far. This collaborative work remains ongoing and is therefore otherwise omitted from this dissertation, however, we hope the example may provide insight to the potential utilities of this assay.

Methods

Specimen collection

Subjects were recruited and enrolled in these cohorts based on sequencing-confirmed infection with BA.1 or BA.5 SARS-CoV-2 variants. Ten milliliters of whole blood were obtained from all subjects with informed consent under a protocol approved by the Arizona State University Institutional Review Board (IRB #0601000548). Blood

was coagulated and processed for serum isolation, aliquoted, and stored at -80°C until thawed for use.

NAb LFA testing

Serum was thawed on ice and mixed well prior to use. NAb LFAs were run in duplicate using 6 μ L of serum, followed by 50 μ L of chase buffer per test. Tests were left to run undisturbed for 10 minutes prior to reading. All tests were read using a RDS-2500 (Detekt Biosciences) portable benchtop densitometer.

Focus Reduction Neutralization Test (FRNT)

To determine IC₅₀ values for serum samples, we performed FRNT assays using 13 convalescent BA.1 sera, and 10 convalescent BA.5 sera. IC₅₀ values for validation of the BA.1 NAb LFA were obtained from FRNT infections using BA.1 virus, and BA.5 IC₅₀ values from BA.5 virus. Assays were performed under high-containment facilities as previously described.

Data analyses

NAb LFA density values and IC₅₀ values were imported into GraphPad Prism, Log₂-transformed, then analyzed using a correlation/linear regression curve fit. Equations derived from the correlation/regression analyses were used to calculate predicted IC₅₀ values, which were extrapolated to NAb titer as previously described (Chapter III, page 49). Data are also normalized to percent neutralization using the limit of detection specific to each assay, as described.^{32,148,166}

Results

To quantify SARS-CoV-2 variant-specific neutralizing antibodies, we developed a BA.1 and BA.5 NAb LFAs in the same manner as the original test. We demonstrate validation of the BA.1 NAb LFA using 13 serum samples from individuals with sequencing-confirmed BA.1 infections and determined IC_{50} values for these samples by FRNT in the BSL-3 laboratory using SARS-CoV-2 BA.1.1.529 virus, such that LFA density values could be correlated with known titers or IC_{50} values. We observed a significant correlation ($r = -0.91$, $p < 0.0001$) between IC_{50} and LFA density (**Figure 31**), indicating the BA.1-specific test was a suitable surrogate for gold-standard neutralization assays.

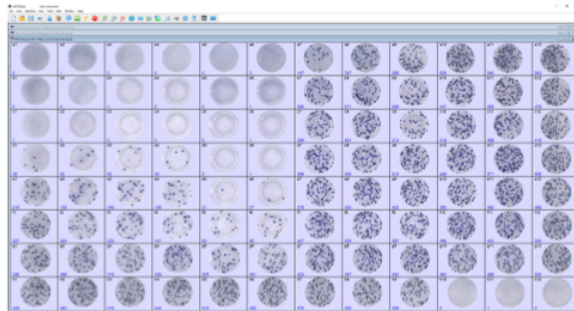
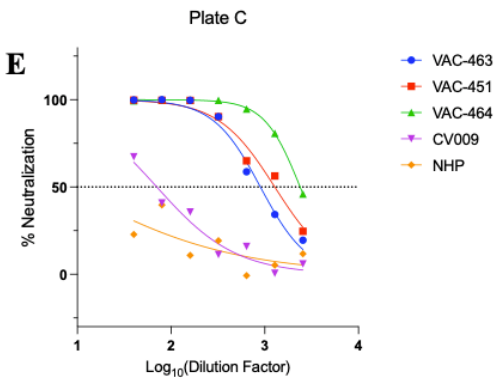
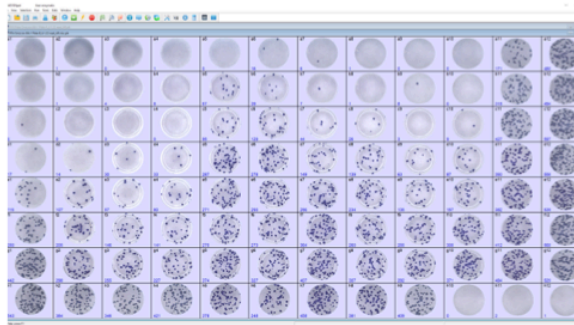
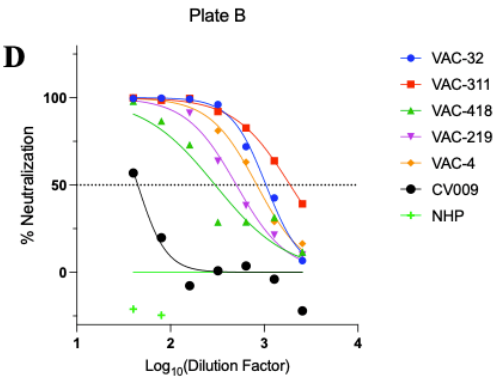
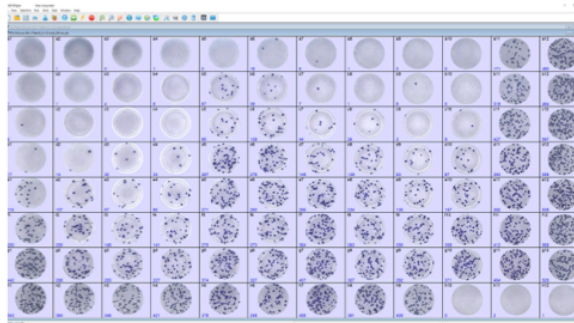
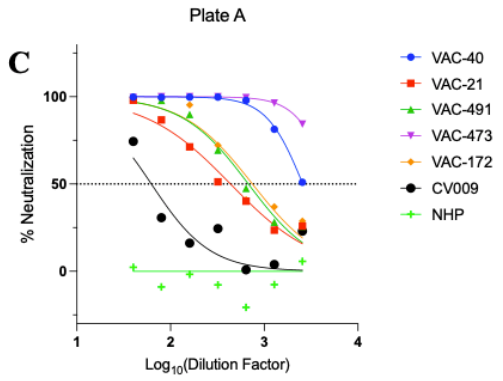
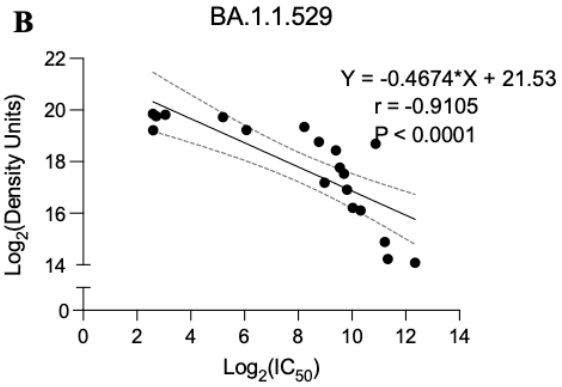
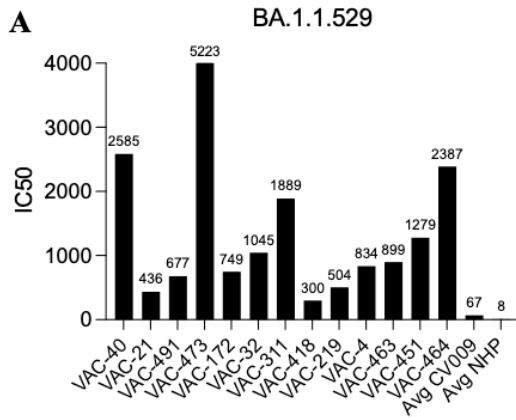


Figure 31. Validation of a BA.1-specific NAb LFA. (A) IC_{50} values for all samples obtained from dilution curves seen in (C-E). (B) Density values and IC_{50} values were Log_2 -transformed and analyzed using a simple linear regression and nonparametric Spearman correlation with two-tailed P value and a 95% confidence interval (CI). Regression analysis with 95% CI boundaries is indicated in solid black and grey dotted lines. Spearman's rho and two-tailed P value are labeled. (C-E) Titration curves from all BA.1-infected FRNT plates (left) represented as Log_{10} dilution factor (x-axis) and percent neutralization (y-axis), and FRNT plate images (left).

Using 10 serum samples isolated from BA.5-infected individuals we performed FFA experiments in the BSL-3 laboratory using SARS-CoV-2 BA.5 virus to determine BA.5-specific NAb titers of the convalescent sera. We observed a significant correlation ($r = -0.81, p < 0.006$) between IC_{50} and NAb LFA density (**Figure 32**), and used the equation ($y = -1.037 * X + 24.90$) derived from a linear regression analysis to predict IC_{50} values from a given LFA density. Using this equation, we established density unit ranges which correspond to predicted IC_{50} calculations, NAb titers, and percent neutralization (**Table 6**).

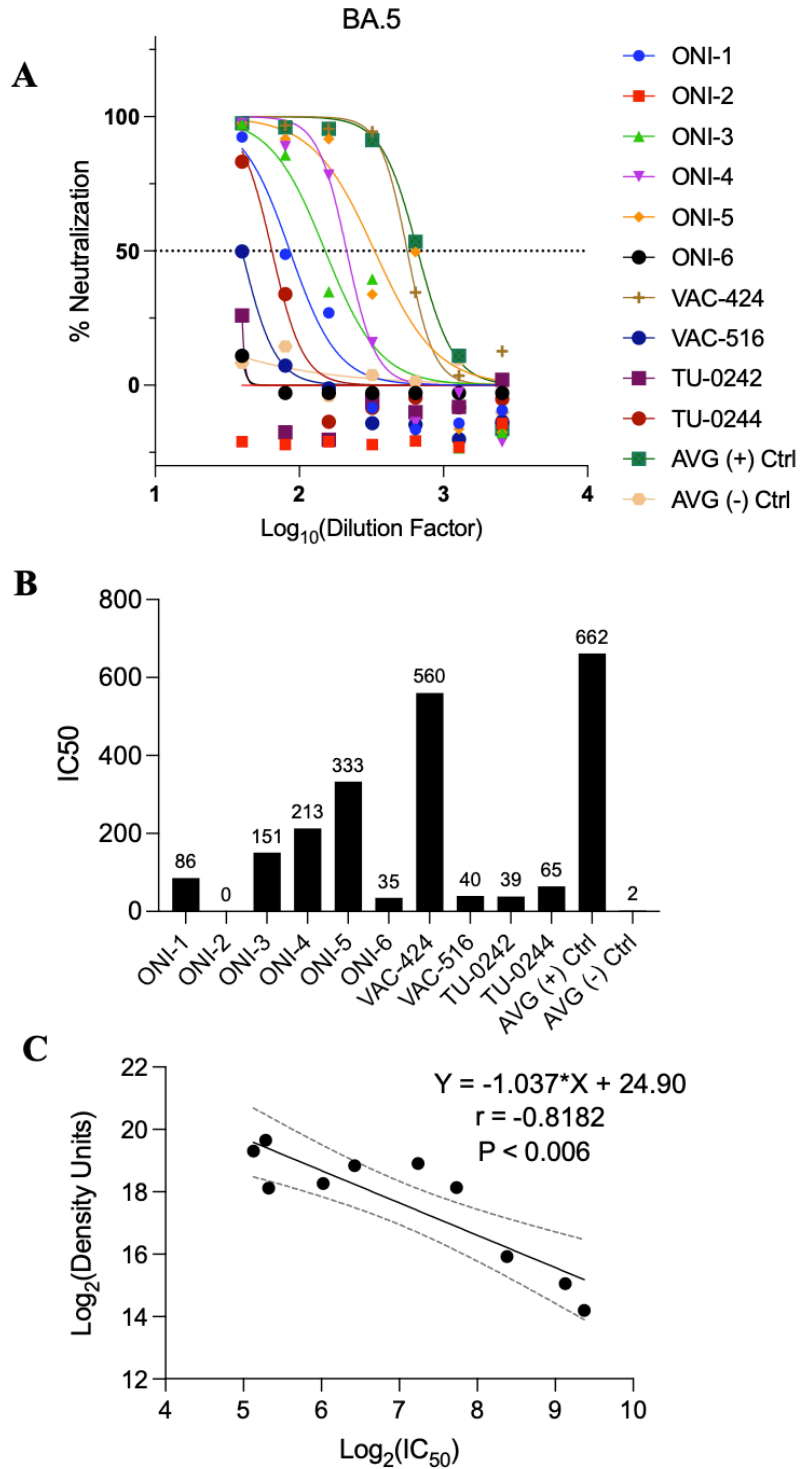


Figure 32. Validation of a BA.5-specific NAb LFA. (A) Serum titration curves from all samples represented as Log_{10} dilution factor (x-axis) and percent neutralization (y axis). Dotted line represents 50% neutralization. (B) IC_{50} values derived from serum titration

curves shown in (A). (C) Density values and IC₅₀ values were Log₂-transformed and analyzed using a simple linear regression and nonparametric Spearman correlation with two-tailed P value and a 95% CI. Regression analysis with 95% CI boundaries is indicated in solid black and grey dotted lines. Spearman's rho and two-tailed P value are labeled.

Density	IC ₅₀	Reciprocal NAb Titer	% Neutralization
37,999 to 18,770	1280.02 to 648.37	1280 to 640	97 to 95%
77,999 - 38,000	648.37 to 324.08	640 to 320	95 to 89%
159,999 - 78,000	324.08 to 162.09	320 to 160	89 to 78%
329,999 - 160,000	162.09 to 80.65	160 to 80	78 to 54%
330,000 - 680,000	80.65 to 40.16	80 to 40	54 to 6%
> 700,000	39.05	≤ 40	3%

Table 6. BA.5 NAb LFA Density unit conversion to IC₅₀, reciprocal NAb titer, and percent neutralization. Density dynamic range is represented as 18,770 density units to >700,000 density units. IC₅₀ dynamic range is represented as 39.05-1280.02, corresponding to NAb titers of ≥ 40 and ≥ 640, respectively. Reciprocal NAb titers range from 40 to 1280, and % neutralization ranges from 3 to 97%.

Discussion

Interestingly, in our original NAb cohort, we found that even subjects with high NAb titers (>1:640) became symptomatically infected once Omicron emerged as the dominant SARS-CoV-2 variant in circulation. This led us to question whether the NAbS measured by our LFA were no longer neutralizing in the context of new circulating SARS-CoV-2 variants. Thus, we validated LFAs for measurement of two SARS-CoV-2 Omicron subvariants, BA.1 and BA.5. We collected convalescent sera from PCR-

confirmed naturally infected subjects and conducted FRNT assays using live SARS-CoV-2 virus for each variant. Through gold standard FRNT assays, we were able to calculate IC_{50} values and reciprocal NAb titers, which were then correlated back to LFA density units to generate a standard curve, such that units can be converted between LFA density ranges, NAb titers, IC_{50} values, and percent neutralization. Successful validation of two additional NAb LFAs that assess neutralization capacity to a SARS-CoV-2 Omicron variants potentially enables: 1) rapid and longitudinal monitoring of antibody responses following new variant specific booster vaccinations, 2) ability to assess neutralization potential (and thus degree of protection) against circulating variants, and 3) investigation into the magnitude of different NAb responses generated against different variants following natural infection or variant-specific immunization.

CHAPTER VI

T CELL AND CYTOKINE PROFILING OF SARS-COV-2 MRNA VACCINE INDUCED NEUTRALIZING ANTIBODY POOR RESPONDERS

Introduction

Severe acute respiratory syndrome coronavirus-2 (SARS-CoV-2), causative pathogen of Coronavirus Disease 2019 (COVID-19), emerged in December of 2019 and was declared a pandemic by World Health Organization (WHO) in March of 2020.⁴⁰ In the first year of the SARS-CoV-2 pandemic, prior to vaccines and monoclonal antibody therapeutics, when COVID-19 convalescent plasma (CCP) was the most specific treatment available, our laboratory developed a ten-minute lateral flow assay (LFA) to quantify SARS-CoV-2 neutralizing antibodies (NAbs) in whole blood, plasma, or serum.³² Initially, we developed this LFA for rapid quantitation NAbs in CCP, as the literature at the time reported ~30% of naturally infected individuals fail to generate NAbs throughout convalescence.⁵² Although CCP administration was near obsolete by the time our assay was validated, we used our NAb LFA to conduct an 18-month longitudinal study which measured COVID-19 mRNA vaccine-induced NAbs after 1st, 2nd, and 3rd doses in more than 500 individuals.¹⁶⁶

Longitudinal NAb surveillance following mRNA vaccination led to the identification of three distinct response groups, each of which exhibited a unique trend in neutralization following 2nd and 3rd vaccinations. First, the vaccine strong responders (VSRs) were those that mounted high NAb titers ($\geq 1:640$) and sustained high titers for several months following 2nd and 3rd vaccinations. Moderate responders (VMRs) initially

mounted high titers, however, the VMR group waned much more rapidly when compared to VSRs, most notably after 3rd dose.¹⁶⁶ Lastly, there remained a small population of individuals for which *three* doses of COVID-19 mRNA vaccine failed to induce peak mean NAb titers $\geq 1:160$, termed, vaccine poor responders (VPRs). Despite low/no titer NAb following 2nd and 3rd vaccination, VPRs are otherwise healthy individuals that range in age from 37 to 73 years old (46% female). Further, all subjects classified as VPRs, VMRs, and VSRs, followed comparable, standard vaccination protocols (informed by CDC and FDA guidance) with respect to timing of first, second, and third immunizations. Consequent to our longitudinal study, we questioned if other immunologic memory compartments were hindered in these VPR individuals, and how they compared to VMR and VSR groups.

Immunologic memory, the basis of vaccination, is often generated naturally following primary pathogen exposure and persists following pathogen clearance. Antigen-specific memory cells of the adaptive immune system (B cells, CD4⁺ T cells, and CD8⁺ T cells) are already primed by vaccination or natural infection to respond to pathogen and thus facilitate early control of pathogen entry and dissemination.^{167,168} The cellular arm of the adaptive immune system refers to antigen-specific CD4⁺ and CD8⁺ T cells that facilitate extracellular and intracellular pathogen clearance through secretion of various inflammatory chemical signals (cytokines and chemokines) or through cell-cell contact mediated killing of virally infected cells, respectively. The humoral arm of the adaptive immune system refers to antigen-specific B cells and the antibodies they secrete. In the context of viral infection, a primary goal of immunization is to elicit the production of neutralizing antibodies (NAbs),¹⁶⁹ such that intracellular infection is limited by a first-

line humoral immune response. An equally crucial goal of immunization is the elicitation of a durable memory CD8⁺ T cell population for early identification and killing of virally infected host cells to limit viral replication and spread. In addition, cytokines and chemokines secreted by memory CD4⁺ T cells limit viral replication at sites of infection.^{170,171} Recently, a critical role for T follicular helper cells (Tfh), a specialized population of CD4⁺ T cells in secondary lymphoid tissues, in facilitating B cell activation/proliferation, germinal center (GC) formation, and production of high affinity NAbs has been described.^{173,174} Although Tfh cells act in lymphoid tissues sites in the context of inflammation/vaccination, a population of circulating Tfh (cTfh) cells have been identified in peripheral blood after GC dissolution. cTfh cells are thought to function as a memory compartment for prior GC reactions, poised to quickly seed formation of GCs upon subsequent antigen encounters.¹⁷²

In the context of SARS-CoV-2, durable anti-spike IgG antibodies, memory B cells, as well as circulating memory CD4⁺ and CD8⁺ T cells have been detected 6-8 months after infection, supporting the idea that diverse memory responses arise following natural infection.¹⁶⁷ In addition to SARS-CoV-2-specific CD4⁺ and CD8⁺ T cell responses, robust circulating follicular helper T cell (cTfh) memory was observed ≥ 6 months post-infection in several cohorts.¹⁷²

T follicular helper (Tfh) cells, conventionally defined as CD4⁺CXCR5⁺ T cells expressing the transcription factor Bcl6, provide critical cognate help to antigen-specific B cells in germinal center (GC) reactions to initiate and maintain humoral immune responses,⁸³ and are crucial for the generation of high affinity NAbs.^{173,174} Upon antigen encounter, Tfh cells can localize to secondary lymphoid tissues where they interact with

cognate B cells at the border between the B cell follicle and T cell zone, to undergo further maturation and imprinting of Tfh fate.^{83,175} Committed Tfh cells can then penetrate the B cell follicle and initiate GC formation.¹⁷⁵ Tfh cells residing within the GC light zone are thought to arbitrate GC B cell affinity-driven competition, as well as GC B cell proliferation and differentiation into plasma or memory B cells which reflect the quality of cognate B and Tfh cell interactions.⁸³ Our interest in Tfh cells arose early in the COVID-19 pandemic, when a loss of Bcl6 expression and GC formation was shown in cohort of individuals with severe natural infections.¹⁷⁶ In several other naturally infected populations, spike-specific cTfh were observed to correlate with NABs and increase during early convalescence.^{172,177} Additionally, cTfh cells were associated with reduced disease severity, and are observed to further increase in frequency over time.¹⁷⁸

In a vaccination context, COVID-19 mRNA vaccines, BNT162b2 (Pfizer) and mRNA-1273 (Moderna), both elicited robust spike-specific CD4⁺ T cell activation comparable to or higher than that of previously infected individuals. Vaccine-induced memory CD4⁺ T cells were detected in nearly 100% of individuals 6 months after second vaccination for both BNT162b2 and mRNA-1273 cohorts.^{179,180,181} Additionally, vaccine-elicited CD4⁺ cTfh numbers were reported to be stably maintained for 6 months post vaccination and strongly correlate with NAb response magnitude.¹⁸² Interestingly, changes in cTfh phenotype have also been observed by multiple groups in the first months following vaccination.^{181,183,184} mRNA vaccine-induced spike-specific CD8⁺ T cells, however, are observed to wane more rapidly in comparison to CD4⁺ cells, although frequencies of vaccine-induced CD8⁺ T cells were comparable to previously infected individuals at 6 months.¹⁷⁹ Spike specific CD8⁺ T cells were detectable in 41-65% of

individuals at 6 months following second mRNA vaccination,¹⁸¹ although more recent reports demonstrate transient re-activation of CD8⁺ T cells following 3rd and 4th vaccine doses.¹⁸⁵

Following our longitudinal NAb study, we hypothesized that vaccine-induced CD4⁺ and CD8⁺ T cells in VPR, VMR, and VSR groups would either be reflective of their NAb response magnitudes (i.e. VPRs show both low T cell and NAb responses vs VMR and VSR), *or* that T cell responses would be enhanced in VPRs to compensate for low NAb titers (i.e. VPRs show stronger T cell activation vs VMR and VSR). We further hypothesized that mRNA vaccine-induced NAb response groups could be defined by unique cellular immunity profiles, including differences in activated CD4⁺ and CD8⁺ T cell abundance, T follicular helper cell activation and abundance, and cytokine mediated signaling.

To assess CD4⁺ and CD8⁺ T cell activation, we used activation-induced marker (AIM) assays to evaluate spike-specific T cell responses in VPR, VMR, and VSR peripheral blood mononuclear cells (PBMCs) following stimulation with overlapping peptide megapools spanning the full-length spike protein. We also evaluated abundance and activation of cTfh cells across NAb response groups. Further, as varying immunophenotypes of CXCR5⁺ Tfh cells have been reported to differentially influence B cell engagement and antibody production, we assessed classically defined cTfh phenotypes by assessment of cell surface expression of chemokine receptor CCR6 and CXCR3.¹⁸⁶ To evaluate cytokine differences, we used a multi-analyte human cytokine bead-based multiplex assay (LegendPLEX, BioLegend) to quantify 25 cytokines in the culture supernatant of peptide-stimulated PBMCs across donor groups.

We observed comparable antigen-specific CD4⁺ and CD8⁺ T cell activation in VPR subjects relative to VMR and VSR groups, indicating that the VPR population indeed generated an antigen-specific T cell response to mRNA vaccination. When evaluating *bulk* cTfh (CD4⁺CXCR5⁺) cells, we observed a significantly increased frequency of CCR6⁺CXCR3⁻ (cTfh17-like) cells in VPRs relative to VMRs, however, *activated* cTfh characterized by OX40 and CD40-L expression demonstrated significantly increased CCR6⁻CXCR3⁺ (cTfh1-like) cells in VPRs, relative to VMRs and VSRs. Interestingly, while analyzing the AIM data set, we also observed increased frequencies of CD4⁺CD8⁺ and CD8^{low} T cells within the VPR group. Most unexpectedly, we observed VPRs to have a significant increase in mean frequency of CXCR5⁺ CD8⁺ T cells as a frequency of CD3⁺ cells, compared to VMRs and VSRs.

Materials and Methods

Experimental Design

The purpose of this study was to evaluate CD4⁺ and CD8⁺ T cell responses in COVID-19 mRNA vaccinated subjects previously classified as having poor (VPR, $n = 11$), moderate (VMR, $n = 5$), or strong (VSR, $n = 7$) NAb responses to vaccination, in addition to naturally infected individuals ($n = 6$) and pre-December 2019 normal donors ($n = 8$). Vaccinated subjects were asked to provide a one-time whole blood donation following informed consent, which was then processed for isolation of PBMCs and plasma. All donor PBMCs and plasma were aliquoted and frozen at -80°C prior to liquid nitrogen preservation, such that a single thaw was applied consistently throughout

experiments. Cells were stimulated with peptide and assessed for antigen-specific activation via multi-color cell surface marker staining, and data were collected via flow cytometry. Supernatant was harvested from stimulated cells, stored at -80°C, then ultimately used for cytokine quantitation via multiplex bead-based assay read via flow cytometry.

Subject Recruitment and Enrollment

Male and female adults ranging in age from 26 – 73 years old upon entry into the study were recruited and enrolled with informed consent under a protocol approved by the institutional review board at Arizona State University (IRB #0601000548). Participants in the T cell study were pre-selected from our previous longitudinal NAb study¹⁶⁶ on the basis of having met criteria for VPR, VMR, and VSR response group status. Subjects were contacted via email as was detailed in the consent initially obtained for NAb study enrollment and asked if they were willing to provide a one-time, 80 mL (8 x 10 mL tubes) blood donation. Willing donors were brought back into the laboratory for blood collection, provided with new informed consent, and were compensated by collection volume at \$0.40/mL, per our IRB protocol.

Inclusion/Exclusion Criteria

Individuals under the age of 18 and older than 80 years old at the time of enrollment were excluded from this study, in addition to patients actively undergoing cancer therapies or treatment for severe autoimmune disease with systemic immunosuppressive therapy. The study population included individuals ranged in age

from 26 – 73 years old, that received at least three doses of COVID-19 mRNA vaccine (BNT162b2 or mRNA-1273) at the time of blood collection, had longitudinal NAb data available for 3-6 months following 2nd and 3rd dose, and could be classified as a VPR, VMR, or VSR. To exclusively evaluate vaccine-induced immunity, all subjects with a history of natural infection after vaccination were excluded from this study. All subjects included denied any history of natural infection at the time of blood donation unless otherwise indicated throughout the manuscript.

Blood Processing and Storage

Upon completion of enrollment, 80 mL of peripheral whole blood was collected using BD Vacutainer Safety-Lok Blood Collection Set into 10 mL sodium heparin-coated vacutainer tubes. Immediately following collection, blood was pooled and processed for isolation of peripheral blood mononuclear cells (PBMCs) using a Ficoll-Paque density gradient and centrifugation. Whole blood layered on Ficoll-Paque was centrifuged at 1900 rpm for 20 minutes without deceleration breaks. Plasma was aspirated and pooled into a separate tube for aliquoting and long-term storage at -80°C. The buffy coat containing lymphocytes was collected from each tube, pooled into two 50 mL conical tubes, and washed three times with 35 mL of 1X PBS. Washed cells were resuspended in 1X PBS + 5% heat-inactivated fetal bovine serum (HI-FBS) then counted via hemocytometer and pelleted for aliquoting and storage. Cell pellets were resuspended in freeze medium (dimethylsulfoxide, DMSO, + 10% HI-FBS) and aliquoted into 1.8 mL cryovials at 10⁶ cells per vial. All donor PBMC vials were stored in liquid nitrogen until thawed for use.

Peptide Megapool Preparation

Individual peptides spanning the full length of SARS-CoV-2 spike glycoprotein and nucleocapsid protein were ordered from Biodefense and Emerging Infections Research Resources Repository (BEI Resources). Peptides are 17-mers or 13-mers with 10 amino acids overlap. Lyophilized peptides were reconstituted at 2 mg/mL in 50% DMSO. Individual peptides were aliquoted and stored in -80°C for future use. Peptide megapools were generated by sequentially pooling 80 μ g of individual peptides, then lyophilizing via Labconco CentriVap Benchtop Concentrator at 40°C for 12-16 hours until all remaining solvent was evaporated. Lyophilized spike and nucleocapsid megapools were reconstituted with 100% DMSO and diluted to 50% DMSO with sterile molecular grade water (REF) at 1 mg/mL of each peptide. Immediately prior to use, megapools were diluted to 2 μ g/mL in Dulbecco's Modified Eagle Medium (DMEM) with 10% FBS. Peptides were plated at a final concentration of 1 μ g/mL each peptide in a 200 μ L final well volume.

T Cell Activation Assays

Frozen PBMCs were thawed into DMEM with 10% FBS, washed, and resuspended in media then rested overnight at 37°C with 5% CO₂. Prior to plating, cells were pelleted and resuspended in fresh media, counted, and assessed for viability. Cells were resuspended at 10×10^6 cells/mL, then plated in round bottom 96 well tissue culture plates at 10^6 cells/well in 100 μ L of media. For activation induced marker (AIM)

assays, cells were stimulated with peptide immediately following plating. For T follicular helper (Tfh) cell assays, all wells were blocked with human anti-CD40 monoclonal antibody at 5 $\mu\text{g}/\text{mL}$ for 15 minutes at 37°C prior to peptide stimulation. All AIM and TFH plates were incubated for 24 hours at 37°C with 5% CO₂. Following incubation, plates were centrifuged at 1400 rpm for 10 minutes, and supernatant was harvested for cytokine multiplex assays. Stimulated cells were washed in 1X PBS and immediately used for AIM cell surface staining.

Activation Induced Marker Cell Surface Staining

Cell surface markers used to assess SARS-CoV-2 antigen-specific T cell responses in our donor cohorts included CD137 and OX40 for CD4⁺ T cells, and CD69 and CD137 for CD8⁺ T cell activation. Prior to staining, cells were resuspended and blocked in 200 μL 1X PAB buffer with 5% FBS for 1 hour at 4°C shaking slowly. Human anti-CD3, CD4, CD8, CD69, CD137, and OX40 antibodies were diluted in blocking/staining buffer and added to all wells in a 50 μL staining volume (see Appendix E, antibody panels). All plates were resuspended and incubated at 4°C for 2 hours shaking and protected from light. Plates were washed and fixed in 4% paraformaldehyde for 30 minutes at 4°C, then washed and resuspended in 200 μL of buffer for analysis by flow cytometry (see Appendix D, gating workflows).

T Follicular Helper Cell Staining

Surface markers used for identification of Tfh cells included human anti-CD3, CD4, CD8, CXCR5, OX40, CD40L, PD-1, CCR6, and CXCR3 (see appendix E,

antibody panels). All plates containing stimulated donor PBMCs were blocked, stained, fixed, and washed as indicated above. Cells were resuspended in 200 μ L of buffer and analyzed by flow cytometry (see Appendix D, gating workflows).

Flow cytometric analyses

All samples were run on a CytoFLEX LX cytometer (Beckman Coulter) using the high throughput plate settings, with 96-well round bottom plates. Data were recorded as 5×10^4 lymphocyte events for AIM, and 1×10^5 lymphocyte events for Tfh wells. Exported .fcs files were imported to FlowJo 10.8.1 for population gating prior to graphic and statistical analyses performed using GraphPad Prism 10.0.

Multiplex Cytokine Assays

Supernatant was harvested from 24-hour AIM plates and stored at -80°C until all T cell stimulation assays had been completed. Cytokines were evaluated using the LegendPLEX multiplex bead arrays (BioLegend) according to manufacturer instruction. We used the Human Cytokine 13-plex and Human T helper (Th) Cytokine 12-plex kits to investigate cytokine profiles between donor groups from stimulated PBMC supernatant. Collectively, these include IL-2, IL-4, IL-5, IL-6, IL-9, IL-10, IL-13, IL-17A, IL-17F, IL-22, IFN γ , TNF α , IL-1a, IL-1b, IFN α 2, IL-12p40, IL-12p70, IL-15, IL-18, IL-21, IL-27, IL-33, GMCSF, and TSLP. Data were recorded on the CytoFLEX instrument using a gating threshold of 3,600 total events per well for the 12-plex, and 3,900 total events for the 13-plex assays. All assays were run with duplicate standard concentrations of each analyte diluted 4-fold per manufacturer instructions. Files were exported and uploaded to

the LegendPLEX Qognit (BioLegend) analysis software, upon which gating of A and B bead populations by size, and each subpopulation within A and B gates by fluorescent intensity was performed manually. Calculated cytokine concentrations derived from standard curve dilutions were exported to Excel and formatted for statistical evaluation using GraphPad Prism 10.

Statistical Analyses

Data were analyzed for statistical significance using GraphPad Prism 10. Significance was assessed using Brown-Forsythe and Welch ANOVA testing to evaluate equality of means between groups using multiple comparisons without correction, such that each comparison stands alone ($p < 0.05$ and 95% CI). All significant p-values are indicated on their respective graphs throughout this chapter.

Results

This study aimed to investigate differences in T cell activation and T cell abundance among three groups of individuals with strong, moderate, and poorly neutralizing anti-spike antibody responses elicited by SARS-CoV-2 mRNA vaccination. Vaccinated NAb response groups are referred to as VSRs, VMRs, and VPRs throughout this manuscript. We used peptide megapools to stimulate donor PBMCs, then measured CD4⁺ and CD8⁺ T cell activation after 24 hours. We did not observe differences in antigen-specific activation of CD4⁺ and CD8⁺ T cells between groups as initially hypothesized, thus, VPRs had mean T cell activation comparable to VMRs and VSRs

upon Spike peptide stimulation *in vitro* (Figure 33).

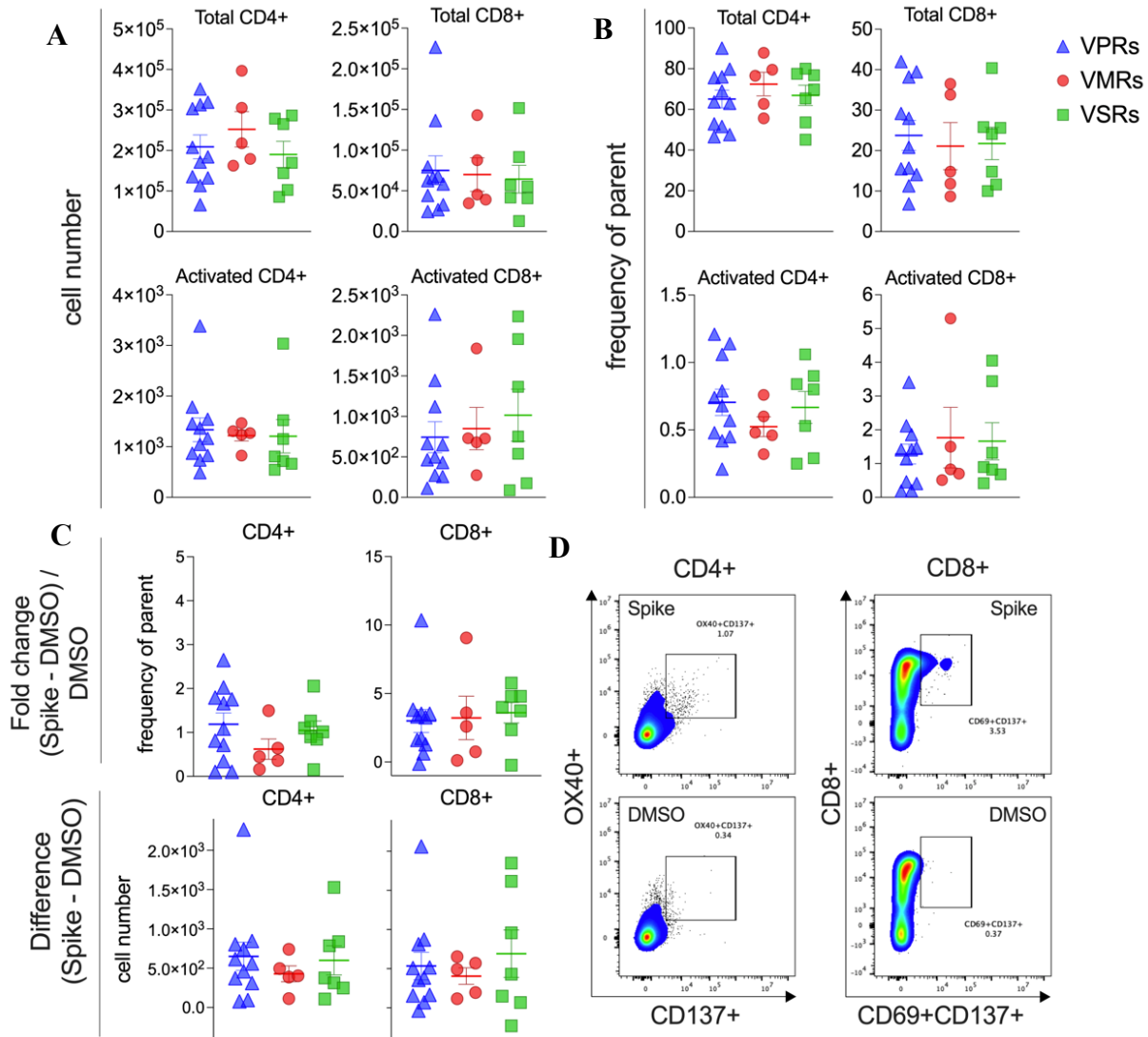


Figure 33. Activation Induced Marker staining of spike peptide stimulated PBMCs. (A) Total CD4⁺ and CD8⁺ T cells (top), and activated CD4⁺ and CD8⁺ T cells (bottom) shown as normalized cell number. Activated CD4⁺ and CD8⁺ populations refer to OX40⁺CD137⁺ and CD69⁺CD137⁺ cells, respectively. (B) Total (top) and activated (bottom) CD4⁺ and CD8⁺ T cells shown as frequency of parent. (C) Baseline-corrected flow cytometric data represented as frequency of parent (top), and normalized cell number (bottom). Data were corrected using a fractional ratio (fold change) of spike-stimulated cells relative to equimolar DMSO-treated cells (top), and calculating the difference between spike and DMSO-treated cells (bottom) using GraphPad Prism 10.0.

(D) Representative pseudo-contour plots demonstrating CD4⁺ (left) and CD8⁺ (right) activation under spike-stimulated (top) and DMSO-treated conditions (bottom).

Interestingly, we observed an increase in cell number and frequency of double positive CD4⁺CD8⁺ T cells in VPRs as compared to VMRs and VSRs (**Figure 34**). As dual expression of CD4 and CD8 is best described in the context of thymic T cell development (immature double-positive thymocytes), we sought to evaluate the maturation status of the CD4⁺CD8⁺ T cells identified in VPRs by assessment of surface CCR7 and CD45RA expression. Unexpectedly, we found this population to be primarily comprised of CCR7⁺CD45RA⁻ cells, indicative of a central memory T (T_{cm}) cell phenotype (**Figure 34**). The data also demonstrated an increased frequency and cell number of CD8^{low} T cells in VPRs, when compared to VMRs, but not VSRs. To summarize these findings and visualize the frequencies of CD4⁺, CD8⁺, and CD4⁺CD8⁺ double positive T cell populations across donor groups following spike-peptide stimulation, we pooled representative VSR, VMR, and VPR samples and generated t-distributed stochastic neighbor embedding (t-SNE) plots from CD3⁺ lymphocytes (Figure 33 E). The t-SNE plots show that while VSR, VMR, and VPR cells all contribute to CD4⁺ and CD8⁺ T cell populations, the CD4⁺CD8⁺ population is uniquely enriched with VPR derived cells.

Interestingly, while CD4⁺CD8⁺ cells highly expressed CD69, they did not express CD137 (41BB) or OX40 (Figure 33E). Additionally, CD8^{low} cells were observed to express higher surface OX40 compared to their CD8^{hi} counterparts (Appendix F, CD8^{hi} vs. CD8^{low} AIM), demonstrating differential activation marker expression within these expanded populations. Antigen specificity of the CD4⁺CD8⁺ and CD8^{low} T cell

populations appears to be more abundant in some VPR individuals than others, as CD4⁺CD8⁺ populations are also present in unstimulated controls. However, CD4⁺CD8⁺ populations were expanded under spike-peptide stimulated conditions to varying degrees (data not shown), suggesting a potential pre-existing or cross-reactive etiology of these cell populations. Ongoing work in our laboratory aims to investigate antigen specificity by tetramer staining a subgroup of VPR, VMR, and VSR in addition to HLA typing of these individuals for evaluation of allele frequency and peptide compatibility.

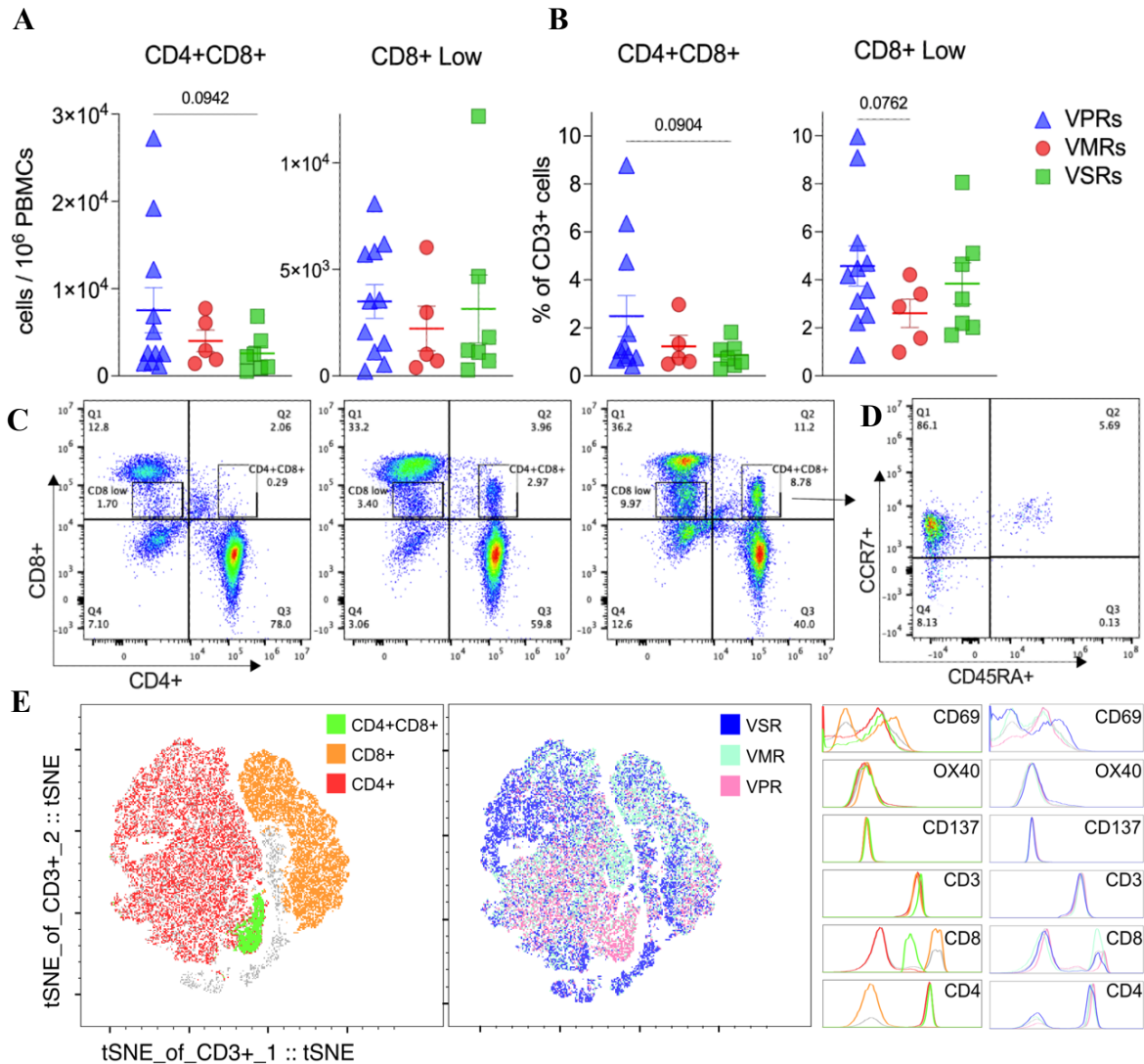


Figure 34. Identification of CD4⁺CD8⁺ and CD8^{low} T cells in VPR subjects. (A) Normalized cell counts and (B) frequencies of CD4⁺CD8⁺ and CD8^{low} cells among CD3⁺ lymphocytes from VSR, VMR, and VPR donors following spike-peptide stimulation. (C) Representative flow cytometric pseudo-color dot plots of CD3⁺ lymphocyte populations from VSR (left), VMR (center), and VPR (right) donors. Uniform gating strategy used for enumeration of CD4⁺CD8⁺ cells and CD8^{low} cell populations from CD3⁺ lymphocytes is demonstrated in quadrants Q1 and Q2. (D) Representative assessment of T cell maturity among the CD4⁺CD8⁺ cell population. The majority of CD4⁺CD8⁺ T cells are CCR7⁺ CD45RA⁻, indicative of a central memory (CM) phenotype. (E) t-distributed stochastic neighbor embedding (t-SNE) visualization of pooled donor CD3⁺ lymphocyte populations with CD4⁺ (red), CD8⁺ (orange), and CD4⁺CD8⁺ (green) T cell populations overlaid (left). Histograms show relative cell surface marker expression for each T cell population. t-SNE visualization of pooled donor CD3⁺ lymphocyte populations with VSR (blue), VMR (teal), and VPR (pink) donor group origin overlaid (right). Histograms show relative cell surface marker expression for each representative donor.

T follicular helper cells classically defined as CD4⁺ T cells expressing the transcription factor Bcl6 and surface chemokine receptor CXCR5, facilitate B cell activation/proliferation, germinal center (GC) formation, and production of high-affinity antibodies in secondary lymphoid tissue.⁸³ Although Tfh cells act in lymphoid tissues sites in the context of inflammation/vaccination, a population of circulating Tfh (cTfh) cells have been identified in peripheral blood after GC dissolution. cTfh cells are thought to function as memory compartment for prior GC reactions, poised to quickly seed formation of GCs upon subsequent antigen encounters.¹⁸⁷ Our interest in Tfh cells initially arose early-pandemic when it was reported that individuals with severe natural infection showed a loss of Bcl6 expression.¹⁷⁶ Considering the differences in NAb response magnitude to mRNA vaccination among individuals that we and others observed,¹⁶⁶ we hypothesized that discordant activation of CD4⁺ cTfh phenotypes could distinguish VPRs from VMR and VSR groups. Due to the low total frequency of cTfh cells in whole PBMCs, we evaluated *bulk* CD4⁺ cTfh (CXCR5⁺) (**Figure 35**) and

activated CD4⁺ cTfh (CXCR5⁺OX40⁺CD40L⁺) (**Figure 36**) abundance. We also assessed differences in cTfh phenotypes, conferred by CXCR3 and CCR6 expression, of bulk and activated cells between groups. cTfh phenotypes are defined as cTfh1 (CXCR3⁺CCR6⁻), cTfh2 (CXCR3⁻CCR6⁻), cTfh17 (CXCR3⁻CCR6⁺), and cTfh1/17 (CXCR3⁺CCR6⁺) cells.¹⁸⁸

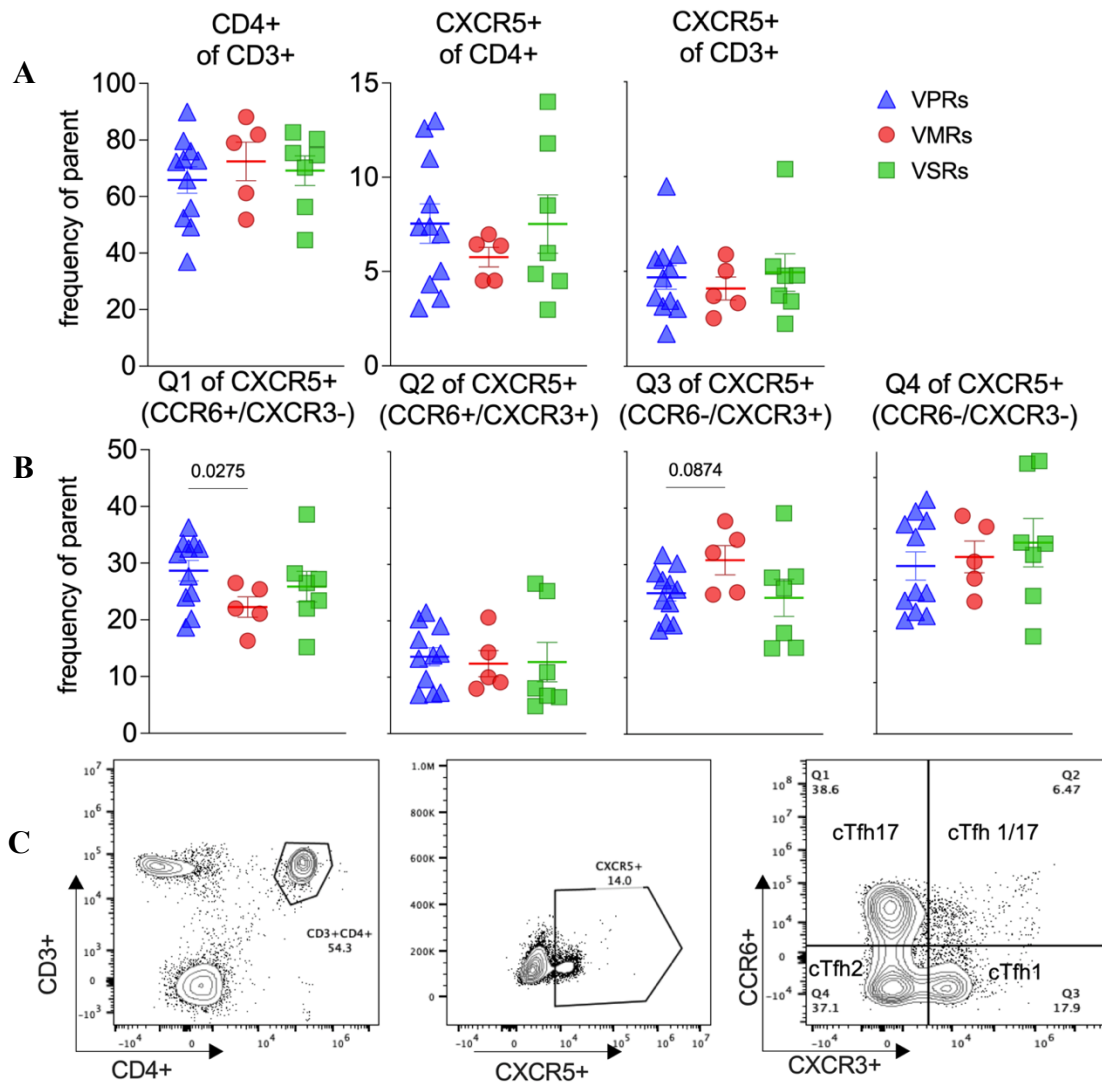


Figure 35. Characterization of *bulk* CD4⁺ cTfh in VPR, VMR, and VSR subjects. (A) Total CD4⁺ T cell abundance represented as a frequency of the CD3⁺ parent

population (left), CXCR5⁺ frequency of CD4⁺ cells (middle), and CXCR5⁺ frequency of CD3⁺ cells (right). **(B)** cTfh phenotype characterization by CXCR3 and CCR6 expression, represented as VPR, VMR, and VSR frequency of CXCR5⁺ cells for all four quadrants seen in (C). Q1 refers to cTfh17 cells (CCR6⁺CXCR3⁻), Q2 refers to cTfh1/17 cells (CCR6⁺CXCR3⁺), Q3 refers to cTfh1 cells (CCR6⁻CXCR3⁺), and Q4 refers to cTfh2 cells (CCR6⁻CXCR3⁻). **(C)** Representative gating workflow for enumeration of bulk CD4⁺ Tfh cells isolated from peripheral blood. Cells are first gated on CD3⁺CD4⁺ populations prior to CXCR5⁺ gating. Data are shown as contour plots at level 10% generated using FlowJo v10 analysis software.

When evaluating bulk CD4⁺ Tfh, we observed a significant increase in the frequency of CCR6⁺CXCR3⁻ (cTfh17, Q1) cells in VPRs as compared to VMRs ($p < 0.05$) (**Figure 35**). However, when we assessed *activated* CD4⁺ Tfh, VPRs demonstrated a significantly increased mean frequency and cell number of CCR6⁻CXCR3⁺ (cTfh1, Q3) cells, in comparison with both VMRs and VSRs ($p < 0.05$) (**Figure 36**). Consequently, or perhaps proportionally, VPRs have a significantly decreased mean frequency of CCR6⁺CXCR3⁺ (cTfh1/17, Q2) cells, in comparison to VSRs (**Figure 36**).

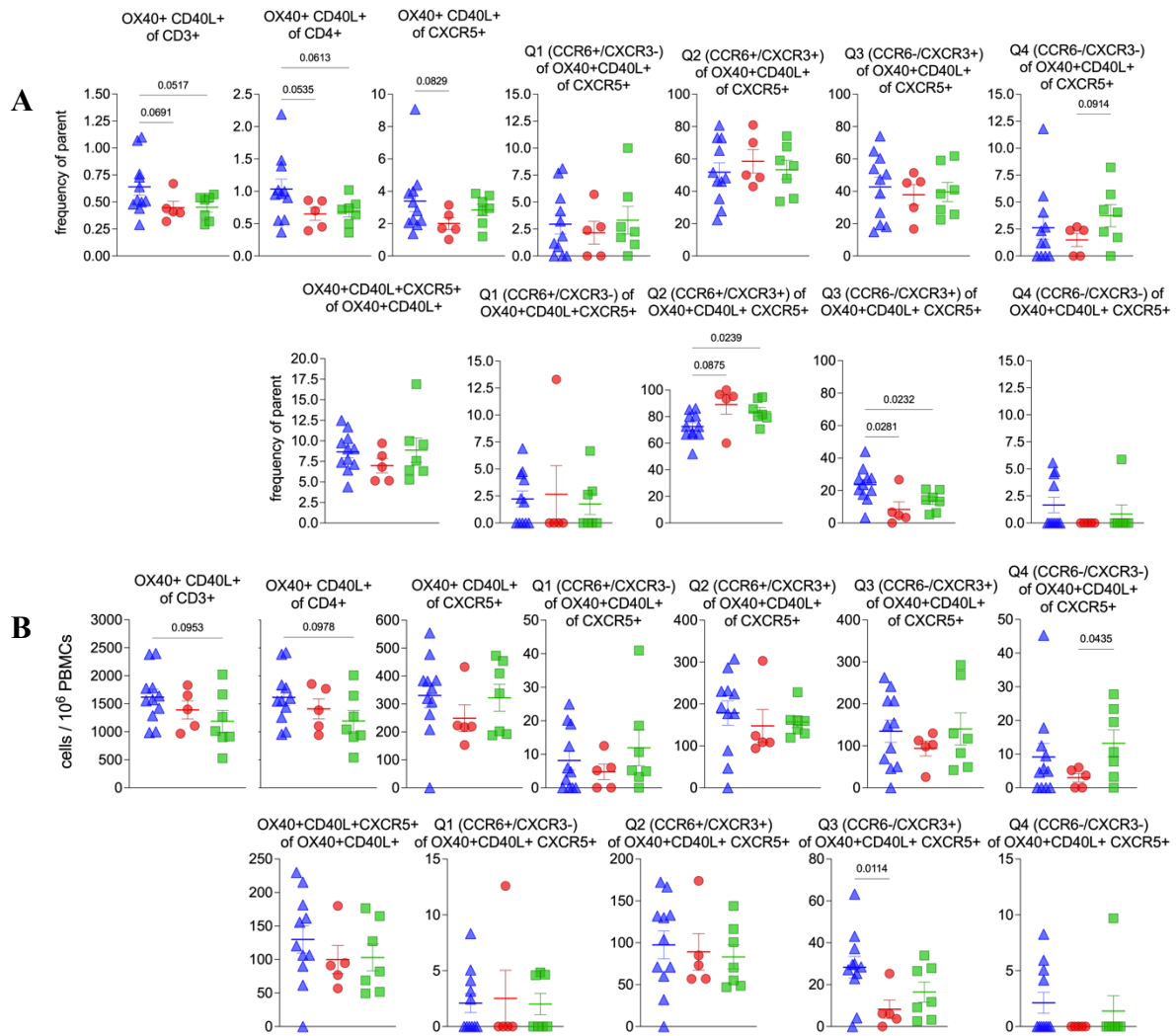


Figure 36. Characterization of activated cTfh in VPR, VMR, and VSR subjects. (A) Frequency of parent and **(B)** normalized cell counts per million PBMCs of activated CD4⁺CXCR5⁺ T cells (cTfh). Enumeration of activated cTfh cells were characterized by OX40 and CD40L surface expression, and cTfh phenotypes were characterized according to CCR6 and CXCR3 expression. Activated cTfh were assessed using two gating strategies in parallel. First, we assessed OX40 and CD40L expression on CXCR5⁺ CD4⁺ T cells (top row A & B), followed by enumeration of CXCR3 and CCR6 expression. Our alternative gating strategy (bottom row A & B) first quantified OX40 and CD40L expression on CD4⁺ cells, then CXCR5⁺ expression, followed by CXCR3 and CCR6 quadrant gating (See Appendix D, gating workflows). Uniform gating strategy was applied to all donors. Statistical testing is described in methods section of the main text and p-values indicated on graphs.

Unexpectedly, we observed several individuals within the VPR population to have an increased number and frequency (among bulk cTfh) of CD8⁺CXCR5⁺ cells, when compared to VMRs and VSRs (**Figure 37**), although differences in activated CD8⁺CXCR5⁺ cells were not seen (data not shown). Lastly, we observed no difference in PD-1 expression in CD4⁺ or CD8⁺ CXCR5⁺ T cell populations between groups (data not shown).

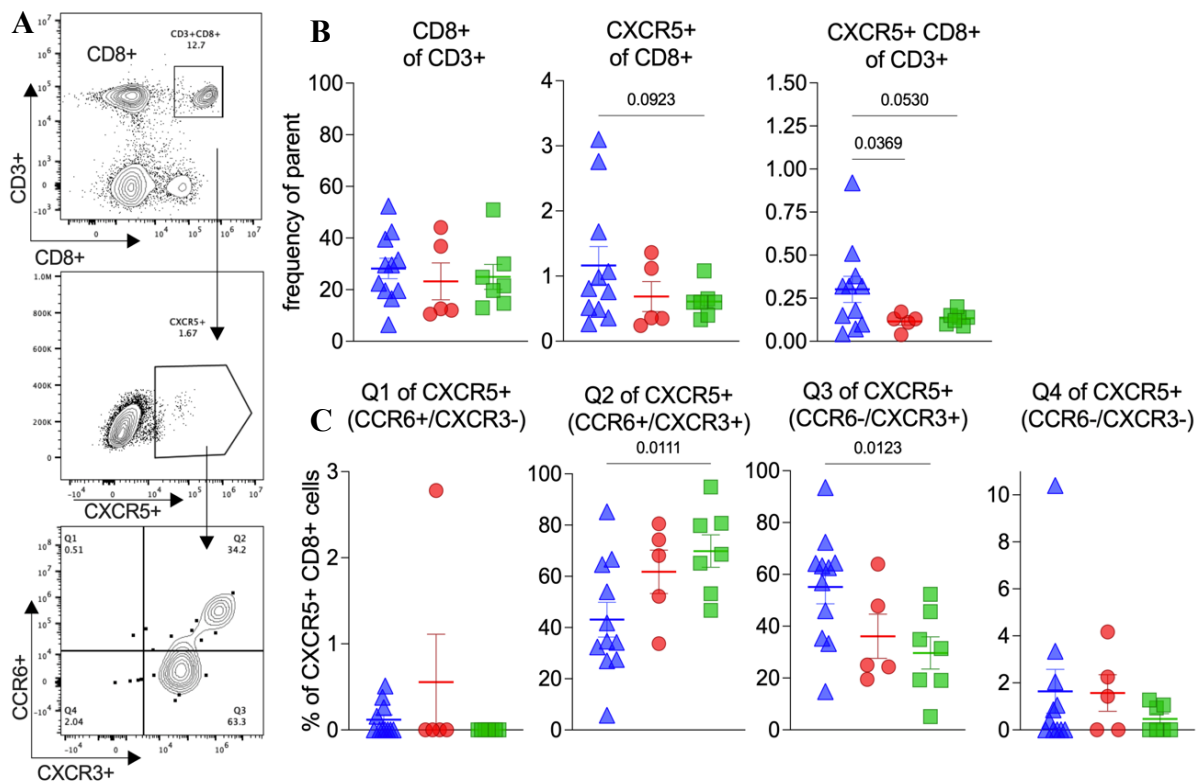


Figure 37. Assessment of *bulk* CD8⁺ T cell CXCR5, CCR6, and CXCR3 expression. (A) Representative gating workflow demonstrating enumeration of CD3⁺CD8⁺ T cells (top), CXCR5⁺ CD8⁺ cells (middle), followed by CCR6 and CXCR3 expression (bottom) of the CXCR5⁺ parent population. (B) Quantitation of total CD8⁺ T cells as a frequency of CD3⁺ cells (left), CXCR5⁺ as a frequency of CD8⁺ cells (middle), and CXCR5⁺CD8⁺ cells as a frequency of CD3⁺ cells (right) are shown for VPR, VMR, and VSR individuals. (C) CCR6 and CXCR3 expression on CXCR5⁺CD8⁺ cell populations, denoted as Q1 (CCR6⁺CXCR3⁻), Q2 (CCR6⁺CXCR3⁺), Q3 (CCR6⁻CXCR3⁺), and Q4

(CCR6⁺CXCR3⁻) graphs listed from left to right. Statistical testing is described in methods section of the main text and p-values are indicated on graphs.

It is important to note that nomenclature with respect to CD8⁺CXCR5⁺ cell populations is not clearly defined nor agreed upon, as their cytotoxic function, in addition to the ability to provide B cell help, has been reported in various other viral and immunologic contexts.^{189,190,191}

Flow cytometric multi-analyte cytokine quantitation by multiplexed bead-based assay

In addition to AIM and cTfh characterization of donor T cell responses to Spike-peptide stimulation *in vitro*, we measured the concentration of 25 different cytokines in culture supernatants following 24-hour peptide stimulation (**Figure 38**), using a bead-based multi-analyte immunosorbent assay (LegendPLEX, BioLegend). Data were collected on CytoFLEX LX (Beckman Coulter) and analyzed using the Qognit © LegendPLEX (BioLegend) analysis software.

Although several cytokines (measured from supernatant) included in our panel were below the assay limit of detection after 24 hour stimulation, we evaluated TNF α , IL-2, IL-27, and IFN γ for statistically significant differences. We found that VPRs and VSRs produced significantly more IFN γ ($p < 0.05$, < 0.03 , respectively), compared to individuals with a past natural infection (NIs). Significant differences between vaccinated groups, however, were not observed in the cell supernatant of stimulated PBMCs for any of the cytokines we measured.

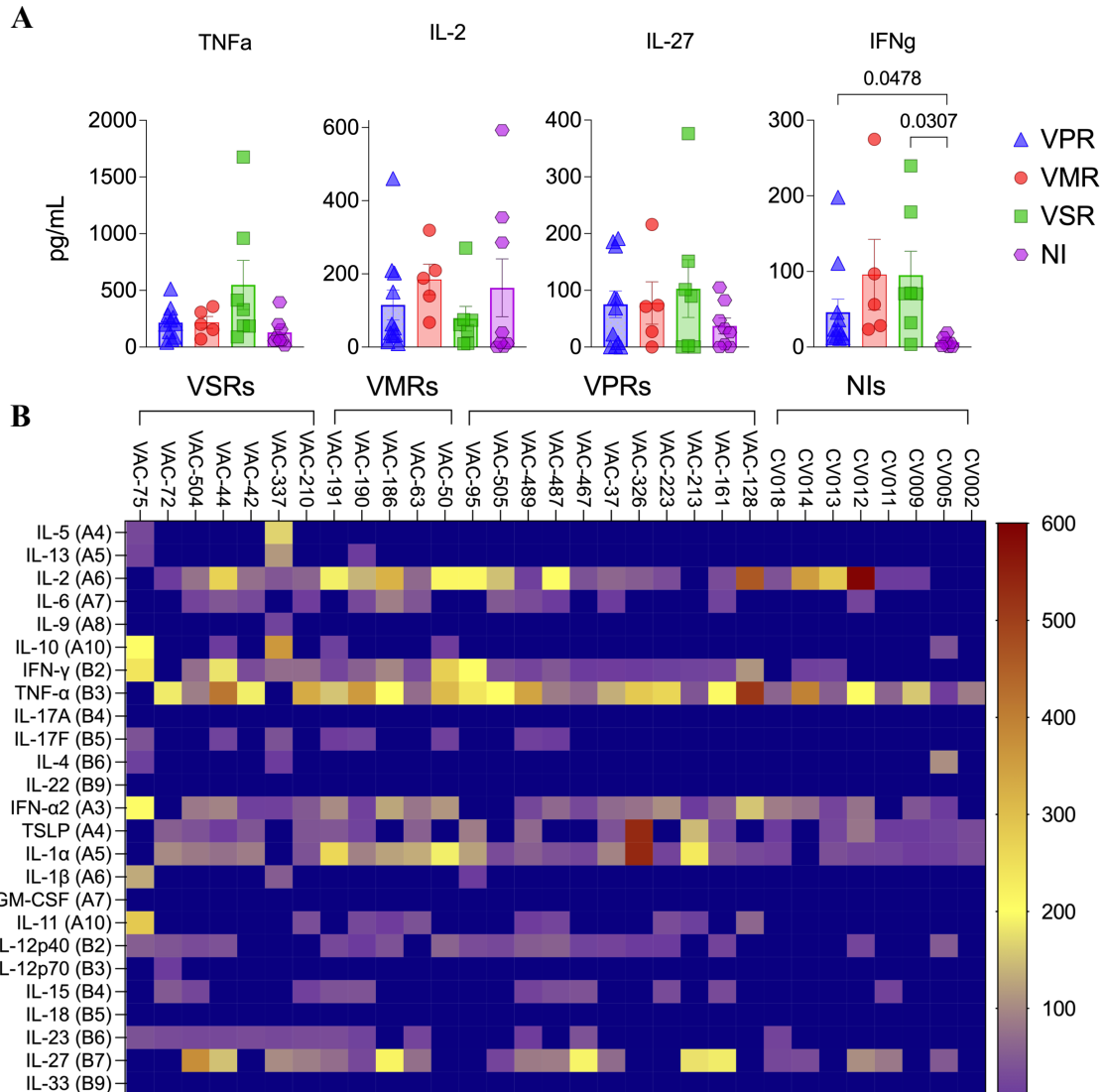


Figure 38. Cytokine profiling of supernatants from peptide-stimulated VPR, VMR, and VSR PBMCs. (A) Cytokines of interest represented as bar graphs with individual symbols corresponding to VPRs, VMRs, and VSRs. Data are represented as picograms/mL, error bars indicate mean \pm SEM. **(B)** Heatmap demonstrating differential cytokine expression across all donor groups. Scale provided is shown in pg/mL.

Discussion

In Chapter VI of this dissertation, we report SARS-CoV-2-specific T cell and cytokine profiling of groups previously identified to elicit strong, moderate, and poorly neutralizing antibody responses to COVID-19 mRNA vaccination.¹⁶⁶ We measured CD4⁺ and CD8⁺ T cell activation following spike-peptide stimulation *in vitro*, using OX40 and CD137 (41BB) to assess CD4⁺ activation, and CD137 and CD69 to assess CD8 activation. We found that poor NAb responders (VPR) had comparable CD4⁺ and CD8⁺ T cell activation compared to moderate (VMR) and strong (VSR) responders, indicating that VPRs indeed mounted an antigen-specific T cell response to mRNA vaccination.

When analyzing the AIM data set for differences between groups, we observed an increased frequency of CD4⁺CD8⁺ T cells in VPR donors, relative to VMRs and VSRs. Peripheral circulating T cells expressing both CD4 and CD8 are present at low frequencies (< 1-3%), have been observed to increase with age > 65 years, and are often thymic-derived, naïve, double positive (DP) thymocytes that escaped prior to positive and negative selection.^{192,193,194} However, when we further evaluated surface marker expression of spike-peptide expanded CD4⁺CD8⁺ T cells, we observed most to be CCR7⁺CD45RA⁻, resembling a central memory (Tcm) phenotype.

We also evaluated circulating CXCR5⁺ T follicular helper cells (cTfh), as a memory population of GC Tfh cells, due to their role in B cell activation/proliferation and neutralizing antibody production.⁸³ We also assessed cTfh phenotype, characterized by CCR6 and CXCR3 chemokine receptor expression on CXCR5⁺ cells. Although the

functional capacities of classically subdivided cTfh populations¹⁸⁸ are diverse and etiologically unclear, their different phenotypes conferring putative TH1, TH2, and TH17-like features have been implicated in various viral and vaccination contexts as correlated with NAb production.^{195,196,197} Due to the low frequency of Tfh in circulation, we measured *bulk* cTfh (total CXCR5⁺) and *activated* cTfh (OX40⁺ CD40L⁺) cells in CD4⁺ and CD8⁺ T cell populations. In bulk CD4⁺ cTfh, we found that VPRs had a significant increase in mean frequency of CCR6⁺CXCR3⁻ (cTfh17) cells in comparison to VMRs. However, when evaluating activated cTfh (CD4⁺CXCR5⁺ OX40⁺CD40L⁺), we found a significant increase in mean frequency of CCR6⁻CXCR3⁺ (cTfh1) cells, compared to both VMRs and VSRs. Further, we observed a significantly decreased mean frequency of activated CCR6⁺CXCR3⁺ (cTfh1/17) in VPRs relative to VSRs, suggesting a difference underlying vaccine-induced T follicular helper immunopathology in these individuals.

Lastly, we investigated the presence of circulating CD8⁺CXCR5⁺ cells in our cohort, as these cell populations have been implicated in various chronic viral infections and immunizations, humoral autoimmunity, several solid tissue cancers, and in the regulation of B cell tolerance.^{189,198} In the same manner as CD4⁺CXCR5⁺ cells, we assessed bulk and activated populations. Surprisingly, we observed significantly increased bulk CD8⁺CXCR5⁺ cells as a frequency of CD3⁺ cells, exclusively in VPRs. No differences in OX40 and CD40L expression were observed for the CD8⁺CXCR5⁺ cells, however, we did observe a significantly *increased* frequency of CCR6⁻CXCR3⁺ (cTfh1) cells and significantly *decreased* frequency of CCR6⁺CXCR3⁺ (cTfh1/17) cells within the bulk CD8⁺CXCR5⁺ population identified in VPR individuals, similarly to

trends seen in bulk CD4⁺ cTfh populations. The implications of identifying such a cell population are controversial, as T follicular helpers are generally regarded exclusively as CD4⁺ cells. However, CD8⁺CXCR5⁺ cells are now a widely recognized CD8⁺ T cell subset that are capable of homing to GCs and secondary lymphoid organs. CD8⁺CXCR5⁺ cells are in some cases referred to as follicular cytotoxic T cells or CD8⁺ T follicular cells (Tfc), however, they are not functionally comparable in all contexts and cannot be generalized as such.

The identification of discordant CD4⁺CD8⁺, CD8^{low}, and CD8⁺CXCR5⁺ cell populations in VPR individuals presents novel findings, however, the relationship between these cell types and NAb generation in the context of COVID-19 mRNA vaccination remains unknown. Further investigation is needed to determine the antigen-specificity of these cell populations, as antigen-specific expansion was more apparent in some donors following peptide stimulation than others. Such investigations might include tetramer staining of stimulated and/or isolated populations of interest, followed by T cell receptor repertoire (TCR) sequencing to evaluate clonal diversity of the isolated populations. Additionally, functional assays in the context of CD8⁺CXCR5⁺ cells may aid in the evaluation of potential phenotypic characteristics such as cytotoxicity, ability to provide B cell help, regulatory functions, cytokine secretion, etc.

In conclusion, we found that all subjects in all three NAb response groups had detectable and comparable frequencies of activated SARS-CoV-2-specific CD4⁺ and CD8⁺ T cells, despite variable NAb responses to mRNA vaccination. We identified elevated frequencies of CD4⁺CD8⁺, CD8^{low}, and CD8⁺CXCR5⁺ T cells in VPR individuals, but not VMR or VSR groups.

This study has several limitations. First, the small total cohort sample size and group size are likely to obfuscate differences that might be seen with a larger cohort. However, subjects were selected on the basis of longitudinal neutralizing antibody data following 2nd and 3rd COVID-19 mRNA vaccinations, thus, our subject pool was limited by the constraints of our experimental design. Another limitation is that only a single timepoint was evaluated for purposes of this study, which was collected ≥ 6 months following 3rd vaccine dose for most individuals. Four VPRs, one VMR, and one VSR received 4th vaccinations prior to the date of collection, thus another limitation is variability in vaccination number at the time of blood donation. Although our AIM assay protocols were adapted from several established methods,^{126,167} the relatively short stimulation period (24 hours) might be considered an additional limitation in the detection of antigen-specific responses.

As is applicable in any SARS-CoV-2-related study, the possibility of unknown asymptomatic infection, despite failure to detect an anti-nucleocapsid humoral or cellular immune response, remains a potential confounding variable. Lastly, as our NAb LFA was designed to measure antibodies that neutralize via the receptor binding domain (RBD) of spike protein,³² the possibility that subjects may neutralize SARS-CoV-2 via sub-immunodominant non-RBD neutralizing epitopes is an additional limitation. Nevertheless, we identified unique cellular immunity characteristics that further distinguish VPR individuals immunologically, indicating that more substantial underlying immunologic differences may be related to the altered NAb response seen in our previous cohort.¹⁶⁶ Finally, this study unequivocally demonstrated detectable SARS-

CoV-2-specific CD4⁺ and CD8⁺ T cell reactivity all mRNA-vaccinated subjects,
independent of NAb response magnitude.

CHAPTER VII

DISCUSSION

SARS-CoV-2 emerged in December of 2019 and COVID-19 was declared a pandemic by March of 2020. Only a year later, in December of 2020, mRNA-1273 (Moderna) and BNT162b2 (Pfizer) vaccines were issued EUA and distribution began the same month.³⁶ During that year, when vaccines had yet to exist, available treatments were failing and infection case numbers along with hospitalizations and deaths were climbing, we developed a lateral flow assay to quantitatively measure SARS-CoV-2 neutralizing antibodies in 10 μ L of peripheral blood from a finger-stick or 6 μ L of plasma/serum (**Chapter II**).³² We developed this test for the purpose of quantifying SARS-CoV-2 NAbs within COVID-19 convalescent plasma (CCP), as CCP was one of the few early pandemic treatment options. However, as we completed clinical agreement and validation studies with our NAb LFA prototype (See Appendix B), the first COVID-19 monoclonal (neutralizing) antibody therapy had become available and vaccines were in the early phases of distribution, rendering CCP near obsolete.

We saw a unique opportunity to measure longitudinally COVID-19 mRNA vaccine-induced spike glycoprotein receptor binding domain (RBD) NAbs using our rapid LFA. For 18 months in over 500 study participants, we measured NAbs in subjects at all stages of vaccination at three testing location sites in vaccine recipients ranging from 18 to 80 in age. Of all participants enrolled, our study population was composed of 57% female and 43% male subjects. Throughout the entirety of this study, many observations were made in real time (detailed throughout this dissertation), as data were

generated and collected relatively rapidly (due to the nature of the assay). One observation was the identification of subgroup of mRNA-vaccinated individuals for which mean RBD-NAb titers failed to exceed 1:160 after 2nd dose, which we termed vaccine poor responders (VPRs). We also observed a small cohort of vaccine recipients who neutralized virus at very high titers compared to other participants in the study; further, their titers did not wane and remained >1:320 throughout the 18 month study, termed vaccine strong responders (VSRs).

In **Chapter III**, we demonstrated that VPRs identified after a two-dose vaccine regimen could be ‘rescued’ by a 3rd dose of mRNA vaccine, regardless of homologous or heterologous vaccination.¹⁴⁸ These findings, submitted in December of 2021 to *Nature Communications Medicine*, demonstrated that 25% of an otherwise healthy cohort failed to generate high titer RBD-NAbs following the initial two-dose vaccination series recommended by regulatory agencies at the time. Importantly, the majority of the VPR individuals identified that received a 3rd dose prior to the submission for publication, received BNT162b2 (Pfizer) two-dose primary series, while only one individual that received the mRNA-1273 primary series was classified as a VPR. At the time, each of the two primary series BNT162b2 vaccine doses contained 30 μ g of mRNA, while the two mRNA-1273 primary vaccine series each contained 100 μ g mRNA.^{199,200} Thus, we likely observed a dose-dependent relationship between COVID-19 mRNA vaccination and NAb elicitation in our initial cohort following primary series vaccination. The CDC’s advisory committee on immunization practices (ACIP) recommended booster (3rd) vaccine doses at the end of September, 2021. We continued conducting longitudinal NAb

testing for an additional 6-8 months after the majority of our study population had received a 3rd vaccine dose and report on this longitudinal study in Chapter IV.

Chapter IV, entitled, “Longitudinal Comparison of Neutralizing Antibody Responses to COVID-19 mRNA Vaccines After 2nd and 3rd Doses” composes the culminating data from the 18-month study conducted using our NAb LFA, published in *Vaccines* in September of 2022.¹⁶⁶ This study demonstrated that a 3rd dose of mRNA vaccine elicits higher and more durable RBD-NAb titers, independent of vaccine manufacturer. Further, we compared homologous 3rd vaccination with heterologous 3rd vaccination (3 doses of BNT162b2 vs 3 doses of mRNA-1273 vs 2 doses of BNT162b2 + 1 dose of mRNA-1273) and found that minimal differences in the early months post-3rd dose. However, we noted that at 5 months post-3rd dose, individuals that received heterologous 3rd vaccines (2 doses of BNT162b2 + 1 dose of mRNA-1273) had significantly higher mean percent neutralization when compared to individuals that received 3 doses of BNT162b2 vaccine. However, by months 6-8, these differences resolved, and all 3rd dose groups had mean percent neutralization $\geq 50\%$. Notably, when evaluating individual NAb responses per timepoint, we observed a more homogenous population distribution at post-3rd dose timepoints as compared to post-2nd dose timepoints, where a large degree of heterogeneity was observed. We suspect that we were among the first to observe a rapid decline in NAb titers within 2-3 months after a second mRNA vaccine dose—and that a third vaccine dose rescued both vaccine poor responders and vaccine recipients whose titers decreased rapidly after a second vaccine dose. Importantly, NAb titers remained elevated ($>50\%$ neutralization) in most vaccine recipients after a third dose.

Additionally, using unsupervised hierarchical clustering and principal component analyses (PCA) of unpaired (total n per timepoint) and paired longitudinal NAb data sets, we identified three distinct groups of mRNA-vaccination individuals with unique RBD-NAb responses to vaccination. The first of these three NAb response groups elicited higher titer NAb following 2nd and 3rd vaccine doses and sustained these titers for longer than the other two groups, thus, they were termed the vaccine strong responders (VSRs). Using the PCA and clustering analyses, we classified 34% of subjects as VSRs after the 2nd vaccine dose, and classified 79% of subjects that were classified as VSRs following 3rd dose. Second, the vaccine moderate responders (VMRs), for whom an initial high titer NAb response was observed in most. However, rapid NAb waning observed in VMRs after both 2nd and 3rd doses largely distinguished the VMR group from the VSR group, particularly after 3rd dose. Lastly, a group of individuals for whom all three doses of COVID-19 mRNA vaccine failed to elicit high titer NAb ($\geq 1:160$ to $1:320$), termed vaccine poor responders (VPRs).

In the final months of our longitudinal study, SARS-CoV-2 BA.1.1.529 (Omicron) emerged in the US, and we observed an unusual number of breakthrough infections in our study population. Several recently (at the time) infected participants had received their 3rd doses just a few weeks prior to Omicron exposure and infection, and despite high titer ($\geq 1:640$) NAb (measured for some only a week prior), mRNA vaccines available at the time failed to protect from symptomatic infection with the Omicron variant¹⁶⁶. However, mRNA vaccines appeared to prevent severe disease and hospitalization in all study participants. Individuals in our cohort of Omicron breakthrough infections reported asymptomatic or very mild, to moderately severe

symptoms, however, none of these subjects were hospitalized throughout natural infection disease course. This large degree of protection is likely attributed to strong innate and cellular immune responses, in addition to high titer binding or effector antibodies which can facilitate viral clearance via various innate and/or adaptive immunologic mechanisms. Further, early Omicron data demonstrated that proximal boosting with ancestral-Spike encoding mRNA vaccines provides some degree of protection against Omicron infection or severe disease, as boosting promotes affinity maturation of binding and neutralizing antibodies elicited by prior immunization.¹³⁹ In contrast, while we did not observe many breakthrough infections throughout Delta and prior waves, those that did occur were almost exclusively in individuals for whom NAb titers were $\leq 1:80$. The difference in breakthrough infections between Delta and Omicron is due to the large number of mutations delineating Omicron from prior variants of concern (VOC), as BA.1.1.529 (Omicron) spike glycoprotein alone contains ≥ 30 mutations in the RBD of spike protein.²⁰¹ Further, vaccines administered at the time, BNT162b2 and mRNA-1273, both target ancestral SARS-CoV-2 spike protein. As Omicron breakthrough infections became more widespread in January of 2022, many studies began reporting similar notions of immune escape.^{202,203,204} The overarching question of “can NAb serve as a correlate of protection?” was quickly confounded by the evolution and emergence of Omicron, and later, Omicron subvariants. Our Omicron breakthrough data, although a small sample size, was indicative of the urgent need for variant-specific vaccine development, and from our laboratory’s perspective, a BA.1.1.529-specific NAb LFA.

In January of 2022, we developed a BA.1.1.529 (Omicron, BA.1) specific NAb LFA using previously published methods.³² The test itself appeared physically identical to the original version, however it contained BA.1.1.529 spike protein rather than ancestral SARS-CoV-2 spike protein. In **Chapter V**, we demonstrate validation of the BA.1 NAb LFA using 13 serum samples from individuals with sequencing-confirmed BA.1 infections. We determined IC₅₀ values for these samples by FRNT in the BSL-3 laboratory using SARS-CoV-2 BA.1.1.529 virus, such that LFA density values could be correlated with known titers or IC₅₀ values. We observed a significant correlation ($r = -0.91, p < 0.0001$) between IC₅₀ and LFA density, suggesting the BA.1-specific test was a suitable surrogate for gold-standard neutralization testing. However, as we completed our validation and correlation analyses, BA.2 had already surpassed BA.1 as the dominant variant in circulation. Like many COVID-19 researchers and vaccine developers around the world, we found ourselves caught in a race with which we could not keep up. The utility of our BA.1 NAb LFA was consequently, limited.

Omicron subvariants rapidly cycled through the population in the months that followed, and BA.4/5 eventually emerged as the dominant variant in the US in July of 2022.¹⁶⁵ We quickly began modification of the BA.1 NAb LFA to contain BA.5 spike protein. Using 10 serum samples isolated from BA.5-infected individuals, we again, performed FFA experiments in the BSL-3 laboratory, this time using SARS-CoV-2 BA.5 virus to determine BA.5-specific NAb titers of the convalescent sera. We observed a significant correlation ($r = -0.81, p < 0.006$) between IC₅₀ and NAb LFA density, and used the equation ($y = -1.037 * X + 24.90$) derived from a linear regression analysis to predict IC₅₀ values from a given LFA density, and extrapolate NAb titer from predicted

IC₅₀ calculations. Similarly to our original NAb LFA, in order to expand the accessibility and interpretation metrics, we use these predicted values derived from IC₅₀ and LFA density correlation/regression analyses for conversion to more clinically relevant indexes. In collaboration with Dr. Vel Murugan's laboratory at the Biodesign Institute, we recently tested 1,060 blinded serum samples on the BA.5 NAb LFA, as part of an ongoing sero-surveillance study to evaluate various aspects of COVID-19 humoral immunity in a large research university population setting. Preliminarily, 28% of the samples tested ($n = 293/1060$) were classified as < 10% neutralization (<1:80 BA.5 NAb titer) as measured by our assay. This collaborative work remains ongoing and is therefore otherwise omitted from this dissertation.

Lastly, in **Chapter VI**, we present findings from a work entitled, "T Cell and Cytokine Profiling of SARS-CoV-2 mRNA Vaccine-Induced Neutralizing Antibody Poor Responders." Here, we investigate SARS-CoV-2 specific CD4⁺ and CD8⁺ T cell response in VPR, VMR, and VSR mRNA-vaccinated populations. We hypothesized that antigen-specific CD4⁺ and CD8⁺ T cell activation and/or abundance would be either be reflective of VPR, VMR, and VSR NAb response magnitudes, or that stronger T cell responses were elicited in VPRs than in moderate and strong NAb response groups, to compensate for poor NAb titers. However, all three groups had comparable CD4⁺ and CD8⁺ T cell responses following peptide megapool stimulation *in vitro*. While analyzing our intended populations, we observed increased frequencies of CD4⁺CD8⁺ double positive and CD8^{low} T cells primarily in VPR individuals. CD4⁺CD8⁺ T cells are typically found in the thymus, as 'double positive' T cells are a normal intermediate stage found in developing thymocytes which precede positive and negative selection,¹⁹³ although they are observed

in the periphery at low frequencies ($\leq 1-3\%$).²⁰⁵ Circulating CD4⁺CD8⁺ T cells are generally regarded as naïve cells that escaped thymocyte development,¹⁹² however, mature peripheral CD4⁺CD8⁺ T cells have been described in various contexts such as viral infection, cancer, and autoimmunity.^{194,206,207} While they remain an understudied, functionally diverse, and etiologically unclear cell population, mature CD4⁺CD8⁺ T cells with memory phenotypes have been reported as highly cytotoxic with anti-viral activity that exceeds their ‘single positive’ counterparts.²⁰⁸ CD8^{low} T cell populations have also been reported in viral contexts such as Epstein-Barr virus (EBV),²⁰⁹ and were also reported as a pathogenic population associated with a progressive form of multiple sclerosis.²¹⁰ Similarly to CD4⁺CD8⁺ T cells, CD8^{low} T cells are an understudied cell population with diverse, highly context-dependent, functional capabilities. As such, further investigation is warranted to determine the functional properties of the CD4⁺CD8⁺ central memory T cells, and CD8^{low} T cells observed in VPR individuals.

In addition to CD4⁺ and CD8⁺ T cell activation, our study aimed to investigate the circulating T follicular helper (cTfh) responses elicited by mRNA vaccines in our VPR, VMR, and VSR donor groups. We hypothesized that VPRs could be further defined by a discordant cTfh phenotype, characterized by chemokine receptor CCR6 and CXCR3 expression. We evaluated bulk cTfh (all CXCR5⁺) and activated cTfh (OX40⁺CD40L⁺ CXCR5⁺ cells) in both CD4⁺ and CD8⁺ T cell populations. We found that while VPRs had increased cTfh17 (CCR6⁺CXCR3⁻) *bulk* CD4⁺CXCR5⁺ cells, they had significantly increased cTfh1 (CCR6⁻CXCR3⁺) *activated* CD4⁺CXCR5⁺ cells. These data support our original hypothesis and lend credence to the possibility of an altered mRNA vaccine-induced immunologic landscape in VPR individuals. In addition to CXCR5 expression on

CD4⁺ cells, we evaluated CD8⁺ cells for CXCR5 surface expression because CXCR5⁺ CD8⁺ T cells have recently been implicated in the regulation of humoral responses to viral infection and vaccination.^{189,211} Surprisingly, in VPRs exclusively, we observed a significant increase in mean frequency and cell count of CD8⁺CXCR5⁺ cells as a frequency of CD3⁺ cells. Although CD8⁺CXCR5⁺ cells are somewhat controversial, as the functions of Tfh cells are generally exclusively attributed to CD4⁺ cells, CXCR5 expression on CD8⁺ cells has been well documented.^{191,211} One group recently described a phenotypically and transcriptionally distinct CD8⁺CXCR5⁺ population in SARS-CoV-2 naturally infected and vaccinated cohorts,²¹² however, their cohort was vaccinated with CoronaVac (Sinovac), an inactivated whole virus immunization platform; thus, results are not comparable.

Our cumulative cTfh data demonstrated an altered immunologic landscape of activated cTfh phenotypes (favoring cTfh1 activation/expansion in VPRs), as well as the expansion CD8⁺CXCR5⁺ T cell populations in VPRs, compared to VMR and VSR groups. Although experiments in the Tfh section of this dissertation are limited to identification and phenotypic characterization of follicular helper cell responses across NAb response groups, several downstream studies may be applicable. As CD8⁺CXCR5⁺ T cells are functionally diverse and have been implicated as cytotoxic, regulatory, and as potent B cell helpers in GC reactions, we suspect that the expansion of CD8⁺CXCR5⁺ cells may be responsible for the altered CD4⁺ Tfh phenotype activation seen in VPRs. However, to address this question experimentally would likely require an adoptive transfer humanized animal model, in which isolated CD8⁺CXCR5⁺ cells are transferred to the animal prior to SARS-CoV-2 mRNA immunization, and peripheral and lymph

node Tfh cells are evaluated over time. To evaluate function of CD8⁺CXCR5⁺ T cells in the context of B cell regulation, *in vitro* co-cultures of isolated CD8⁺CXCR5⁺ T cells and B cells from selected VPR, VMR, and VSR individuals could be used to assess antibody isotype, neutralization capacity, and cytokine secretion induced by experimental microenvironments over time. Further, quantitative transcriptomic evaluation of expanded populations may elucidate functional properties of CD8⁺CXCR5⁺ cells, such as the level of Bcl6 expression in a classical Tfh context, or forkhead box P3 (FOXP3) in a regulatory T cell context. To evaluate a potential cytotoxic role for these cell populations, one can perform *in vitro* cytotoxicity assays in addition to flow cytometric assessment of granzyme and perforin expression, or quantification of apoptotic cells via Annexin V staining assays. These suggested experiments are by no means limited, and simply aim to provide an example of the ample downstream investigation potential for further characterization of unique cell populations identified in individuals with impaired neutralizing antibody responses to COVID-19 mRNA vaccination.

Finally, we evaluated 25 different cytokines in the supernatant of spike-peptide megapool stimulated PBMCs from all donors using a flow cytometric bead-based multiplex assay. Several cytokines in our panel were below the limit of detection, however, those of interest included tumor necrosis factor alpha (TNF α), interleukin-2 (IL-2), interleukin-27 (IL-27), and interferon gamma (IFN γ). No differences were observed between vaccinated groups, although significantly increased IFN γ concentrations were observed in VPRs and VSRs, relative to naturally infected individuals.

The results of this research provide novel insight into the vast heterogeneity of human immunologic responses to COVID-19 mRNA vaccination. The foremost intention at the beginning of this project was to increase the accessibility of SARS-CoV-2 NAb quantitation via development of a surrogate assay to the laborious, expensive, and time-consuming gold-standard live virus neutralization assay. This work cumulatively highlights the critical need for COVID-19 NAb testing accessibility to all individuals, such that VPRs can be identified (voluntarily) following standard vaccination protocol and make personal protective decisions accordingly, under the guidance and supervision of their healthcare provider. Moreover, we highlight the differences in underlying immunologic response to mRNA vaccination in VPR individuals, likely reflective of population-level heterogeneity.

REFERENCES

1. Li Y, Wang X, Nair H. Global Seasonality of Human Seasonal Coronaviruses: A Clue for Postpandemic Circulating Season of Severe Acute Respiratory Syndrome Coronavirus 2? *J Infect Dis.* 2020;222(7):1090-1097. doi:10.1093/infdis/jiaa436
2. Edridge AWD, Kaczorowska J, Hoste ACR, et al. Seasonal coronavirus protective immunity is short-lasting. *Nat Med.* 2020;26(11):1691-1693. doi:10.1038/s41591-020-1083-1
3. Cherry JD, Krogstad P. SARS: The First Pandemic of the 21st Century. *Pediatr Res.* 2004;56(1):1-5. doi:10.1203/01.PDR.0000129184.87042.FC
4. Vu HT, Leitmeyer KC, Le DH, et al. Clinical description of a completed outbreak of SARS in Vietnam, February-May 2003. *Emerg Infect Dis.* 2004;10(2):334-338. doi:10.3201/eid1002.030761
5. Wilder-Smith A, Telemann MD, Heng BH, Earnest A, Ling AE, Leo YS. Asymptomatic SARS coronavirus infection among healthcare workers, Singapore. *Emerg Infect Dis.* 2005;11(7):1142-1145. doi:10.3201/eid1107.041165
6. Corman VM, Muth D, Niemeyer D, Drosten C. Hosts and Sources of Endemic Human Coronaviruses. In: *Advances in Virus Research.* Vol 100. Elsevier; 2018:163-188. doi:10.1016/bs.aivir.2018.01.001
7. Zaki AM, van Boheemen S, Bestebroer TM, Osterhaus ADME, Fouchier RAM. Isolation of a novel coronavirus from a man with pneumonia in Saudi Arabia. *N Engl J Med.* 2012;367(19):1814-1820. doi:10.1056/NEJMoa1211721
8. Ahmed AE. The predictors of 3- and 30-day mortality in 660 MERS-CoV patients. *BMC Infect Dis.* 2017;17(1):615. doi:10.1186/s12879-017-2712-2
9. Oh M don, Park WB, Park SW, et al. Middle East respiratory syndrome: what we learned from the 2015 outbreak in the Republic of Korea. *Korean J Intern Med.* 2018;33(2):233-246. doi:10.3904/kjim.2018.031
10. Sheahan TP, Sims AC, Leist SR, et al. Comparative therapeutic efficacy of remdesivir and combination lopinavir, ritonavir, and interferon beta against MERS-CoV. *Nat Commun.* 2020;11(1):222. doi:10.1038/s41467-019-13940-6
11. Rabaan AA, Alahmed SH, Bazzi AM, Alhani HM. A review of candidate therapies for Middle East respiratory syndrome from a molecular perspective. *J Med Microbiol.* 2017;66(9):1261-1274. doi:10.1099/jmm.0.000565

12. Arabi Y, Balkhy H, Hajeer AH, et al. Feasibility, safety, clinical, and laboratory effects of convalescent plasma therapy for patients with Middle East respiratory syndrome coronavirus infection: a study protocol. *SpringerPlus*. 2015;4(1):709. doi:10.1186/s40064-015-1490-9
13. Briggs N, Gormally MV, Li F, et al. Early but not late convalescent plasma is associated with better survival in moderate-to-severe COVID-19. Chen RJ, ed. *PLoS ONE*. 2021;16(7):e0254453. doi:10.1371/journal.pone.0254453
14. Ripoll JG, van Helmond N, Senefeld JW, et al. Convalescent Plasma for Infectious Diseases: Historical Framework and Use in COVID-19. *Clin Microbiol Newsl*. 2021;43(4):23-32. doi:10.1016/j.clinmicnews.2021.02.001
15. Piyush R, Rajarshi K, Khan R, Ray S. Convalescent plasma therapy: a promising coronavirus disease 2019 treatment strategy. *Open Biol*. 2020;10(9):200174. doi:10.1098/rsob.200174
16. Keller MA, Stiehm ER. Passive immunity in prevention and treatment of infectious diseases. *Clin Microbiol Rev*. 2000;13(4):602-614. doi:10.1128/CMR.13.4.602
17. Garraud O. Use of convalescent plasma in Ebola virus infection. *Transfusion and Apheresis Science*. 2017;56(1):31-34. doi:10.1016/j.transci.2016.12.014
18. Al-Tawfiq JA, Arabi Y. Convalescent plasma therapy for coronavirus infection: experience from MERS and application in COVID-19. *Hum Vaccin Immunother*. 2020;16(12):2973-2979. doi:10.1080/21645515.2020.1793712
19. Gharbharan A, Jordans CCE, GeurtsvanKessel C, et al. Effects of potent neutralizing antibodies from convalescent plasma in patients hospitalized for severe SARS-CoV-2 infection. *Nat Commun*. 2021;12(1):3189. doi:10.1038/s41467-021-23469-2
20. Duan K, Liu B, Li C, et al. Effectiveness of convalescent plasma therapy in severe COVID-19 patients. *Proc Natl Acad Sci USA*. 2020;117(17):9490-9496. doi:10.1073/pnas.2004168117
21. Meekins DA, Gaudreault NN, Richt JA. Natural and Experimental SARS-CoV-2 Infection in Domestic and Wild Animals. *Viruses*. 2021;13(10):1993. doi:10.3390/v13101993
22. Rahman MT, Sobur MA, Islam MS, et al. Zoonotic Diseases: Etiology, Impact, and Control. *Microorganisms*. 2020;8(9):1405. doi:10.3390/microorganisms8091405
23. Messenger AM, Barnes AN, Gray GC. Reverse zoonotic disease transmission (zooanthroponosis): a systematic review of seldom-documented human biological threats to animals. *PLoS One*. 2014;9(2):e89055. doi:10.1371/journal.pone.0089055

24. Lim YX, Ng YL, Tam JP, Liu DX. Human Coronaviruses: A Review of Virus-Host Interactions. *Diseases*. 2016;4(3):26. doi:10.3390/diseases4030026
25. Cui J, Li F, Shi ZL. Origin and evolution of pathogenic coronaviruses. *Nat Rev Microbiol*. 2019;17(3):181-192. doi:10.1038/s41579-018-0118-9
26. Pormohammad A, Ghorbani S, Khatami A, et al. Comparison of confirmed COVID-19 with SARS and MERS cases - Clinical characteristics, laboratory findings, radiographic signs and outcomes: A systematic review and meta-analysis. *Rev Med Virol*. 2020;30(4):e2112. doi:10.1002/rmv.2112
27. Zhou P, Yang XL, Wang XG, et al. A pneumonia outbreak associated with a new coronavirus of probable bat origin. *Nature*. 2020;579(7798):270-273. doi:10.1038/s41586-020-2012-7
28. Lu R, Zhao X, Li J, et al. Genomic characterisation and epidemiology of 2019 novel coronavirus: implications for virus origins and receptor binding. *Lancet*. 2020;395(10224):565-574. doi:10.1016/S0140-6736(20)30251-8
29. Lau SKP, Luk HKH, Wong ACP, et al. Possible Bat Origin of Severe Acute Respiratory Syndrome Coronavirus 2. *Emerg Infect Dis*. 2020;26(7):1542-1547. doi:10.3201/eid2607.200092
30. Lytras S, Hughes J, Martin D, et al. Exploring the Natural Origins of SARS-CoV-2 in the Light of Recombination. Stern A, ed. *Genome Biology and Evolution*. 2022;14(2):evac018. doi:10.1093/gbe/evac018
31. Huang XY, Chen Q, Sun MX, et al. A pangolin-origin SARS-CoV-2-related coronavirus: infectivity, pathogenicity, and cross-protection by preexisting immunity. *Cell Discov*. 2023;9(1):59. doi:10.1038/s41421-023-00557-9
32. Lake DF, Roeder AJ, Kaleta E, et al. Development of a rapid point-of-care test that measures neutralizing antibodies to SARS-CoV-2. *Journal of Clinical Virology*. 2021;145:105024. doi:10.1016/j.jcv.2021.105024
33. She J, Jiang J, Ye L, Hu L, Bai C, Song Y. 2019 novel coronavirus of pneumonia in Wuhan, China: emerging attack and management strategies. *Clin Transl Med*. 2020;9(1):19. doi:10.1186/s40169-020-00271-z
34. *WHO Novel Coronavirus (2019-nCoV) Situation Report 1*. Accessed October 14, 2023. <https://www.who.int/docs/default-source/coronaviruse/situation-reports/20200121-sitrep-1-2019-ncov.pdf>
35. Holshue ML, DeBolt C, Lindquist S, et al. First Case of 2019 Novel Coronavirus in the United States. *N Engl J Med*. 2020;382(10):929-936. doi:10.1056/NEJMoa2001191

36. CDC Museum COVID-19 Timeline. Accessed October 14, 2023. <https://www.cdc.gov/museum/timeline/covid19.html>
37. Jiang S, Shi Z, Shu Y, et al. A distinct name is needed for the new coronavirus. *The Lancet*. 2020;395(10228):949. doi:10.1016/S0140-6736(20)30419-0
38. CDC, Washington State Report First COVID-19 Death. Accessed October 14, 2023. <https://www.cdc.gov/media/releases/2020/s0229-COVID-19-first-death.html>
39. CDC Morbidity and Mortality Weekly Report - Public Health Responses to COVID-19 Outbreaks on Cruise Ships - Worldwide, February-March 2020.; 2020. Accessed October 14, 2023. <https://www.cdc.gov/mmwr/volumes/69/wr/pdfs/mm6912e3-H.pdf>
40. Cucinotta D, Vanelli M. WHO Declares COVID-19 a Pandemic. *Acta Biomed*. 2020;91(1):157-160. doi:10.23750/abm.v91i1.9397
41. NIH Clinical Trial of Investigational Vaccine for COVID-19 Begins.; 2020. Accessed October 14, 2023. <https://www.nih.gov/news-events/news-releases/nih-clinical-trial-investigational-vaccine-covid-19-begins>
42. Leitner WW, Ying H, Restifo NP. DNA and RNA-based vaccines: principles, progress and prospects. *Vaccine*. 1999;18(9-10):765-777. doi:10.1016/s0264-410x(99)00271-6
43. Plotkin SA. Vaccines: past, present and future. *Nat Med*. 2005;11(4 Suppl):S5-11. doi:10.1038/nm1209
44. Plotkin S. History of vaccination. *Proc Natl Acad Sci U S A*. 2014;111(34):12283-12287. doi:10.1073/pnas.1400472111
45. Gottlieb RL, Vaca CE, Paredes R, et al. Early Remdesivir to Prevent Progression to Severe Covid-19 in Outpatients. *N Engl J Med*. 2022;386(4):305-315. doi:10.1056/NEJMoa2116846
46. Clancy CJ, Nguyen MH. A First Draft of the History of Treating Coronavirus Disease 2019: Use of Repurposed Medications in United States Hospitals. *Open Forum Infect Dis*. 2021;8(2):ofaa617. doi:10.1093/ofid/ofaa617
47. McCreary EK, Pogue JM. Coronavirus Disease 2019 Treatment: A Review of Early and Emerging Options. *Open Forum Infectious Diseases*. 2020;7(4):ofaa105. doi:10.1093/ofid/ofaa105
48. Joyner MJ, Bruno KA, Klassen SA, et al. Safety Update. *Mayo Clinic Proceedings*. 2020;95(9):1888-1897. doi:10.1016/j.mayocp.2020.06.028

49. Jaafar R, Boschi C, Aherfi S, et al. High Individual Heterogeneity of Neutralizing Activities against the Original Strain and Nine Different Variants of SARS-CoV-2. *Viruses*. 2021;13(11):2177. doi:10.3390/v13112177
50. Stoddard M, Yuan L, Sarkar S, et al. Heterogeneity in Vaccinal Immunity to SARS-CoV-2 Can Be Addressed by a Personalized Booster Strategy. *Vaccines (Basel)*. 2023;11(4):806. doi:10.3390/vaccines11040806
51. Chen X, Pan Z, Yue S, et al. Disease severity dictates SARS-CoV-2-specific neutralizing antibody responses in COVID-19. *Sig Transduct Target Ther*. 2020;5(1):180. doi:10.1038/s41392-020-00301-9
52. Wu F, Wang A, Liu M, et al. *Neutralizing Antibody Responses to SARS-CoV-2 in a COVID-19 Recovered Patient Cohort and Their Implications*. *Infectious Diseases (except HIV/AIDS)*; 2020. doi:10.1101/2020.03.30.20047365
53. *Convalescent Plasma EUA Letter of Authorization 12282021*.; 2021. Accessed October 14, 2023. <https://www.fda.gov/media/141478/download>
54. Franchini M. Convalescent plasma therapy for managing infectious diseases: a narrative review. *Ann Blood*. 2021;6:17-17. doi:10.21037/aob-2020-cp-03
55. Sun M, Xu Y, He H, et al. A potentially effective treatment for COVID-19: A systematic review and meta-analysis of convalescent plasma therapy in treating severe infectious disease. *Int J Infect Dis*. 2020;98:334-346. doi:10.1016/j.ijid.2020.06.107
56. Pandey S, Vyas GN. Adverse effects of plasma transfusion. *Transfusion*. 2012;52 Suppl 1(Suppl 1):65S-79S. doi:10.1111/j.1537-2995.2012.03663.x
57. Filippatos C, Ntanasis-Stathopoulos I, Sekeri K, et al. Convalescent Plasma Therapy for COVID-19: A Systematic Review and Meta-Analysis on Randomized Controlled Trials. *Viruses*. 2023;15(3):765. doi:10.3390/v15030765
58. Vegivinti CTR, Pederson JM, Saravu K, et al. Efficacy of convalescent plasma therapy for COVID-19: A systematic review and meta-analysis. *J Clin Apher*. 2021;36(3):470-482. doi:10.1002/jca.21881
59. *Updated Evidence to Support the Emergency Use of COVID-19 Convalescent Plasma – as of 9/23/2020*. Accessed October 14, 2023. <https://www.fda.gov/media/142386/download>
60. Liu KT, Han YJ, Wu GH, Huang KYA, Huang PN. Overview of Neutralization Assays and International Standard for Detecting SARS-CoV-2 Neutralizing Antibody. *Viruses*. 2022;14(7):1560. doi:10.3390/v14071560

61. *Bamlanivimab EUA Letter of Authorization 03022021.*; 2020. Accessed October 14, 2023. <https://www.fda.gov/media/143602/download>
62. *Promising Interim Results from Clinical Trial of NIH-Moderna COVID-19 Vaccine.*; 2020. Accessed October 23, 2023. <https://www.nih.gov/news-events/news-releases/promising-interim-results-clinical-trial-nih-moderna-covid-19-vaccine>
63. Baden LR, El Sahly HM, Essink B, et al. Efficacy and Safety of the mRNA-1273 SARS-CoV-2 Vaccine. *N Engl J Med.* 2021;384(5):403-416. doi:10.1056/NEJMoa2035389
64. *Pfizer and BioNTech Conclude Phase 3 Study of COVID-19 Vaccine Candidate, Meeting All Primary Efficacy Endpoints.*; 2020. Accessed October 23, 2023. <https://www.pfizer.com/news/press-release/press-release-detail/pfizer-and-biontech-conclude-phase-3-study-covid-19-vaccine>
65. Polack FP, Thomas SJ, Kitchin N, et al. Safety and Efficacy of the BNT162b2 mRNA Covid-19 Vaccine. *N Engl J Med.* 2020;383(27):2603-2615. doi:10.1056/NEJMoa2034577
66. Fortner A, Schumacher D. First COVID-19 Vaccines Receiving the US FDA and EMA Emergency Use Authorization. *Discoveries (Craiova).* 2021;9(1):e122. doi:10.15190/d.2021.1
67. Feldman RA, Fuhr R, Smolenov I, et al. mRNA vaccines against H10N8 and H7N9 influenza viruses of pandemic potential are immunogenic and well tolerated in healthy adults in phase 1 randomized clinical trials. *Vaccine.* 2019;37(25):3326-3334. doi:10.1016/j.vaccine.2019.04.074
68. Lowe R, Barcellos C, Brasil P, et al. The Zika Virus Epidemic in Brazil: From Discovery to Future Implications. *Int J Environ Res Public Health.* 2018;15(1):96. doi:10.3390/ijerph15010096
69. Tebas P, Roberts CC, Muthumani K, et al. Safety and Immunogenicity of an Anti-Zika Virus DNA Vaccine. *N Engl J Med.* 2021;385(12):e35. doi:10.1056/NEJMoa1708120
70. *VRC 705: A Zika Virus DNA Vaccine in Healthy Adults and Adolescents (DNA).*; 2023. Accessed October 14, 2023. <https://clinicaltrials.gov/study/NCT03110770>
71. Kamboj M, Sepkowitz KA. Risk of transmission associated with live attenuated vaccines given to healthy persons caring for or residing with an immunocompromised patient. *Infect Control Hosp Epidemiol.* 2007;28(6):702-707. doi:10.1086/517952

72. Pöyhönen L, Bustamante J, Casanova JL, Jouanguy E, Zhang Q. Life-Threatening Infections Due to Live-Attenuated Vaccines: Early Manifestations of Inborn Errors of Immunity. *J Clin Immunol*. 2019;39(4):376-390. doi:10.1007/s10875-019-00642-3
73. Valenzuela P, Medina A, Rutter WJ, Ammerer G, Hall BD. Synthesis and assembly of hepatitis B virus surface antigen particles in yeast. *Nature*. 1982;298(5872):347-350. doi:10.1038/298347a0
74. Nascimento IP, Leite LCC. Recombinant vaccines and the development of new vaccine strategies. *Braz J Med Biol Res*. 2012;45(12):1102-1111. doi:10.1590/s0100-879x2012007500142
75. de Pinho Favaro MT, Atienza-Garriga J, Martínez-Torró C, et al. Recombinant vaccines in 2022: a perspective from the cell factory. *Microb Cell Fact*. 2022;21(1):203. doi:10.1186/s12934-022-01929-8
76. Joshi G, Borah P, Thakur S, Sharma P, Mayank null, Poduri R. Exploring the COVID-19 vaccine candidates against SARS-CoV-2 and its variants: where do we stand and where do we go? *Hum Vaccin Immunother*. 2021;17(12):4714-4740. doi:10.1080/21645515.2021.1995283
77. Sadoff J, Gray G, Vandebosch A, et al. Safety and Efficacy of Single-Dose Ad26.COVS.2 Vaccine against Covid-19. *N Engl J Med*. 2021;384(23):2187-2201. doi:10.1056/NEJMoa2101544
78. Voysey M, Clemens SAC, Madhi SA, et al. Safety and efficacy of the ChAdOx1 nCoV-19 vaccine (AZD1222) against SARS-CoV-2: an interim analysis of four randomised controlled trials in Brazil, South Africa, and the UK. *Lancet*. 2021;397(10269):99-111. doi:10.1016/S0140-6736(20)32661-1
79. Pollet J, Chen WH, Strych U. Recombinant protein vaccines, a proven approach against coronavirus pandemics. *Adv Drug Deliv Rev*. 2021;170:71-82. doi:10.1016/j.addr.2021.01.001
80. Heath PT, Galiza EP, Baxter DN, et al. Safety and Efficacy of NVX-CoV2373 Covid-19 Vaccine. *N Engl J Med*. 2021;385(13):1172-1183. doi:10.1056/NEJMoa2107659
81. Le TT, Cramer JP, Chen R, Mayhew S. Evolution of the COVID-19 vaccine development landscape. *Nat Rev Drug Discov*. 2020;19(10):667-668. doi:10.1038/d41573-020-00151-8
82. McCrone JT, Hill V, Bajaj S, et al. Context-specific emergence and growth of the SARS-CoV-2 Delta variant. *medRxiv*. Published online December 21, 2021:2021.12.14.21267606. doi:10.1101/2021.12.14.21267606

83. Crotty S. T follicular helper cell differentiation, function, and roles in disease. *Immunity*. 2014;41(4):529-542. doi:10.1016/j.immuni.2014.10.004
84. Ghinai I, McPherson TD, Hunter JC, et al. First known person-to-person transmission of severe acute respiratory syndrome coronavirus 2 (SARS-CoV-2) in the USA. *The Lancet*. 2020;395(10230):1137-1144. doi:10.1016/S0140-6736(20)30607-3
85. Huang C, Wang Y, Li X, et al. Clinical features of patients infected with 2019 novel coronavirus in Wuhan, China. *The Lancet*. 2020;395(10223):497-506. doi:10.1016/S0140-6736(20)30183-5
86. Li R, Pei S, Chen B, et al. Substantial undocumented infection facilitates the rapid dissemination of novel coronavirus (SARS-CoV-2). *Science*. 2020;368(6490):489-493. doi:10.1126/science.abb3221
87. Widge AT, Roupheal NG, Jackson LA, et al. Durability of Responses after SARS-CoV-2 mRNA-1273 Vaccination. *N Engl J Med*. 2021;384(1):80-82. doi:10.1056/NEJMc2032195
88. Robbiani DF, Gaebler C, Muecksch F, et al. *Convergent Antibody Responses to SARS-CoV-2 Infection in Convalescent Individuals*. *Immunology*; 2020. doi:10.1101/2020.05.13.092619
89. Juno JA, Tan HX, Lee WS, et al. *Immunogenic Profile of SARS-CoV-2 Spike in Individuals Recovered from COVID-19*. *Infectious Diseases (except HIV/AIDS)*; 2020. doi:10.1101/2020.05.17.20104869
90. Han Z, Battaglia F, Terlecky SR. Discharged COVID-19 patients testing positive again for SARS-CoV-2 RNA: A minireview of published studies from China. *Journal of Medical Virology*. 2021;93(1):262-274. doi:10.1002/jmv.26250
91. Ye G, Pan Z, Pan Y, et al. Clinical characteristics of severe acute respiratory syndrome coronavirus 2 reactivation. *Journal of Infection*. 2020;80(5):e14-e17. doi:10.1016/j.jinf.2020.03.001
92. Hoang VT, Dao TL, Gautret P. Recurrence of positive SARS-CoV-2 in patients recovered from COVID-19. *Journal of Medical Virology*. 2020;92(11):2366-2367. doi:10.1002/jmv.26056
93. Wang Q, Zhang Y, Wu L, et al. Structural and Functional Basis of SARS-CoV-2 Entry by Using Human ACE2. *Cell*. 2020;181(4):894-904.e9. doi:10.1016/j.cell.2020.03.045
94. Premkumar L, Segovia-Chumbez B, Jadi R, et al. The receptor-binding domain of the viral spike protein is an immunodominant and highly specific target of antibodies in SARS-CoV-2 patients. *Sci Immunol*. 2020;5(48):eabc8413. doi:10.1126/sciimmunol.abc8413

95. Tan CW, Chia WN, Qin X, et al. A SARS-CoV-2 surrogate virus neutralization test based on antibody-mediated blockage of ACE2–spike protein–protein interaction. *Nat Biotechnol.* 2020;38(9):1073-1078. doi:10.1038/s41587-020-0631-z
96. Xie X, Muruato A, Lokugamage KG, et al. An Infectious cDNA Clone of SARS-CoV-2. *Cell Host & Microbe.* 2020;27(5):841-848.e3. doi:10.1016/j.chom.2020.04.004
97. Giavarina D. Understanding Bland Altman analysis. *Biochem Med.* 2015;25(2):141-151. doi:10.11613/BM.2015.015
98. Doğan NÖ. Bland-Altman analysis: A paradigm to understand correlation and agreement. *Turkish Journal of Emergency Medicine.* 2018;18(4):139-141. doi:10.1016/j.tjem.2018.09.001
99. Obuchowski NA, Bullen JA. Receiver operating characteristic (ROC) curves: review of methods with applications in diagnostic medicine. *Phys Med Biol.* 2018;63(7):07TR01. doi:10.1088/1361-6560/aab4b1
100. Nakas CT, Yiannoutsos CT. Ordered multiple-class ROC analysis with continuous measurements. *Statistics in Medicine.* 2004;23(22):3437-3449. doi:10.1002/sim.1917
101. Schober P, Boer C, Schwarte LA. Correlation Coefficients: Appropriate Use and Interpretation. *Anesthesia & Analgesia.* 2018;126(5):1763-1768. doi:10.1213/ANE.0000000000002864
102. Rights JD, Sterba SK. Quantifying explained variance in multilevel models: An integrative framework for defining R-squared measures. *Psychological Methods.* 2019;24(3):309-338. doi:10.1037/met0000184
103. Rights JD, Sterba SK. A framework of R-squared measures for single-level and multilevel regression mixture models. *Psychological Methods.* 2018;23(3):434-457. doi:10.1037/met0000139
104. Rights JD, Sterba SK. New Recommendations on the Use of R-Squared Differences in Multilevel Model Comparisons. *Multivariate Behavioral Research.* 2020;55(4):568-599. doi:10.1080/00273171.2019.1660605
105. Jackson LA, Anderson EJ, Roupael NG, et al. An mRNA Vaccine against SARS-CoV-2 — Preliminary Report. *N Engl J Med.* 2020;383(20):1920-1931. doi:10.1056/NEJMoa2022483
106. Lombardi A, Bozzi G, Ungaro R, et al. Mini Review Immunological Consequences of Immunization With COVID-19 mRNA Vaccines: Preliminary Results. *Front Immunol.* 2021;12:657711. doi:10.3389/fimmu.2021.657711

107. Sahin U, Muik A, Derhovanessian E, et al. COVID-19 vaccine BNT162b1 elicits human antibody and TH1 T cell responses. *Nature*. 2020;586(7830):594-599. doi:10.1038/s41586-020-2814-7
108. Anderson EJ, Roupael NG, Widge AT, et al. Safety and Immunogenicity of SARS-CoV-2 mRNA-1273 Vaccine in Older Adults. *N Engl J Med*. 2020;383(25):2427-2438. doi:10.1056/NEJMoa2028436
109. Doria-Rose N, Suthar MS, Makowski M, et al. Antibody Persistence through 6 Months after the Second Dose of mRNA-1273 Vaccine for Covid-19. *N Engl J Med*. 2021;384(23):2259-2261. doi:10.1056/NEJMc2103916
110. Ebinger JE, Fert-Bober J, Printsev I, et al. Antibody responses to the BNT162b2 mRNA vaccine in individuals previously infected with SARS-CoV-2. *Nat Med*. 2021;27(6):981-984. doi:10.1038/s41591-021-01325-6
111. Chi X, Yan R, Zhang J, et al. A neutralizing human antibody binds to the N-terminal domain of the Spike protein of SARS-CoV-2. *Science*. 2020;369(6504):650-655. doi:10.1126/science.abc6952
112. Liu L, Wang P, Nair MS, et al. Potent neutralizing antibodies against multiple epitopes on SARS-CoV-2 spike. *Nature*. 2020;584(7821):450-456. doi:10.1038/s41586-020-2571-7
113. Cai Y, Zhang J, Xiao T, et al. Distinct conformational states of SARS-CoV-2 spike protein. *Science*. 2020;369(6511):1586-1592. doi:10.1126/science.abd4251
114. Richardson SI, Madzorera VS, Spencer H, et al. SARS-CoV-2 Omicron triggers cross-reactive neutralization and Fc effector functions in previously vaccinated, but not unvaccinated, individuals. *Cell Host & Microbe*. 2022;30(6):880-886.e4. doi:10.1016/j.chom.2022.03.029
115. Díez JM, Romero C, Cruz M, et al. Anti-Severe Acute Respiratory Syndrome Coronavirus 2 Hyperimmune Immunoglobulin Demonstrates Potent Neutralization and Antibody-Dependent Cellular Cytotoxicity and Phagocytosis Through N and S Proteins. *The Journal of Infectious Diseases*. 2022;225(6):938-946. doi:10.1093/infdis/jiab540
116. Wu Y, Wang F, Shen C, et al. A noncompeting pair of human neutralizing antibodies block COVID-19 virus binding to its receptor ACE2. *Science*. 2020;368(6496):1274-1278. doi:10.1126/science.abc2241
117. Khoury DS, Cromer D, Reynaldi A, et al. Neutralizing antibody levels are highly predictive of immune protection from symptomatic SARS-CoV-2 infection. *Nat Med*. 2021;27(7):1205-1211. doi:10.1038/s41591-021-01377-8

118. Brouwer PJM, Caniels TG, van der Straten K, et al. Potent neutralizing antibodies from COVID-19 patients define multiple targets of vulnerability. *Science*. 2020;369(6504):643-650. doi:10.1126/science.abc5902
119. Ju B, Zhang Q, Ge X, et al. *Potent Human Neutralizing Antibodies Elicited by SARS-CoV-2 Infection*. *Immunology*; 2020. doi:10.1101/2020.03.21.990770
120. Weinreich DM, Sivapalasingam S, Norton T, et al. REGN-COV2, a Neutralizing Antibody Cocktail, in Outpatients with Covid-19. *N Engl J Med*. 2021;384(3):238-251. doi:10.1056/NEJMoa2035002
121. Bertram S, Blazquez-Navarro A, Seidel M, et al. Predictors of impaired SARS-CoV-2 immunity in healthcare workers after vaccination with BNT162b2. *Sci Rep*. 2022;12(1):6243. doi:10.1038/s41598-022-10307-8
122. Achiron A, Mandel M, Gurevich M, et al. Immune response to the third COVID-19 vaccine dose is related to lymphocyte count in multiple sclerosis patients treated with fingolimod. *J Neurol*. 2022;269(5):2286-2292. doi:10.1007/s00415-022-11030-0
123. Armbruster DA, Pry T. Limit of blank, limit of detection and limit of quantitation. *Clin Biochem Rev*. 2008;29 Suppl 1(Suppl 1):S49-52.
124. Gilbert PB, Montefiori DC, McDermott AB, et al. Immune correlates analysis of the mRNA-1273 COVID-19 vaccine efficacy clinical trial. *Science*. 2022;375(6576):43-50. doi:10.1126/science.abm3425
125. Addetia A, Crawford KHD, Dingens A, et al. Neutralizing Antibodies Correlate with Protection from SARS-CoV-2 in Humans during a Fishery Vessel Outbreak with a High Attack Rate. McAdam AJ, ed. *J Clin Microbiol*. 2020;58(11):e02107-20. doi:10.1128/JCM.02107-20
126. Grifoni A, Weiskopf D, Ramirez SI, et al. Targets of T Cell Responses to SARS-CoV-2 Coronavirus in Humans with COVID-19 Disease and Unexposed Individuals. *Cell*. 2020;181(7):1489-1501.e15. doi:10.1016/j.cell.2020.05.015
127. Le Bert N, Tan AT, Kunasegaran K, et al. SARS-CoV-2-specific T cell immunity in cases of COVID-19 and SARS, and uninfected controls. *Nature*. 2020;584(7821):457-462. doi:10.1038/s41586-020-2550-z
128. Sekine T, Perez-Potti A, Rivera-Ballesteros O, et al. *Robust T Cell Immunity in Convalescent Individuals with Asymptomatic or Mild COVID-19*. *Immunology*; 2020. doi:10.1101/2020.06.29.174888
129. Harris RJ, Hall JA, Zaidi A, Andrews NJ, Dunbar JK, Dabrera G. Effect of Vaccination on Household Transmission of SARS-CoV-2 in England. *N Engl J Med*. 2021;385(8):759-760. doi:10.1056/NEJMc2107717

130. Thomas SJ, Moreira ED, Kitchin N, et al. Safety and Efficacy of the BNT162b2 mRNA Covid-19 Vaccine through 6 Months. *N Engl J Med.* 2021;385(19):1761-1773. doi:10.1056/NEJMoa2110345
131. Levin EG, Lustig Y, Cohen C, et al. Waning Immune Humoral Response to BNT162b2 Covid-19 Vaccine over 6 Months. *N Engl J Med.* 2021;385(24):e84. doi:10.1056/NEJMoa2114583
132. Aleman A, Upadhyaya B, Tuballes K, et al. Variable cellular responses to SARS-CoV-2 in fully vaccinated patients with multiple myeloma. *Cancer Cell.* 2021;39(11):1442-1444. doi:10.1016/j.ccell.2021.09.015
133. Caillard S, Thaunat O. COVID-19 vaccination in kidney transplant recipients. *Nat Rev Nephrol.* 2021;17(12):785-787. doi:10.1038/s41581-021-00491-7
134. Marion O, Del Bello A, Abravanel F, et al. Safety and Immunogenicity of Anti-SARS-CoV-2 Messenger RNA Vaccines in Recipients of Solid Organ Transplants. *Ann Intern Med.* 2021;174(9):1336-1338. doi:10.7326/M21-1341
135. Mazzola A, Todesco E, Drouin S, et al. Poor Antibody Response After Two Doses of Severe Acute Respiratory Syndrome Coronavirus 2 (SARS-CoV-2) Vaccine in Transplant Recipients. *Clinical Infectious Diseases.* Published online June 24, 2021:ciab580. doi:10.1093/cid/ciab580
136. Simon D, Tascilar K, Fagni F, et al. SARS-CoV-2 vaccination responses in untreated, conventionally treated and anticytokine-treated patients with immune-mediated inflammatory diseases. *Ann Rheum Dis.* 2021;80(10):1312. doi:10.1136/annrheumdis-2021-220461
137. Wiedermann U, Garner-Spitzer E, Wagner A. Primary vaccine failure to routine vaccines: Why and what to do? *Human Vaccines & Immunotherapeutics.* 2016;12(1):239-243. doi:10.1080/21645515.2015.1093263
138. Hannoun C, Megas F, Piercy J. Immunogenicity and protective efficacy of influenza vaccination. *Virus Research.* 2004;103(1-2):133-138. doi:10.1016/j.virusres.2004.02.025
139. Schmidt F, Muecksch F, Weisblum Y, et al. Plasma Neutralization of the SARS-CoV-2 Omicron Variant. *N Engl J Med.* Published online December 30, 2021:NEJMc2119641. doi:10.1056/NEJMc2119641
140. Lipsitch M, Krammer F, Regev-Yochay G, Lustig Y, Balicer RD. SARS-CoV-2 breakthrough infections in vaccinated individuals: measurement, causes and impact. *Nat Rev Immunol.* 2022;22(1):57-65. doi:10.1038/s41577-021-00662-4

141. Bergwerk M, Gonen T, Lustig Y, et al. Covid-19 Breakthrough Infections in Vaccinated Health Care Workers. *N Engl J Med*. 2021;385(16):1474-1484. doi:10.1056/NEJMoa2109072
142. Goldberg Y, Mandel M, Bar-On YM, et al. Waning Immunity after the BNT162b2 Vaccine in Israel. *N Engl J Med*. 2021;385(24):e85. doi:10.1056/NEJMoa2114228
143. Gharpure R, Sami S, Vostok J, et al. Multistate Outbreak of SARS-CoV-2 Infections, Including Vaccine Breakthrough Infections, Associated with Large Public Gatherings, United States. *Emerg Infect Dis*. 2022;28(1):35-43. doi:10.3201/eid2801.212220
144. Juthani PV, Gupta A, Borges KA, et al. Hospitalisation among vaccine breakthrough COVID-19 infections. *The Lancet Infectious Diseases*. 2021;21(11):1485-1486. doi:10.1016/S1473-3099(21)00558-2
145. Kuhlmann C, Mayer CK, Claassen M, et al. Breakthrough infections with SARS-CoV-2 omicron despite mRNA vaccine booster dose. *The Lancet*. Published online January 2022:S0140673622000903. doi:10.1016/S0140-6736(22)00090-3
146. Williams E, Colson J, Valiathan R, et al. *PERMISSIVE OMICRON BREAKTHROUGH INFECTIONS IN INDIVIDUALS WITH BINDING OR NEUTRALIZING ANTIBODIES TO ANCESTRAL SARS-CoV-2*. *Infectious Diseases (except HIV/AIDS)*; 2022. doi:10.1101/2022.04.17.22273938
147. Arora P, Zhang L, Rocha C, et al. Comparable neutralisation evasion of SARS-CoV-2 omicron subvariants BA.1, BA.2, and BA.3. *The Lancet Infectious Diseases*. 2022;22(6):766-767. doi:10.1016/S1473-3099(22)00224-9
148. Lake DF, Roeder AJ, Gonzalez-Moa MJ, et al. Third COVID-19 vaccine dose boosts neutralizing antibodies in poor responders. *Commun Med*. 2022;2(1):85. doi:10.1038/s43856-022-00151-2
149. Ghosh N, Nandi S, Saha I. A review on evolution of emerging SARS-CoV-2 variants based on spike glycoprotein. *International Immunopharmacology*. 2022;105:108565. doi:10.1016/j.intimp.2022.108565
150. Flores-Vega VR, Monroy-Molina JV, Jiménez-Hernández LE, Torres AG, Santos-Preciado JI, Rosales-Reyes R. SARS-CoV-2: Evolution and Emergence of New Viral Variants. *Viruses*. 2022;14(4):653. doi:10.3390/v14040653
151. Legros V, Denolly S, Vogrig M, et al. A longitudinal study of SARS-CoV-2-infected patients reveals a high correlation between neutralizing antibodies and COVID-19 severity. *Cell Mol Immunol*. 2021;18(2):318-327. doi:10.1038/s41423-020-00588-2

152. Evans JP, Zeng C, Carlin C, et al. Neutralizing antibody responses elicited by SARS-CoV-2 mRNA vaccination wane over time and are boosted by breakthrough infection. *Sci Transl Med*. 2022;14(637):eabn8057. doi:10.1126/scitranslmed.abn8057
153. Vassilaki N, Gargalionis AN, Bletsas A, et al. Impact of Age and Sex on Antibody Response Following the Second Dose of COVID-19 BNT162b2 mRNA Vaccine in Greek Healthcare Workers. *Microorganisms*. 2021;9(8):1725. doi:10.3390/microorganisms9081725
154. Bignucolo A, Scarabel L, Mezzalana S, Polesel J, Cecchin E, Toffoli G. Sex Disparities in Efficacy in COVID-19 Vaccines: A Systematic Review and Meta-Analysis. *Vaccines*. 2021;9(8):825. doi:10.3390/vaccines9080825
155. Klein SL, Flanagan KL. Sex differences in immune responses. *Nat Rev Immunol*. 2016;16(10):626-638. doi:10.1038/nri.2016.90
156. TGen Arizona COVID-19 Sequencing Dashboard. <https://pathogen.tgen.org/covidseq-tracker/>
157. Barnes CO, West AP, Huey-Tubman KE, et al. Structures of Human Antibodies Bound to SARS-CoV-2 Spike Reveal Common Epitopes and Recurrent Features of Antibodies. *Cell*. 2020;182(4):828-842.e16. doi:10.1016/j.cell.2020.06.025
158. Food and Drug Administration, FDA authorizes bamlanivimab and etesevimab monoclonal antibody therapy for post-exposure prophylaxis (prevention) for COVID-19 (2021). (available at <https://www.fda.gov/drugs/drug-safety-and-availability/fda-authorizes-bamlanivimab-and-etesevimab-monoclonal-antibody-therapy-post-exposure-prophylaxis#:~:text=FDA%20authorizes%20bamlanivimab%20and%20etesevimab,%2D19%20%7C%20FDA.>).
159. Cromer D, Steain M, Reynaldi A, et al. Neutralising antibody titres as predictors of protection against SARS-CoV-2 variants and the impact of boosting: a meta-analysis. *The Lancet Microbe*. 2022;3(1):e52-e61. doi:10.1016/S2666-5247(21)00267-6
160. Centers for Disease Control and Prevention, CDC COVID-19 vaccine and booster recommendations (2022). <https://www.cdc.gov/coronavirus/2019-ncov/vaccines/stay-up-to-date.html#recommendations>
161. Amanatidou E, Gkiouliava A, Pella E, et al. Breakthrough infections after COVID-19 vaccination: Insights, perspectives and challenges. *Metabolism Open*. 2022;14:100180. doi:10.1016/j.metop.2022.100180
162. Khandia R, Singhal S, Alqahtani T, et al. Emergence of SARS-CoV-2 Omicron (B.1.1.529) variant, salient features, high global health concerns and strategies to

- counter it amid ongoing COVID-19 pandemic. *Environ Res.* 2022;209:112816.
doi:10.1016/j.envres.2022.112816
163. Goldblatt D, Alter G, Crotty S, Plotkin SA. Correlates of protection against SARS-CoV-2 infection and COVID-19 disease. *Immunol Rev.* 2022;310(1):6-26.
doi:10.1111/imr.13091
164. Tegally H, Moir M, Everatt J, et al. Emergence of SARS-CoV-2 Omicron lineages BA.4 and BA.5 in South Africa. *Nat Med.* 2022;28(9):1785-1790.
doi:10.1038/s41591-022-01911-2
165. Tanne JH. Covid-19: BA.5 variant is now dominant in US as infections rise. *BMJ.* Published online July 18, 2022;o1770. doi:10.1136/bmj.o1770
166. Roeder AJ, Koehler MA, Jasbi P, et al. Longitudinal Comparison of Neutralizing Antibody Responses to COVID-19 mRNA Vaccines after Second and Third Doses. *Vaccines.* 2022;10(9):1459. doi:10.3390/vaccines10091459
167. Dan JM, Mateus J, Kato Y, et al. Immunological memory to SARS-CoV-2 assessed for up to 8 months after infection. *Science.* 2021;371(6529):eabf4063.
doi:10.1126/science.abf4063
168. Cantrell D. Signaling in lymphocyte activation. *Cold Spring Harb Perspect Biol.* 2015;7(6):a018788. doi:10.1101/cshperspect.a018788
169. Sadarangani M, Marchant A, Kollmann TR. Immunological mechanisms of vaccine-induced protection against COVID-19 in humans. *Nat Rev Immunol.* 2021;21(8):475-484. doi:10.1038/s41577-021-00578-z
170. Gilbert SC. T-cell-inducing vaccines - what's the future. *Immunology.* 2012;135(1):19-26. doi:10.1111/j.1365-2567.2011.03517.x
171. Thimme R, Wieland S, Steiger C, et al. CD8(+) T cells mediate viral clearance and disease pathogenesis during acute hepatitis B virus infection. *J Virol.* 2003;77(1):68-76. doi:10.1128/jvi.77.1.68-76.2003
172. Boppana S, Qin K, Files JK, et al. SARS-CoV-2-specific circulating T follicular helper cells correlate with neutralizing antibodies and increase during early convalescence. *PLoS Pathog.* 2021;17(7):e1009761.
doi:10.1371/journal.ppat.1009761
173. Zahran AM, Abdel-Rahim MH, Nasif KA, et al. Association of follicular helper T and follicular regulatory T cells with severity and hyperglycemia in hospitalized COVID-19 patients. *Virulence.* 2022;13(1):569-577.
doi:10.1080/21505594.2022.2047506

174. Yan L, de Leur K, Hendriks RW, et al. T Follicular Helper Cells As a New Target for Immunosuppressive Therapies. *Front Immunol.* 2017;8:1510. doi:10.3389/fimmu.2017.01510
175. Yeh CH, Finney J, Okada T, Kurosaki T, Kelsoe G. Primary germinal center-resident T follicular helper cells are a physiologically distinct subset of CXCR5hiPD-1hi T follicular helper cells. *Immunity.* 2022;55(2):272-289.e7. doi:10.1016/j.immuni.2021.12.015
176. Kaneko N, Kuo HH, Boucay J, et al. Loss of Bcl-6-Expressing T Follicular Helper Cells and Germinal Centers in COVID-19. *Cell.* 2020;183(1):143-157.e13. doi:10.1016/j.cell.2020.08.025
177. Zhang J, Wu Q, Liu Z, et al. Spike-specific circulating T follicular helper cell and cross-neutralizing antibody responses in COVID-19-convalescent individuals. *Nat Microbiol.* 2020;6(1):51-58. doi:10.1038/s41564-020-00824-5
178. Rydyznski Moderbacher C, Ramirez SI, Dan JM, et al. Antigen-Specific Adaptive Immunity to SARS-CoV-2 in Acute COVID-19 and Associations with Age and Disease Severity. *Cell.* 2020;183(4):996-1012.e19. doi:10.1016/j.cell.2020.09.038
179. Mateus J, Dan JM, Zhang Z, et al. Low-dose mRNA-1273 COVID-19 vaccine generates durable memory enhanced by cross-reactive T cells. *Science.* 2021;374(6566):eabj9853. doi:10.1126/science.abj9853
180. Guerrera G, Picozza M, D'Orso S, et al. BNT162b2 vaccination induces durable SARS-CoV-2-specific T cells with a stem cell memory phenotype. *Sci Immunol.* 2021;6(66):eabl5344. doi:10.1126/sciimmunol.abl5344
181. Goel RR, Painter MM, Apostolidis SA, et al. mRNA vaccines induce durable immune memory to SARS-CoV-2 and variants of concern. *Science.* 2021;374(6572):abm0829. doi:10.1126/science.abm0829
182. Zhang Z, Mateus J, Coelho CH, et al. *Humoral and Cellular Immune Memory to Four COVID-19 Vaccines.* *Immunology;* 2022. doi:10.1101/2022.03.18.484953
183. Wragg KM, Lee WS, Koutsakos M, et al. Establishment and recall of SARS-CoV-2 spike epitope-specific CD4+ T cell memory. *Nat Immunol.* 2022;23(5):768-780. doi:10.1038/s41590-022-01175-5
184. Mudd PA, Minervina AA, Pogorelyy MV, et al. SARS-CoV-2 mRNA vaccination elicits a robust and persistent T follicular helper cell response in humans. *Cell.* 2022;185(4):603-613.e15. doi:10.1016/j.cell.2021.12.026
185. Reinscheid M, Luxenburger H, Karl V, et al. COVID-19 mRNA booster vaccine induces transient CD8+ T effector cell responses while conserving the memory pool

for subsequent reactivation. *Nat Commun.* 2022;13(1):4631. doi:10.1038/s41467-022-32324-x

186. Song W, Craft J. T follicular helper cell heterogeneity: Time, space, and function. *Immunol Rev.* 2019;288(1):85-96. doi:10.1111/imr.12740
187. Brenna E, Davydov AN, Ladell K, et al. CD4⁺ T Follicular Helper Cells in Human Tonsils and Blood Are Clonally Convergent but Divergent from Non-Tfh CD4⁺ Cells. *Cell Rep.* 2020;30(1):137-152.e5. doi:10.1016/j.celrep.2019.12.016
188. Schmitt N, Bentebibel SE, Ueno H. Phenotype and functions of memory Tfh cells in human blood. *Trends Immunol.* 2014;35(9):436-442. doi:10.1016/j.it.2014.06.002
189. He R, Hou S, Liu C, et al. Follicular CXCR5⁻ expressing CD8(+) T cells curtail chronic viral infection. *Nature.* 2016;537(7620):412-428. doi:10.1038/nature19317
190. Valentine KM, Hoyer KK. CXCR5⁺ CD8 T Cells: Protective or Pathogenic? *Front Immunol.* 2019;10:1322. doi:10.3389/fimmu.2019.01322
191. Fousteri G, Kuka M. The elusive identity of CXCR5⁺ CD8 T cells in viral infection and autoimmunity: Cytotoxic, regulatory, or helper cells? *Mol Immunol.* 2020;119:101-105. doi:10.1016/j.molimm.2020.01.007
192. de Meis J, Aurélio Farias-de-Oliveira D, Nunes Panzenhagen PH, et al. Thymus atrophy and double-positive escape are common features in infectious diseases. *J Parasitol Res.* 2012;2012:574020. doi:10.1155/2012/574020
193. Overgaard NH, Jung JW, Steptoe RJ, Wells JW. CD4⁺/CD8⁺ double-positive T cells: more than just a developmental stage? *Journal of Leukocyte Biology.* 2015;97(1):31-38. doi:10.1189/jlb.1RU0814-382
194. Choi SM, Park HJ, Choi EA, Jung KC, Lee JI. Cellular heterogeneity of circulating CD4⁺CD8⁺ double-positive T cells characterized by single-cell RNA sequencing. *Sci Rep.* 2021;11(1):23607. doi:10.1038/s41598-021-03013-4
195. Vella LA, Herati RS, Wherry EJ. CD4⁺ T Cell Differentiation in Chronic Viral Infections: The Tfh Perspective. *Trends in Molecular Medicine.* 2017;23(12):1072-1087. doi:10.1016/j.molmed.2017.10.001
196. Wijesinghe A, Gamage J, Goonewardena H, et al. Phenotype and functionality of follicular helper T cells in patients with acute dengue infection. *J Biomed Sci.* 2020;27(1):50. doi:10.1186/s12929-020-00641-2
197. Zoldan K, Ehrlich S, Killmer S, et al. Th1-Biased Hepatitis C Virus-Specific Follicular T Helper-Like Cells Effectively Support B Cells After Antiviral Therapy. *Front Immunol.* 2021;12:742061. doi:10.3389/fimmu.2021.742061

198. Chen Y, Yu M, Zheng Y, et al. CXCR5+PD-1+ follicular helper CD8 T cells control B cell tolerance. *Nat Commun.* 2019;10(1):4415. doi:10.1038/s41467-019-12446-5
199. *Emergency Use Authorization for Pfizer-BioNTech COVID-19 Vaccine Review Memo.* Accessed October 14, 2023. <https://www.fda.gov/media/144416/download>
200. *Moderna COVID-19 Vaccine Health Care Provider Fact Sheet.* Accessed October 14, 2023. <https://www.fda.gov/media/144637/download>
201. Mohseni Afshar Z, Tavakoli Pirzaman A, Karim B, et al. SARS-CoV-2 Omicron (B.1.1.529) Variant: A Challenge with COVID-19. *Diagnostics (Basel).* 2023;13(3):559. doi:10.3390/diagnostics13030559
202. Cao Y, Wang J, Jian F, et al. Omicron escapes the majority of existing SARS-CoV-2 neutralizing antibodies. *Nature.* Published online December 23, 2021. doi:10.1038/s41586-021-04385-3
203. Hu J, Peng P, Cao X, et al. Increased immune escape of the new SARS-CoV-2 variant of concern Omicron. *Cell Mol Immunol.* Published online January 11, 2022. doi:10.1038/s41423-021-00836-z
204. Willett BJ, Grove J, MacLean OA, et al. SARS-CoV-2 Omicron is an immune escape variant with an altered cell entry pathway. *Nat Microbiol.* 2022;7(8):1161-1179. doi:10.1038/s41564-022-01143-7
205. Blue ML, Daley JF, Levine H, Schlossman SF. Coexpression of T4 and T8 on peripheral blood T cells demonstrated by two-color fluorescence flow cytometry. *The Journal of Immunology.* 1985;134(4):2281-2286. doi:10.4049/jimmunol.134.4.2281
206. Bohner P, Chevalier MF, Cesson V, et al. Double Positive CD4+CD8+ T Cells Are Enriched in Urological Cancers and Favor T Helper-2 Polarization. *Front Immunol.* 2019;10:622. doi:10.3389/fimmu.2019.00622
207. Giraldo NA, Bolaños NI, Cuellar A, et al. Increased CD4+/CD8+ Double-Positive T Cells in Chronic Chagasic Patients. Rodrigues MM, ed. *PLoS Negl Trop Dis.* 2011;5(8):e1294. doi:10.1371/journal.pntd.0001294
208. Nascimbeni M, Shin EC, Chiriboga L, Kleiner DE, Rehmann B. Peripheral CD4+CD8+ T cells are differentiated effector memory cells with antiviral functions. *Blood.* 2004;104(2):478-486. doi:10.1182/blood-2003-12-4395
209. Trautmann A, Rückert B, Schmid-Grendelmeier P, et al. Human CD8 T cells of the peripheral blood contain a low CD8 expressing cytotoxic/effector subpopulation. *Immunology.* 2003;108(3):305-312. doi:10.1046/j.1365-2567.2003.01590.x

210. Izad M, Harirchian MH, Amiri H, Najafi F, Ghaflati Z, Salehi Z. Low and high CD8 positive T cells in multiple sclerosis patients. *Iran J Allergy Asthma Immunol.* 2013;12(3):276-280.
211. Tyllis TS, Fenix KA, Norton TS, et al. CXCR5+CD8+ T Cells Shape Antibody Responses In Vivo Following Protein Immunisation and Peripheral Viral Infection. *Front Immunol.* 2021;12:626199. doi:10.3389/fimmu.2021.626199
212. Zhou P, Gong F, Ji T, Cao C, Zheng T. Enriched CXCR3+ CXCR5+ CD8+ T cells in SARS-CoV-2 infected and vaccinated individuals effectively respond to the antigen in recall. *Journal of Infection.* 2023;86(5):497-499. doi:10.1016/j.jinf.2023.02.022

APPENDIX A
STATEMENT OF PERMISSIONS

All co-authors have granted their permission for the use of the articles presented in this dissertation.

APPENDIX B

SARS-COV-2 NEUTRALIZING ANTIBODY LATERAL FLOW ASSAY

CLINICAL AGREEMENT AND VALIDATION STUDIES

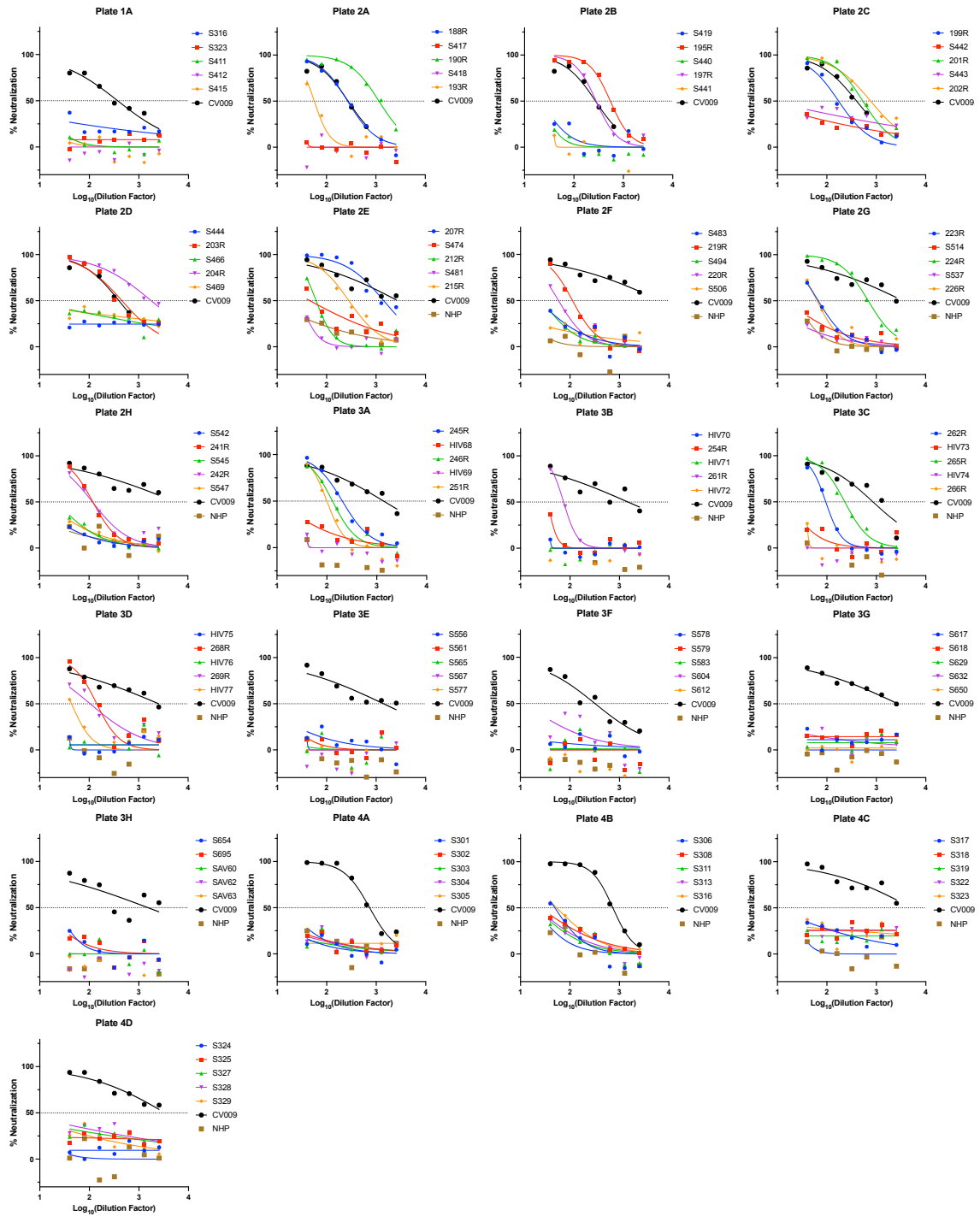


Figure 1. SARS-CoV-2 NAb LFA validation data set.

Sample ID	IC50	Reciprocal Titer	Density Units
188R	269	160	374770
190R	1155	640	87151
193R	57	40	683320
195R	546	320	54370
197R	282	160	270713
199R	173	160	467905
201R	535	320	583088
202R	769	640	312516
203R	462	320	824844
204R	1801	1280	57481
207R	1428	1280	112023
212R	61	40	1024369
215R	282	160	170650
219R	113	80	721586
220R	59	40	700201
223R	67	40	359723
224R	690	640	60639
226R	64	40	126477
241R	119	80	693428
242R	117	80	270305
245R	205	160	868519
246R	130	80	739227
251R	100	80	606793
254R	35	20	1046521
261R	74	40	462301
262R	95	80	726823
265R	230	160	389631
266R	38	20	797636
268R	142	80	627052
269R	105	80	458631
HIV68	10	0	832321
HIV69	37	20	798070
HIV70	37	20	933033
HIV71	0	0	853477
HIV72	0	0	1270656
HIV73	16	0	1003183
HIV74	0	0	1083644
HIV75	0	0	1361471
HIV76	0	0	1056155
HIV77	44	40	1019498
S301	5	0	1233303
S302	2	0	1140550
S303	1	0	1272560
S304	1	0	1085154
S305	0	0	1164398
S306	50	40	866335
S308	25	20	1179183
S311	20	20	1157597
S313	21	2	1291301
S316	0	0	1238273
S316	54	40	1085448
S317	7	0	1135441

Sample ID	IC50	Reciprocal Titer	Density Units
S318	0	0	1150060
S319	0	0	899112
S322	0	0	1107033
S323	0	0	1025706
S323	0	0	958239
S324	0	0	848878
S325	0	0	1089202
S327	1	0	1061677
S328	3	0	1095870
S329	3	0	1194879
S411	11	0	962435
S412	0	0	1013325
S415	6	0	1092463
S417	32	20	1064887
S418	0	0	1166137
S419	22	20	1011284
S440	21	20	926672
S441	37	20	1000844
S442	3	0	981888
S443	7	0	871883
S444	0	0	1188161
S466	6	0	1142105
S469	1	0	1113319
S474	46	40	780280
S481	29	20	1248317
S483	23	20	1174262
S494	27	20	1144064
S506	1	0	932677
S514	15	0	1150494
S537	5	0	1079687
S542	7	0	1189236
S545	22	20	1212776
S547	12	0	1024074
S556	4	0	1132113
S561	10	0	1149996
S565	2	0	1150720
S567	0	0	801701
S577	0	0	994422
S578	0	0	1075530
S579	0	0	1203387
S583	0	0	949402
S604	12	0	1165519
S612	0	0	933738
S617	0	0	919449
S618	0	0	1077343
S629	0	0	1255364
S632	0	0	605716
S650	0	0	1064286
S654	23	20	948276
S695	11	0	1092731
SAV60	2	0	1101658
SAV62	0	0	800966
SAV63	0	0	1128588

Table 1. NAb LFA Test Line Densities (TLD) for validation data set.

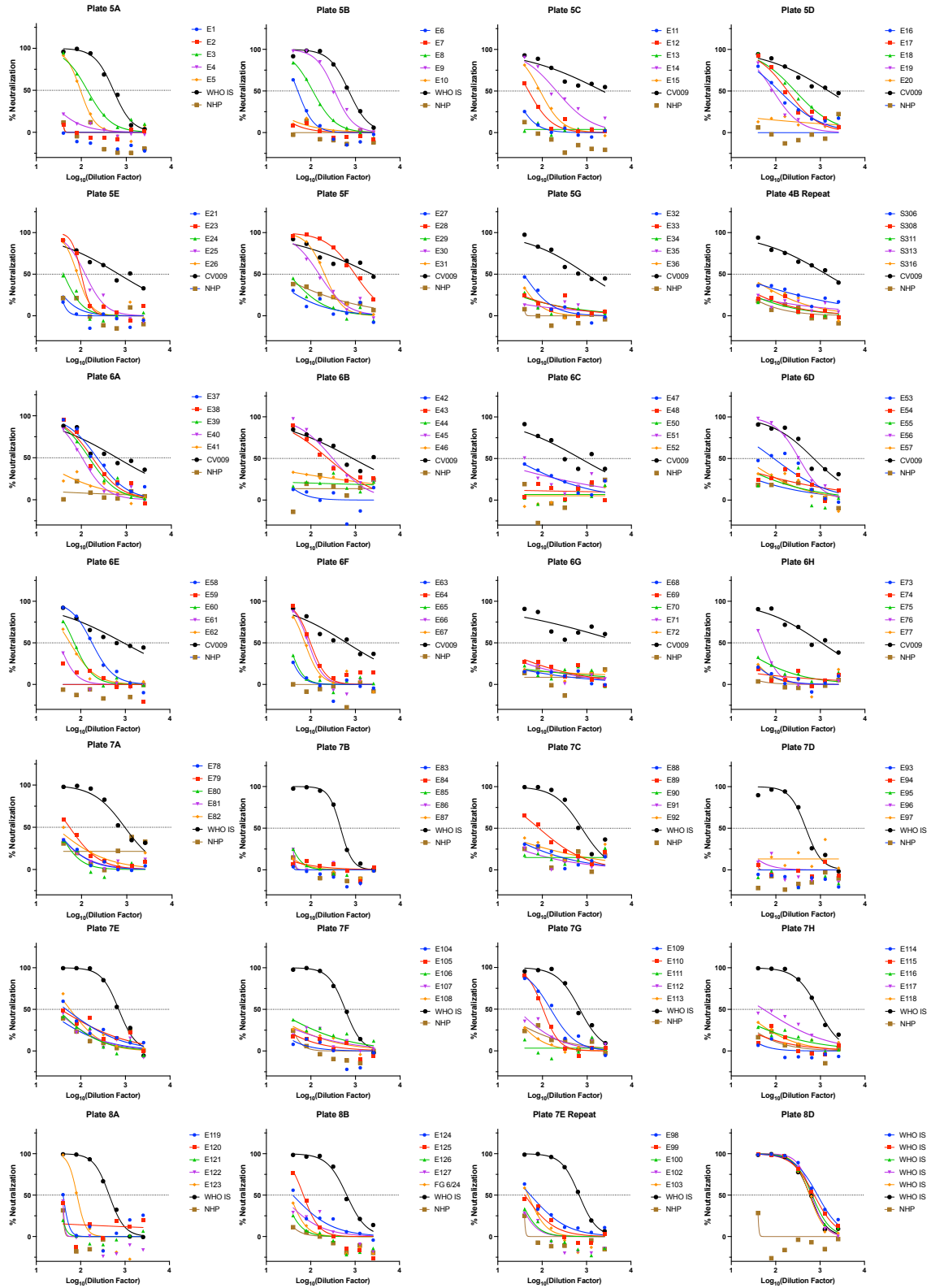


Figure 2. SARS-CoV-2 NAb LFA clinical agreement data set.

APPENDIX C

PROTOCOL FOR VALIDATION OF FOCUS REDUCTION NEUTRALIZATION

TEST (FRNT) AT ARIZONA STATE UNIVERSITY

**Protocol for Validation of Focus Reduction Neutralization Test (FRNT) at
Arizona State University**

Validation Protocol for FRNT Assay

Protocol Number: ASU-210113

PROTOCOL APPROVAL

AUTHOR: ___Alexa Roeder___  ___Date: 8/26/2021___

APPROVED BY: ___Douglas Lake___  ___Date: 8/26/2021___

1. STUDY

Plaque assays are a classic methodology for detecting infectious viruses, including Beta coronaviruses like SARS-CoV-2. However, this method is labor-intensive, costly, low throughput, and is not efficient for performing large-scale neutralization assays on patient specimens or monoclonal antibodies.

Neutralization tests that can be performed in 96-well microtiter plates are higher throughput, conserve reagents, and are more accurate than traditional plaque assays in 6-well or 24-well plates. We adapted a microneutralization focus reduction neutralization test (FRNT) that measures the ability of serum samples to prevent SARS-CoV-2 from infecting permissive Vero E6 cells (Vanderheiden et al., 2020) as measured by detecting SARS-CoV-2 spike protein infected cell foci using anti-spike monoclonal antibody CR3022 (Suthar et al 2020). The data reported from this microneutralization test are in IC₅₀ format, which indicates the dilution of serum that inhibits 50% of the virus from infecting Vero E6 cells. This Protocol provides step-by-step instructions for performing microneutralization assay and applies to performing a SARS-CoV-2 neutralization assay on human plasma or serum samples.

The following analytical performance characteristics or validation tests will be determined during this validation:

2. MATERIALS AND METHODS

- Vero C1008 cells (clone E6), (ATCC, cat. no. CRL-1586)
- Dulbecco's Modified Eagle Medium, DMEM (VWR, cat. no. 45000-304)
- Minimal Essential Medium, MEM (Sigma, cat. no. M0275)
- Fetal Bovine Serum, FBS, heat inactivated (Sigma cat. no. F4135)
- Complete DMEM (see recipe in Appendix)
- Complete DMEM containing 2% FBS, 10mM HEPES, 100U/mL penicillin/100U/mL streptomycin, store sterile filtered at 4°C.
- Dulbecco's phosphate-buffered saline, DPBS (VWR, cat. no. 45000-436)
- 0.25% trypsin-EDTA (Corning, cat. no. 25-053-CI)
- Trypan blue (Beta South Technologies, cat. no. T8154)
- Human serum/plasma samples
 1. The serum samples used in this validation study were collected at Mayo Clinic Arizona as leftover samples from the clinical laboratory with waived consent. Collection of the samples was approved by Mayo Clinic IRB# 20-004544.
 2. Post collection, serum was stored at -80°C and not freeze-thawed more than twice. Twenty µL of serum is needed to run one assay in duplicates.
- SARS-CoV-2 isolate USA-WA/012020 (BEI, cat. no. NR-52281)
- 2.0% methylcellulose (see recipe in Appendix)

- 2X MEM prepared at twice the normal concentration containing 4% FBS, 20 mM HEPES, 0.42% (w/v) sodium bicarbonate, 200 IU penicillin G/mL, 100 µg streptomycin/mL.
- Fixation buffer: 4% (v/v) paraformaldehyde (PFA) in 1x PBS (see recipe in Appendix)
- Permeabilization buffer (see recipe in Appendix)
- KPL TrueBlue Peroxidase Substrate (VWR, cat. no. 95059-168)
- Recombinant anti-SARS-CoV-2 Spike Glycoprotein S1 antibody (CR3022, Abcam, cat. no. ab273073)
- Goat Anti-Human IgG (Fc specific)-horseradish peroxidase antibody (Sigma-Aldrich, cat. no. A0170)
- Laminar flow hood (Labconco Purifier BSC Class II, or equivalent)
- Tissue culture microscope (Nikon or equivalent)
- 175-cm² (T-175) cell culture flasks (ThermoFisher, Cat. no. 159910)
- 96-well flat bottom cell culture-treated microplate (Corning, cat. no. 3599)
- 96-well V-bottom cell culture-treated microplate (Grenier Bio-One cat. no. 651180)
- Multichannel pipettes (200 and 20 µL)
- Tips for micropipettes, sterile (Rainin LTS or equivalent) and wide-mouth pipette tips
- 1.5-ml RNase/DNase free tubes (VWR, cat. no. 10160-142, or equivalent)
- Heat block or water bath (set to 56°C)
- Benchtop microcentrifuge, refrigerated
- Falcon 96-well U-bottom plate (Corning, cat. no. 353077)
- Tissue culture incubator (set to 37°C with 5% CO₂)
- Serological pipettes, sterile (VWR or equivalent)
- Labnet Rocker 25 (Model S2025-XLD-B)
- Benchmark Scientific Everlast Rocker 247
- ELISPOT reader (CTL ImmunoSpot S6 Universal Analyzer)
- Additional reagents and equipment for cell culture including trypsinization and counting viable cells by trypan blue exclusion (see Current Protocols article: Phelan & May, 2015)

3. SAFETY PRECAUTIONS

1. SARS-CoV-2 is a Biosafety Level 3 (BSL-3) pathogen. Investigators should seek guidance from their local institutional environmental health and safety office to determine the appropriate protocols for working in BSL-3 and removal of samples from BSL-3.
2. All personnel performing this work should have read the protocol and received appropriate training and certification for work in a BSL3 environment. Appropriate BSL3 safety operating procedures should be used at all times and all methods should be performed in appropriate BSL3 certified labs.

3. All blood samples should be handled and processed according to Institutional Biosafety Guidelines. This procedure should be performed in accordance with all applicable safety procedures.

4. METHODS AND PERFORMANCE CHARACTERISTICS EVALUATED

4.1 Preparation

- Cells: Prepare four 96-well flat-bottom plates of Vero E6 cells for subsequent inoculation with SARS-CoV-2. Plates should be seeded with 2.5×10^5 cells/mL in 100 μ L complete DMEM, 12-18 hours prior to inoculation. Cells should be just recently confluent at the time of inoculation.
- Serum samples: 20 μ L aliquots of sera should be prepared just before inoculation. Note: In preliminary experiments we heat-inactivated serum, but the serum formed a gel upon 56°C heat-inactivation. We presume this is due to serum separator tubes that Mayo Clinic employs for peripheral blood collection. Therefore, we did not heat-inactivate any serum used in the validation or clinical agreement studies. An hour prior to inoculation, serum samples should be diluted 10-fold using 180 μ L infection medium (see recipe in Appendix). Prior to dilution, serum aliquots should be stored on ice or at 4°C.

4.2 FRNT50 Assay

Serum and virus dilutions

- Prepare four 96-well V-bottom dilution plates by adding 60 μ L infection medium to all wells.
- Vortex or vigorously pipette 10-fold diluted serum and add 60 μ L to wells A1-A2 for duplicate replicates. Repeat with four additional serum samples in wells A3-A4, A5-A6, A7-A8, and A9-A10. Negative and positive SARS-CoV-2 neutralizing antibody controls should be run in lane 11 and 12, respectively, for every plate. Transfer 60 μ L of pooled normal human serum to well A11 and 60 μ L neutralizing antibody control. CV009 was used as a control serum for all of the experiments in the validation study.
- Prepare serial two-fold dilutions of sera in the 96-well V-bottom plate using a multichannel pipettor, from the initial dilution (1:20). After virus is added, the final dilution of the starting concentration of sera is 1:40.
- Perform two-fold serial dilutions by transferring 60 μ L from row A through row G in the plate such that row G contains a final dilution of 1:2560, discarding the final 60 μ L. Row H should contain infection medium without antibody to serve as a virus only control except for wells H10, H11 and H12 which contain cells alone without virus.
- Prepare the SARS-CoV-2 (WA01/2020 isolate) virus dilution as shown below, mix and transfer to multichannel pipette reservoir. Prepare 60 μ L virus

per well for 120 wells (to allow extra for pipetting). Total volume per plate should be 7.2 mL.

$60 \mu\text{L}/\text{well} \times 120 \text{ wells} = 2.88 \times 10^5 \text{ pfu in } 7.2 \text{ mL}$

$\text{Stock virus} = 2 \times 10^4 \text{ pfu}/\mu\text{L}$

$2.88 \times 10^5 \text{ pfu} / 2 \times 10^4 \text{ pfu}/\mu\text{L} = 14.4 \mu\text{L virus added to } 7.186 \text{ mL diluent (infection medium).}$

- Using the multichannel pipettor, inoculate 60 μL of virus into each of the wells containing serum dilutions. Take care not to immerse the pipet tips into the sample. Start at the last (row H, no Ab) row and only add virus to wells H1-H9. Inoculate 60 μL of virus into every well of the remaining rows, working bottom to top. Add 60 μL media without virus to the last three wells (H10-H12). These wells will contain cells only. Incubate the samples at 37°C for 60 minutes in a 5% CO₂ incubator.
- Remove assay plates containing Vero E6 cells from incubator and aspirate medium from each well. Remove dilution plates containing antibody and virus after 60 minutes incubation. Starting from the bottom row (most dilute), transfer 100 μL of antibody + virus from dilution plate to assay plate. Incubate assay plates at 37°C for 60 minutes in a 5% CO₂ incubator.

4.3 Methylcellulose Overlay

- Prepare 40 mL of overlay medium by mixing 20 mL of 2X MEM with 20 mL of 2% Methylcellulose in 1:1 (v/v) ratio. Ensure equal volumes of methylcellulose and MEM is mixed evenly by vigorous serological pipetting. If prepared beforehand and stored at 4°C, allow overlay to heat in a 37°C water bath during the previous incubation.
- Pipette 100 μL of methylcellulose overlay per well: dispense the overlay onto the side of the well to avoid damaging the monolayer.
- Incubate the plates 24 hours at 37°C in a 5% CO₂ incubator.

4.4 Immunostaining Virally Infected Foci

- Remove methylcellulose overlay by carefully aspirating remaining media, taking care not to disturb infected monolayers.
- Transfer 300 μL 4% paraformaldehyde in 1X PBS to each well. Incubate at room temperature for 20 minutes. Remove paraformaldehyde into appropriate waste container.
- Wash cells with 200 μL permeabilization buffer six times to remove any overlay and formaldehyde. Replace last wash with DPBS. Plates can be stored at 4°C in 200 μL DPBS and removed from BSL3 for staining at this point.
- Remove DPBS and add 50 $\mu\text{L}/\text{well}$ primary antibody (CR3022, Abcam, ab273073) at 1 $\mu\text{g}/\text{mL}$ (1:1000 stock) diluted in permeabilization buffer. Incubate plates overnight at 4°C without rocking.
- Wash three times with 200 $\mu\text{L}/\text{well}$ of PBS + 0.01% Tween 20.
- Add 50 $\mu\text{L}/\text{well}$ secondary antibody (goat anti-human IgG(Fc)-HRP, Sigma-Aldrich, A0170) diluted 1:2000 in permeabilization buffer. Incubate for 2 hours at room temperature, gently rocking.

- Wash three times with 200 μ L/well of PBS + 0.01% Tween 20.
- Add 50 μ L/well KPL TrueBlue Substrate (VWR, cat. no. 95059-168). Incubate for 15 minutes at room temperature, gently rocking.
- Wash three times with 200 μ L/well of ddH₂O. Tap plates dry on a paper towel and image on AID ELISPOT reader.

4.5 Data

- Export data from AID ELISPOT reader in Microsoft Excel and PowerPoint formats.
- Data are formatted in excel to display the average of duplicate wells at each dilution, for a given serum sample. The average of nine virus only (no antibody) wells and three cell only (no virus or antibody) wells are calculated for data normalization using GraphPad Prism 9.0 (GraphPad Software Inc.).
- Data are transformed to percentage neutralization by normalization using the average number of viral foci in virus only wells (maximum infection/least neutralization) and cells only wells (minimum infection/greatest neutralization).
- Normalized data are then curve fit using a non-linear regression and analyzed for IC₅₀ in GraphPad Prism 9.0 using parameters and constraints described by Ferrara and Temperton, 2018.

4.6. Interpretation and Determination of Titer

- The principle is to determine the highest dilution of serum that inhibits (reduces) plaque formation by a given amount. The given amount varies by investigators and virus, but most of the time 50% reduction is appropriate. In that case, the neutralizing titer of the sample would be the reciprocal of the highest dilution of serum that inhibits >50% of the plaques relative to no serum or non-immune serum controls.

Example:

- The no serum control wells contain 100 plaques, such that 50% reduction is defined as a well having 50 or fewer plaques. Assume that the plaque counts for serum dilutions of 1:40, 80, 160, 320, 640, 1280 and 2560 were 0, 2, 13, 31, >50, >50.
- In the above example, the 50% neutralizing titer would be 1:320.

5. REAGENTS & RECIPES

Complete DMEM for Vero cell culture.

*For 1 L:

Dulbecco's Modified Eagle Medium (high glucose) supplemented to contain:

10% heat-inactivated fetal bovine serum
1% Glutamax
10 mM HEPES
100 U/mL penicillin/100 U/mL streptomycin

Sterile filter and store at 4°C.

*Vero-furin media is as stated above with the addition of 5 µg/ml blasticidin.

Infection medium

*For 1 L:

Dulbecco's Modified Eagle Medium (high glucose) supplemented to contain:

2% heat-inactivated fetal bovine serum

10 mM HEPES

100U/mL penicillin/100U/mL streptomycin

2X minimal essential medium + 4% FBS

*For 1 L:

200 mL 10X MEM (Sigma #M0275)

20 mL of 1 M L-glutamine

20 mL 1 M HEPES

40 mL heat-inactivated fetal bovine serum

4.2 g sodium bicarbonate

20 mL of 10,000 IU/ml penicillin +10,000 µg/ml streptomycin

Deionized distilled (Milli-Q) water to 1 L

Sterile filter and store at 4°C.

2% methylcellulose

Autoclave a 250 mL glass bottle containing 2 g carboxymethylcellulose powder (Sigma #M0512) and a stir bar.

Autoclave 100 mL deionized distilled (Milli-Q) water. When water is cool enough to handle, add to methylcellulose containing bottle. Stir mixture overnight at 4°C and then store at 4°C until ready for use.

4% Paraformaldehyde in 1X PBS

*For 1L:

Dissolve 40g paraformaldehyde powder (Sigma, Cat. No. 158127) into 800 mL 60°C 1X PBS

pH with 1N NaOH until solution clears

Add 1X PBS to 1L, allow to cool to room temperature

Adjust pH to 6.9 with 10M HCl

Permeabilization buffer

*For 1L:

1 g of saponin (Sigma, Cat. No: S7900)

1 g of bovine serum albumin (Fraction V)

To volume with 1 L phosphate buffered saline (without Ca or Mg)
Filter sterilize and store at 4°C until ready for use.

PBS + Tween wash

1 L 10X PBS

9 L ddH₂O

50 mL 10% Tween-20

References

1. ASU SOP: Focus Reduction Neutralization Test (FRNT) for Determination of Antibody to SARS-CoV-2.
2. Suhtar et al. Rapid Generation of Neutralizing Antibody Responses in COVID-19 Patients. *Cell Rep. Med.* 2020; 1(3):100040.
3. Vanderheiden et al. Development of a Rapid Focus Reduction Neutralization Test Assay for Measuring SARS-CoV-2 Neutralizing Antibodies. *Curr. Protoc. Immunol.* 2020; 131(1):e116.
4. Ferrara F., Temperton N., Pseudotype Neutralization Assays: From Laboratory Bench to Data Analysis. *Methods Protoc.* 2018;1(1):8.

APPENDIX D

FLOW CYTOMETRIC T CELL ASSAY GATING WORKFLOWS

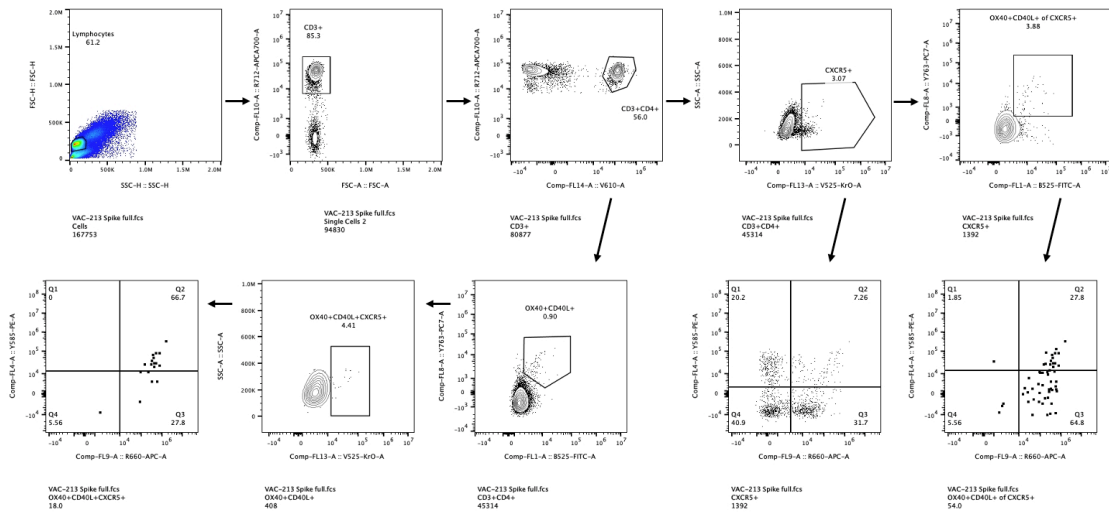


Figure 1. Gating workflow for identification of bulk and activated T follicular helper cells.

APPENDIX E

FLOW CYTOMETRIC T CELL ASSAY MULTICOLOR ANTIBODY PANELS

Activation Induced Marked (AIM) assays:

Antibody	Dilution	Reference
α -hu-CD3-AF700	1:25	56-0038-82 (eBiosciences)
α -hu-CD4-BV605	1:25	BDB562658 (BD)
α -hu-CD8-EF450	1:50	48-0088-42 (Invitrogen)
α -hu-OX40-PECy7	1:50	350012 (Biolegend)
α -hu-CD137-APC	1:25	309810 (Biolegend)
α -hu-CD69-PE	1:10	BDB555531 (BD)

T follicular helper cell assays:

Antibody	Dilution	Reference
α -hu-CD3-AF700	1:25	56-0038-82 (eBiosciences)
α -hu-CD4-BV605	1:25	BDB562658 (BD)
α -hu-CD8-EF450	1:50	48-0088-42 (Invitrogen)
α -hu-OX40-PECy7	1:50	350012 (Biolegend)
α -hu-CXCR5-BV510	1:50	BDB563105 (BD)
α -hu-CXCR3-APR	1:25	353708 (Biolegend)
α -hu-CCR6-PE	1:25	353410 (Biolegend)
α -hu-PD-1-PerCPCy5.5	1:25	367410 (Biolegend)
α -hu-CD40L-FITC	1:50	310804 (Biolegend)

APPENDIX F

CD8^{HI} VS CD8^{LOW} ACTIVATION INDUCED MARKER EXPRESSION

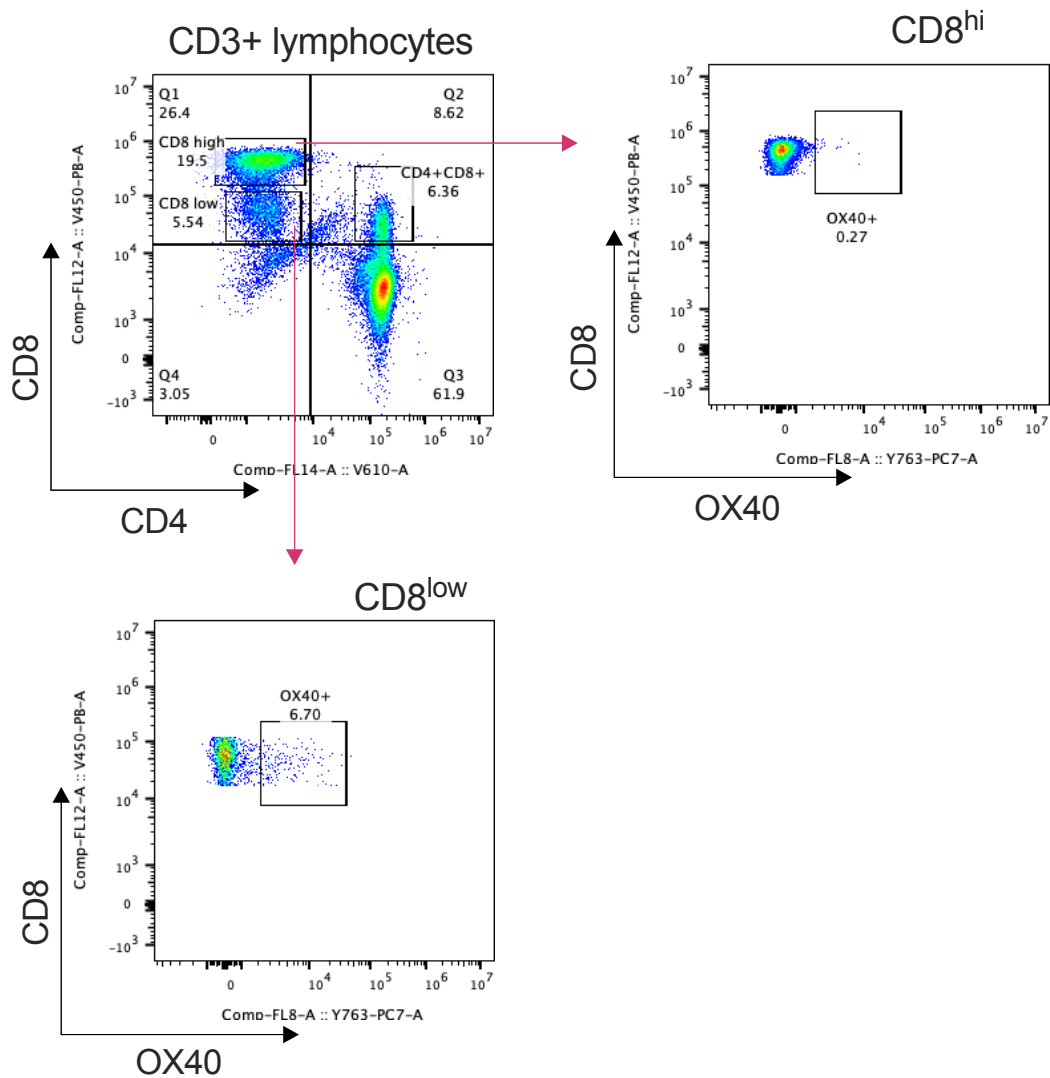


Figure 1. Differential surface expression of OX40 on CD8^{hi} and CD8^{low} T cell populations. This figure shows a representative VPR with expanded CD8^{low} T cells under spike-peptide stimulated conditions. Flow cytometric pseudo-color dot plots show enumeration of CD8^{hi}, CD8^{low}, and CD4⁺CD8⁺ T cells within the CD3⁺ lymphocyte parent population. Red arrows show that CD8^{hi} and CD8^{low} populations were independently assessed for OX40 expression.